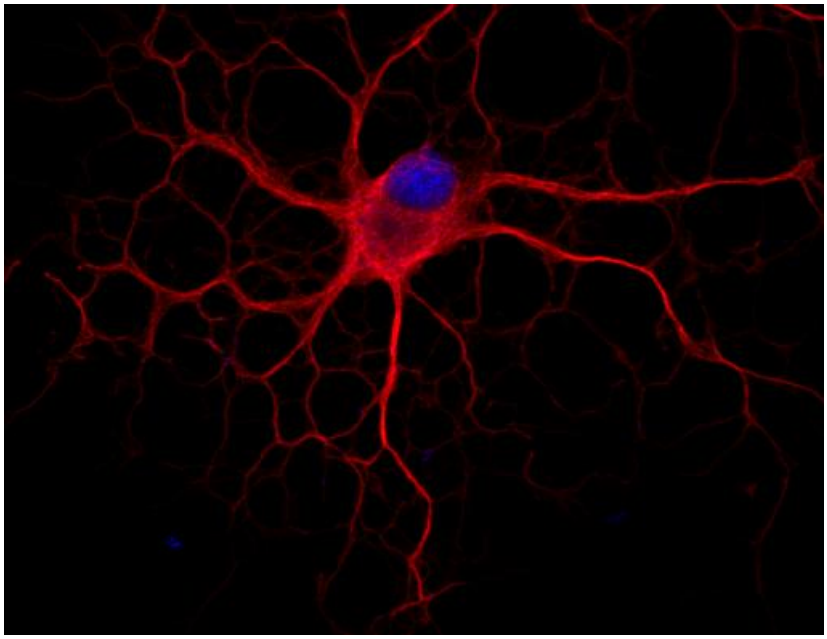

The oligodendrocyte "processosome": novel regulators of differentiation and myelination

Ana Filipa Bouçanova da Silva

Mestrado em Bioquímica

Departamento de Química e Bioquímica

2015

Orientador

Doutora Helena Sofia Domingues, PhD, Instituto de Investigação e Inovação em Saúde – Instituto de Biologia Molecular e Celular

Co-orientador

Doutor João Bettencourt Relvas, PhD, Instituto de Investigação e Inovação em Saúde –Instituto de Biologia Molecular e Celular

INSTITUTO DE INVESTIGAÇÃO E INOVAÇÃO EM SAÚDE
UNIVERSIDADE DO PORTO

IBMC
INSTITUTO DE BIOLOGIA MOLECULAR E CELULAR
INSTITUTE FOR MOLECULAR AND CELL BIOLOGY

U.PORTO

INSTITUTO DE CIÊNCIAS BIOMÉDICAS ABEL SALAZAR
UNIVERSIDADE DO PORTO

U.PORTO

FACULDADE DE CIÊNCIAS
UNIVERSIDADE DO PORTO

Todas as correções determinadas pelo júri, e só essas, foram efetuadas.

O Presidente do Júri,

Porto, _____/_____/_____

Este trabalho foi financiado por fundos FEDER através do Programa Operacional de Competitividade – COMPETE –, por fundos nacionais através da Fundação para a Ciência e a Tecnologia – FCT – ao abrigo do projeto FCOMP-01-0124-FEDER 021333 (PTDC/SAU/NMC/119937/2010) e pelas Ações Marie Curie – Bolsa Intra-Europeia inserida no 7º programa Quadro (MC-IEF-2010 #276322).

O “processossoma” do oligodendrócito: novos reguladores da diferenciação e mielinização

The oligodendrocyte “processosome”: novel regulators of differentiation and myelination

Ana Filipa Bouçanova da Silva

Orientador: Doutora Helena Sofia Domingues

Coorientador: Doutor João Bettencourt Relvas

Faculdade de Ciências da Universidade do Porto

Instituto de Ciências Biomédicas Abel Salazar da Universidade do Porto

Instituto de Investigação e Inovação em Saúde

Instituto de Biologia Molecular e Celular

Setembro 2015

Agradecimentos

Lembro-me de, por volta dos dez anos, ter visto um documentário sobre as profundezas dos oceanos. Fiquei fascinada pelos animais que lá habitam e, desse dia em diante, decidi que queria ser cientista. Depois do meu primeiro amor pela biologia marinha, descobri a química, a física e finalmente encontrei o meu lugar nesta grande casa que é a Bioquímica. Uma casa que me ensinou tanta coisa e à qual eu devo tanto.

Quero por isso agradecer a todos os professores da Faculdade de Ciências e do Instituto de Ciências Biomédicas Abel Salazar da Universidade do Porto, nomeadamente aos que mais me marcaram: Alexandre Quintanilha, Eulália Pereira, Rosário Almeida, Nuno Mateus, Claudio Sunkel e Paula Ferreira. Agradeço também aos orientadores e colegas de laboratório que me guiaram e ajudaram neste projeto – Sofia Domingues, João Bettencourt Relvas, Andrea Cruz, Joana Paes de Faria, Maria Azevedo, Ana Seixas, Ana Keating, Nuno Dias, Camila Cabral, Renato Socodato, Cátia Silva e Teresa Canedo. Quero agradecer ao André Maia pela ajuda preciosa no desenvolvimento dos protocolos automáticos de análise de imagem.

Quero também agradecer aos meus colegas e amigos que tornaram o percurso mais fácil, com muitas gargalhadas e “nerdice” – João Santos, Ana Gomes, Filipe Marques, Margarida Moura, Abigail Ferreira, Ricardo Vieira, Carla Gonçalves, Miguel Gonçalves, Tiago Silva, João Garcia e Ivo Barros.

Claro que não me poderia esquecer dos “meus” médicos – João Paulo Caldas, Sónia Moreira, Susana Costa, Fernanda Rosa e Eugénia Silva – e do “meu” engenheiro biomédico – Guilherme Costa: um dia iremos abrir a nossa clínica e curar todas as doenças do mundo.

E porque os últimos são os primeiros, quero agradecer aos meus pais, pois nada disto teria sido possível sem o seu apoio. É graças a vocês que estou aqui hoje e agradeço-vos do fundo do coração. Quero agradecer também à minha irmã, Sofia, e ao meu cunhado, André, pelas conversas e desabafos durante as crises existenciais que tive nos últimos 23 anos.

Finalmente, quero dedicar este trabalho ao meu sobrinho e afilhado Gabriel e a todas as pessoas que sofrem de Esclerose Múltipla no mundo.

Os dados científicos apresentados nesta tese de Mestrado contribuem para dois projetos independentes, derivados de um estudo de transcriptómica desenvolvido no grupo de Biologia Celular da Glia do IBMC. Estes projetos são liderados pelas investigadoras Helena Sofia Domingues e Andrea Cruz e estão atualmente a ser preparados para publicação. Deste trabalho resultaram várias comunicações em poster e estão a ser preparadas duas publicações. Por motivos de terminologia científica, esta tese foi escrita em inglês.

Comunicações em poster

Domingues, HS; Cruz, A; **Bouçanova, F**; Azevedo, M; Seixas, AI; Braz, S and Relvas, JB (2015). The oligodendrocyte “processosome”: identification of new regulators of differentiation and myelination. Poster apresentado no XII European Meeting on Glial Cells in Health and Disease. Bilbau, Espanha, 15 – 18 julho.

Domingues, HS; Cruz, A; **Bouçanova, F**; Azevedo, M; Seixas, AI; Braz, S and Relvas, JB (2015). The oligodendrocyte “processosome”: identification of new regulators of differentiation and myelination. Poster apresentado no XIV Encontro da Sociedade Portuguesa de Neurociências. Póvoa de Varzim, Portugal, 4-5 julho.

Cruz, A; Domingues, HS; Braz, S; **Bouçanova, F**; Moreira, A and Relvas, JB (2015). Role of PABPC1 and YBX1 In oligodendrocyte differentiation. Poster apresentado no XIV Encontro da Sociedade Portuguesa de Neurociências. Póvoa de Varzim, Portugal, 4-5 julho.

Domingues, HS; Cruz, A; **Bouçanova, F**; Azevedo, M; Seixas, AI; Braz, S and Relvas, JB (2014). The oligodendrocyte “processosome”: identification of new regulators of differentiation and myelination. Poster apresentado no IV Encontro do I3S. Póvoa de Varzim, Portugal, 30-31 outubro.

Publicações

Domingues, HS; Cruz, A; **Bouçanova, F**; Azevedo, M; Seixas, AI; Braz, S and Relvas, JB (em preparação). The oligodendrocyte “processosome”: identification of new regulators of differentiation and myelination.

Cruz, A; Domingues, HS; Braz, S; **Bouçanova, F**; Moreira, A and Relvas, JB (em preparação). Role of PABPC1 and YBX1 In oligodendrocyte differentiation

The scientific data presented in this Master thesis contributes to two independent projects, which derived from a transcriptomics study developed in the Glial Cell Biology group at IBMC. These are led by the researchers Helena Sofia Domingues and Andrea Cruz and are currently being prepared for publication. Of this work resulted several poster communications and two publications are in preparation.

Poster communications

Domingues, HS; Cruz, A; **Bouçanova, F**; Azevedo, M; Seixas, AI; Braz, S and Relvas, JB (2015). The oligodendrocyte “processosome”: identification of new regulators of differentiation and myelination. Poster presented at the XII European Meeting on Glial Cells in Health and Disease. Bilbao, Spain, July 15 – 18.

Domingues, HS; Cruz, A; **Bouçanova, F**; Azevedo, M; Seixas, AI; Braz, S and Relvas, JB (2015). The oligodendrocyte “processosome”: identification of new regulators of differentiation and myelination. Poster presented at the XIV Meeting of the Portuguese Society for Neuroscience. Póvoa de Varzim, Portugal, June 4-5.

Cruz, A; Domingues, HS; Braz, S; **Bouçanova, F**; Moreira, A and Relvas, JB (2015). Role of PABPC1 and YBX1 in oligodendrocyte differentiation. Poster presented at the XIV Meeting of the Portuguese Society for Neuroscience. Póvoa de Varzim, Portugal, June 4-5.

Domingues, HS; Cruz, A; **Bouçanova, F**; Azevedo, M; Seixas, AI; Braz, S and Relvas, JB (2014). The oligodendrocyte “processosome”: identification of new regulators of differentiation and myelination. Poster presented at the IV I3S Meeting. Póvoa de Varzim, Portugal, October 30-31.

Publications

Domingues, HS; Cruz, A; **Bouçanova, F**; Azevedo, M; Seixas, AI; Braz, S and Relvas, JB (in preparation). The oligodendrocyte “processosome”: identification of new regulators of differentiation and myelination.

Cruz, A; Domingues, HS; Braz, S; **Bouçanova, F**; Moreira, A and Relvas, JB (in preparation). Role of PABPC1 and YBX1 in oligodendrocyte differentiation.

Resumo

Os oligodendrócitos (OL) são as células mielinizantes do sistema nervoso central (SNC). A Esclerose Múltipla (EM) é a doença desmielinizante mais frequente do SNC e pensa-se que a sua progressão é devida à incapacidade das células precursoras de oligodendrócitos (OPC) se diferenciarem em novas células mielinizantes no microambiente inibidor das lesões da EM. Durante a diferenciação, uma OPC é inicialmente bipolar e estende os seus processos para depois ramificar (OL imaturo) e finalmente produzir uma membrana de mielina. Este OL maduro pode, assim, contactar com um axónio para o mielinizar.

Globalmente, o objetivo deste projeto é identificar e estudar o papel de novas moléculas que tenham um papel importante da diferenciação de OL e mielinização. Para tal, estabeleceu-se previamente uma técnica para separar fisicamente o soma dos processos das OPC e sequenciaram-se os mRNAs das duas frações. Hipotetizámos que os mRNAs enriquecidos nos processos teriam uma maior probabilidade de ter um papel relevante na diferenciação e mielinização de OL. Vários mRNAs foram identificados como estando significativamente enriquecidos nos processos das OPC e, destes, foram selecionados quatro candidatos com base no seu envolvimento na modulação do citoesqueleto e regulação da tradução proteica: Kank2, Dusp19, PABPC1 e YBX1.

Em particular, o objetivo principal desta tese de Mestrado é estudar o papel funcional de Kank2, Dusp19, PABPC1 e YBX1 na diferenciação de OL, nomeadamente a nível da extensão e ramificação dos processos bem como da produção de mielina. Neste contexto, pretendemos também desenvolver um protocolo de análise automática da morfologia de OL. Os nossos resultados mostram que os OL onde foi feita a depleção do mRNA de Kank2, Dusp19, PABPC1 e YBX1 sofreram um atraso na diferenciação quando comparados com o controlo. Este atraso caracteriza-se por um enriquecimento da população de células em estadios de diferenciação mais precoces (análise manual por categorização). Também se verifica uma redução da percentagem de células com marcação positiva para a MBP (*myelin basic protein*, proteína básica da mielina) após depleção do mRNA de Kank2, Dusp19 e PABPC1. No caso da depleção de YBX1 verifica-se um aumento não significativo da percentagem de células com marcação positiva para MBP. Deste modo, pudemos concluir que os candidatos identificados por sequenciação de RNA têm, de facto, um papel relevante na diferenciação dos OL.

Palavras-chave

Oligodendrócito, mielina, citosqueleto, proteínas de ligação ao RNA, diferenciação morfológica, análise de imagem de elevado rendimento.

Abstract

The oligodendrocyte (OL) is the myelinating cell in the central nervous system (CNS). Multiple Sclerosis (MS) is the most frequent demyelinating disease in the CNS and it is thought that its progression is due to oligodendrocyte progenitor cells’ (OPC) inability to differentiate into new myelinating cells in the inhibitory microenvironment of MS lesions. During differentiation, an OPC is initially bipolar and extends its processes, which become ramified (immature OL) and finally produce a myelin membrane. This mature OL can contact an axon and myelinate it.

Globally, the aim of this project is to identify and study novel molecules, which may have an important role in OL differentiation and myelination. To do so, a technique was established to physically separate OPC soma from processes and mRNA from these two fractions was sequenced. It was hypothesized that mRNAs enriched in the processes would have a higher probability of having an important role in OL process extension, branching and myelination. Several mRNAs were identified to be significantly enriched in OPC process and, of these, four candidates were selected based on their role in cytoskeleton modulation and regulation of protein translation: Kank2, Dusp19, PABPC1 and YBX1.

In particular, the main purpose of this Master thesis is to study the functional role of Kank2, Dusp19, PABPC1 and YBX1 in OL differentiation, with special regard to process extension and ramification as well as myelin production. In this context, we also intend to develop an automated analysis protocol of OL morphology. Our results show a delay in OL process extension when Kank2, Dusp19, PABPC1 and YBX1 mRNAs are depleted, relatively to control. This delay is characterized by an enrichment of cells in earlier stages of differentiation (manual categorization analysis). There is also a reduction in the percentage of cells positively stained for MBP (myelin basic protein) after depletion of Kank2, Dusp19 and PABPC1 mRNAs. In the case of depletion of YBX1, there is a non-significant increase in the percentage of cells with MBP staining. Thus, we could conclude that the candidates identified by RNA sequencing do have an important role in OL differentiation.

Keywords

Oligodendrocyte, myelin, cytoskeleton, RNA-binding proteins, morphological differentiation, high-throughput image analysis

Abbreviations List

A2RE – A2 responsive element

ADF – Actin depolymerizing factor

ASK1 – Apoptosis signal-regulating kinase 1

CNPase – 2',3'-Cyclic-nucleotide 3'-phosphodiesterase

CNS – Central nervous system

CA – Constitutively active

DN – Dominant negative

DNA – Deoxyribonucleic acid

DSP/Dusp – Dual-specificity phosphatase

Dusp19 – Dual-specificity phosphatase 19

EAE – Experimental allergic encephalomyelitis

ECM – Extracellular matrix

ERK – Extracellular signal-regulated kinase

FAK – Focal adhesion kinase

hnRNPs – Heterogeneous nuclear ribonucleoproteins

GAP – GTPase-activating protein

GEF – Guanine nucleotide exchange factor

IFN – Interferon

ILK – Integrin-linked kinase

JNK – c-Jun NH_2-terminal kinase

Kank2 – Kank N-motif and ankyrin repeat domain-containing protein 2/ Kidney ankyrin repeat domain-containing protein 2

MAG – Myelin-associated glycoprotein

MAP1B – Microtubule-associated protein 1B

MAPK – Mitogen-activated protein kinase

MBP – Myelin basic protein

MEK – Mitogen/Extracellular signal-activated kinase

MKK – MAPK kinase

MOBP – Myelin-associated oligodendrocytic basic protein

MOG – Myelin-oligodendrocyte glycoprotein

mRNA – Messenger ribonucleic acid

MS – Multiple Sclerosis

OL – Oligodendrocyte

OPC – Oligodendrocyte progenitor cell

PABPC1 – PolyA-Binding Protein Cytoplasmic 1

PDGF-Rα – Platelet-derived growth factor receptor α

PI3K – Phosphoinositol 3-kinase

PI(4,5)P_2/PIP_2 – Phosphatidylinositol-4,5-bisphosphate

PLP – Proteolipid protein

PPMS – Primary progressive form of Multiple Sclerosis

RBP – RNA-binding protein

RhoGDI – Rho GDP-dissociation inhibitor

RNP – Ribonucleoprotein particle

RRMS – Relapsing and remitting phase of Multiple Sclerosis

SAPK – Stress-activated protein kinase

SPMS – Secondary progressive phase of Multiple Sclerosis

UTR – Untranslated region

YB-1/YBX1 – Y-Box binding protein 1

Zfp536 – Zinc-finger protein 536

Table of Contents

Agradecimentos i
Comunicações em poster iii
Publicações iii
Poster communications v
Publications v
Resumo vii
Palavras-chave vii
Abstract ix
Keywords ix
Abbreviations List xi
Table of Figures xvii
1. Introduction 1
1.1. Developmental myelination in the Central Nervous System 3
1.2. The oligodendrocyte (OL) cytoskeleton 11
1.2.1. Tubulin and Actin 11
1.2.2. β1-Integrin signaling 12
1.2.3. Rho GTPases 16
1.2.4. Mitogen-activated protein kinases (MAPK) – JNK pathway 18
1.3. Local mRNA translation in OL 21
1.4. Transcriptomics of CNS resident cells 23
1.5. Demyelination and remyelination in Multiple Sclerosis (MS) 25
1.6. RNA Sequencing of Oligodendrocyte soma *versus* processes 27
1.6.1. Kank N-motif and ankyrin repeat domain-containing protein 2 or Kidney ankyrin repeat domain-containing protein 2 – Kank2 29
1.6.2. Dual specificity phosphatase 19 – Dusp19 31
1.6.3. PolyA-Binding Protein Cytoplasmic 1 – PABPC1 32
1.6.4. Y-Box binding protein 1 – YBX1 32
1.7. Image analysis for morphological studies 35
1.7.1. Manual Categorization 35
1.7.2. Sholl Analysis 36

1.7.3. High-throughput Image Analysis 37
1.8 Aim 41
2. Materials and Methods 43
2.1. Reagents 43
2.2. Mixed Glial Cell Cultures 44
2.3. Oligodendrocyte Progenitor Cells isolation and culture 44
2.4. Lentivirus production and OPC infection 45
2.5. RNA isolation and cDNA synthesis 46
2.6. Quantitative Real-Time Polymerase Chain Reaction 47
2.7. Immunocytochemistry (ICC) 48
2.8. Image acquisition 49
2.9. Image Analysis using INCell Developer Toolbox software 49
2.10. Morphological Categorization by Manual Image Analysis 50
2.11. Sholl Analysis 50
2.12. Statistical Analysis 50
3. Results and Discussion 51
3.1 Development of high-throughput protocols for image analysis using INCell Developer Toolbox 51
3.1.1. Development of an automated protocol for morphological analysis of OL 51
3.1.2. Development of an automated protocol for quantification of myelin production 57
3.2. Functional study of Kank2, Dusp19, PABPC1 and YBX1 in OL differentiation and myelination 61
3.2.1. Kank2 61
3.2.2. Dusp19 67
3.2.3. Sholl Analysis of Kank2 and Dusp19 knockdown 73
3.2.4. PABPC1 75
3.2.5. YBX1 79
4. Conclusions 83
5. Future perspectives 85
6. Challenges 87

7. References 89

Notes 100

Table of Figures

Figure 1 Oligodendrocyte differentiation *in vitro* and *in vivo* 1
Figure 2 "Liquid croissant" model of axon ensheathment by oligodendrocytes 3
Figure 3 Model of a developing myelin sheath 4
Figure 4 Model of MBP regulation of actin disassembly during myelination 5
Figure 5 Model of actin-driven OL process wrapping 6
Figure 6 Saltatory conduction in nerve fibers 7
Figure 7 Structure of the nodal, paranodal and juxtaparanodal regions of axons 8
Figure 8 Localization of myelin proteins in the CNS. 9
Figure 9 Oligodendrocyte cytoskeleton. 12
Figure 10 Integrin activation and interaction with actin cytoskeleton 13
Figure 11 Switch between proliferation and differentiation in OL is mediated by integrin signaling.. 14
Figure 12 OL lacking β1 integrin produce smaller myelin sheets 15
Figure 13 Over-expression of constitutively active (CA) and dominant-negative (DN) forms of Rho, Rac and Cdc42 GTPases 17
Figure 14 The MAPK/JNK pathway in oligodendrocytes. 19
Figure 15 Transport and local translation of MBP mRNA 22
Figure 16 MRI comparing a healthy and an MS patient's brains 25
Figure 17 Physical separation of OPC soma and processes 27
Figure 18 RNA sequencing of OPC soma vs. process 28
Figure 19 Schematic representations of the structure of human Kank family proteins. 29
Figure 20 Over-expression of Kank2-4 reduces the formation of actin stress fibers. ... 30
Figure 21 Possible roles of Dusp19 in JNK pathway. 31
Figure 22 Branching categorization of OPC/OL 35
Figure 23 Sholl Analysis of a neuron 36
Figure 24 Sholl Profile of neurons.. 37
Figure 25 2.5D image acquisition mode 38
Figure 26 Image segmentation 52
Figure 27 Image analysis of oligodendrocytes at OL3d 52
Figure 28 Image analysis of oligodendrocytes 54
Figure 29 Image analysis of oligodendrocytes 56
Figure 30 Segmentation steps used in the automated protocol for analysis of MBP^+ cells.. 57
Figure 31 Result of the analysis using the automated protocol for MBP+ cells. 58
Figure 32 Morphological categorization of OL development. 62

Figure 33 Representative picture of control and Kank2 knockdown cells at OL3d..... 63
Figure 34 Representative picture of control and Kank2 knockdown cells at OL5d..... 64
Figure 35 Representative picture of control and Dusp19 knockdown cells at OL3d 68
Figure 36 Representative picture of control and Dusp19 knockdown cells at OL5d 69
Figure 37 Representative picture of control and PABPC1 knockdown cells at OL3d... 76
Figure 38 Representative picture of control and PABPC1 knockdown cells at OL5d... 77
Figure 39 Representative picture of control and YBX1 knockdown cells at OL3d..... 80
Figure 40 Representative picture of control and YBX1 knockdown cells at OL5d..... 81

Graph 1 Graphical representations of number of processes, branch points and end nodes of OL at OL3d..... 55
Graph 2 Knockdown efficiency of Kank2 shRNA..... 62
Graph 3 Distribution of Olig2^{+}GFP^{+} cells in four morphological stages..... 63
Graph 4 MBP production of control and Kank2 knockdown cells 64
Graph 5 Knockdown of Kank2 leads to a reduction of MBP mRNA levels..... 65
Graph 6 Knockdown efficiency of Dusp19 shRNA 67
Graph 7 Distribution of Olig2^{+}GFP^{+} cells in four morphological stages..... 68
Graph 8 MBP production of control and Dusp19 knockdown cells 69
Graph 9 Knockdown of Dusp19 leads to a reduction of MBP mRNA levels..... 70
Graph 10 Sholl Analysis of OL at OL3d 73
Graph 11 Knockdown efficiency of PABPC1 shRNA..... 75
Graph 12 Distribution of Olig2^{+}GFP^{+} cells in four morphological stages..... 76
Graph 13 MBP production of control and PABPC1 knockdown cells..... 77
Graph 14 Knockdown of PABPC1 leads to a reduction of MBP mRNA levels..... 78
Graph 15 Knockdown efficiency of YBX1 shRNA..... 79
Graph 16 Distribution of Olig2^{+}GFP^{+} cells in four morphological stages..... 80
Graph 17 MBP production of control and YBX1 knockdown cells 81
Graph 18 Knockdown of YBX1 leads to an increase of MBP mRNA levels..... 82

Table 1 Some image processing tools available in INCell Developer Toolbox software. 39
Table 2 shRNA sequences for mRNA knockdown. 46
Table 3 Primer sequences used for qPCR. 47
Table 4 List of primary antibodies, secondary antibodies and stains used for immunocytochemistry. 48

1. Introduction

The oligodendrocyte (OL) is the myelinating cell of the central nervous system (CNS). It is responsible for the formation and maintenance of myelin sheaths, which enwrap axonal internodes, and for trophic support of neurons. Myelin is a lipid-rich substance necessary for electric insulation of axons that allows saltatory conduction of nerve impulses, making it faster and more energy efficient (Hartline and Colman, 2007).

Oligodendrocyte-lineage cells arise from the ventral regions of the prosencephalon and spinal cord during embryonic development (Kessaris et al., 2006; Noll and Miller, 1993). In humans, oligodendrocyte progenitor cells (OPC) appear at the forebrain at 10 weeks of gestation. At around 20 weeks, OPC and pre-oligodendrocytes are the main forms of oligodendroglia and, ten weeks later, it is possible to find more complex immature OL and a few myelinating mature OL in the subcortical regions (Craig et al., 2003). At 40 weeks, end of gestation, around 5% of total brain volume is myelinated, defining the white matter region (Back et al., 2001).

OPC are small bipolar cells expressing platelet-derived growth factor receptor α (PDGF-Rα) (Pringle et al., 1992) and proteoglycan NG2 at the cell surface (Chittajallu et al., 2004; Nishiyama et al., 1996). As they differentiate *in vitro*, OPC become pre-oligodendrocytes – multipolar cells with slightly ramified processes expressing ganglioside A2B5 at the surface, – immature OL – processes become increasingly branched and complex, and cells express sulfatide recognized by O4 antibody (Sommer and Schachner, 1981) – and finally mature OL – highly complex cells able to produce myelin components such as myelin basic protein (MBP) (Reynolds and Wilkin, 1988) **(Figure 1)** (Jackman et al., 2009).

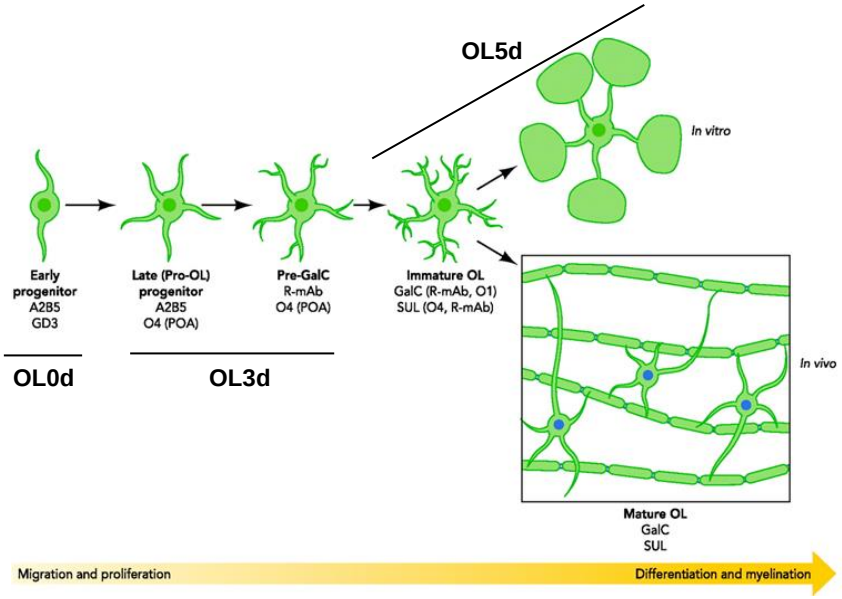

Figure 1 **Oligodendrocyte differentiation *in vitro* and *in vivo*.** Morphological stages found at 0, 3 and 5 days of *in vitro* differentiation (OL0d, OL3d and OL5d). Adapted from Jackman *et al.* (2009).

1.1. Developmental myelination in the Central Nervous System

In vivo, pre-myelinating oligodendrocytes emit multiple radially oriented processes which reach a maximum distance of 50µm of the cell body (Hardy and Friedrich, 1996). These exploratory processes are constantly being extended and retracted as a means of sensing the environment until the OL finds a suitable axon to myelinate. Once OL establish contacts with appropriate axons, myelination is initiated: the cytoplasmic processes begin to spiral around axons to form internodes and the remaining radial processes are retracted (Colognato et al., 2002).

One recent model for myelin ensheathment of axons is called the “liquid croissant model” (Sobottka et al., 2011). Just like making a croissant, OL emit triangular cytoplasmic processes, which may attach to putative surface molecules on axons, and begin wrapping. With each new turn, the inner tongue moves under the outer tongue and myelin spreads outwards along the axon, possibly guided by molecules at the axonal surface **(Figure 2)**. This model accounts for the irregular texture of internodes and for the fact that myelin is thicker in the middle of the internode and thinner at the edges.

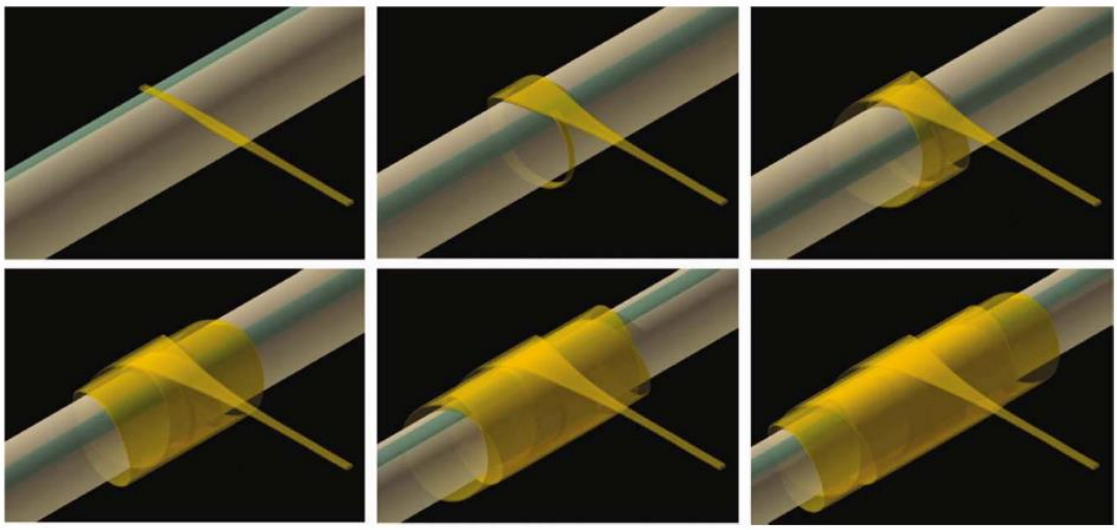

Figure 2 **“Liquid croissant” model of axon ensheathment by oligodendrocytes.** Yellow – oligodendrocyte process, white – axon, blue – putative adhesion molecules on axonal surface**.** Adapted from Sobottka *et al.* (2011).

While accounting for some characteristics of the internode that had not been previously explained, this model fails. A recent work using 3D electron microscopy reconstruction showed that the outermost layer of myelin is continuous and the longest **(Figure 3)** (Snaidero et al., 2014). The irregular texture of the internode is due to the organization of the inner layers, which are gradually shorter, being the inner tongue the shortest.

Two different motions are at play – the leading edge at the inner tongue wraps around the axon while the upper layers extend laterally along the axon.

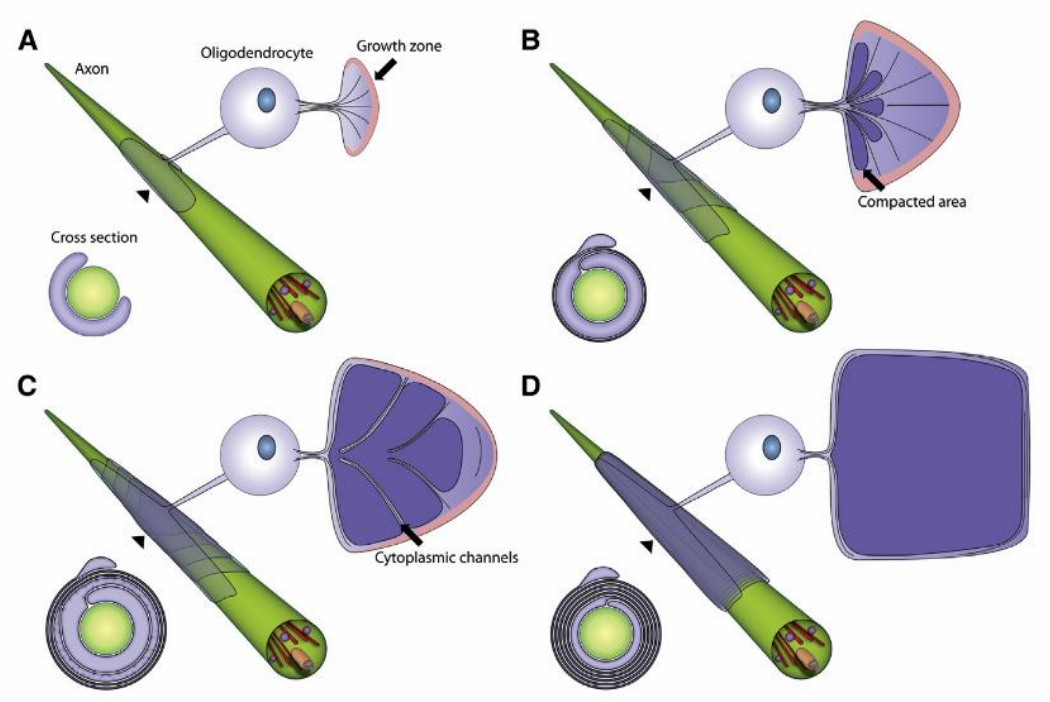

Figure 3 Model of a developing myelin sheath. The unwrapped representation shows the shape of the sheath and the localization of the cytoplasmic channels. The growth zone is colored in pink and the compacted myelin is in dark purple. The wrapped representation shows the position of the layers when wrapped around the axon. The cross-sections show the state of compaction during myelin growth. Adapted from Snaidero *et al.* (2014)

Such a tightly confined space generates pressure that can help push the leading edge forward (blebbing motility) (Paluch and Raz, 2013). However, classic blebbing involves actomyosin contractility, which doesn’t exist in OL (myosin is down-regulated (Zhang et al., 2014b)), therefore there must be other mechanisms regulating inner tongue progression. Indeed, it has been recently found that the actin cytoskeleton is disassembled in mature OL, with F-actin (filamentous) limited to the rim of the OL membrane, *in vitro* (Nawaz et al., 2015; Zuchero et al., 2015). *In vivo*, wild type mice spinal cords show early OL membranes wrapping around axons, which are poor in myelin basic protein (MBP) and rich in actin, as well as more mature OL membranes with an opposite staining pattern (high MBP, low actin). Additionally, *shiverer* mice (knockout for MBP (Readhead and Hood, 1990)) present increased actin staining in white matter tracts. The model proposes that, initially, process extension and branching rely on Arp2/3-dependent actin assembly: OL treated with Arp2/3 inhibitor show a reduced ability to ensheath axons in a dose-dependent manner (Zuchero et al., 2015). However, as OL mature and increase the production of MBP, actin staining along processes disappears and becomes restricted to the outer rim of the OL membrane.

This is supported by the observation that induced conditional knockout of Arp2/3 during ensheathment (10 to 14 days post natal development, P10-P14) doesn't alter the number of myelin wraps in the optic nerve at P30, suggesting that Arp2/3-dependent actin assembly is not needed for myelin wrapping. Treating pre-myelinating but morphologically differentiated OL with an actin-depolymerizing drug overnight dramatically increases MBP production, further suggesting that actin depolymerization drives myelination.

Actin disassembly is usually triggered by depolymerizing factors like gelsolin and cofilin (Hilpelä et al., 2004). These proteins are associated with membrane phosphatidylinositol-4,5-bisphosphate ($PI(4,5)P_2$ or PIP_2) in an inactive state and, when PIP_2 is hydrolyzed by phospholipase C, they are released to the cytoplasm. However, MBP also associates with PIP_2 in order to promote myelin compaction (Nawaz et al., 2009). Therefore, PIP_2 hydrolysis does not seem to be the mechanism by which actin depolymerizing factors become active. It may be due to a competition between MBP and gelsolin/cofilin for the binding to membrane PIP_2. An *in vitro* test using PIP_2-coated beads incubated with cofilin-1 or gelsolin and increasing amounts of MBP showed that MBP was able to compete with the actin depolymerizing factors for binding to the beads. This further suggests that MBP binding to PIP_2 may be a triggering factor of actin cytoskeleton disassembly **(Figure 4)**.

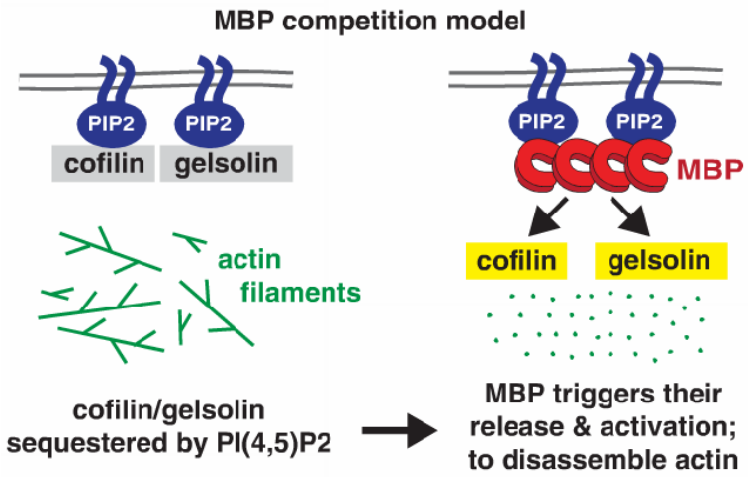

Figure 4 **Model of MBP regulation of actin disassembly during myelination.** Actin disassembly factors cofilin and gelsolin are normally sequestered by $PI(4,5)P_2$ (PIP_2), preventing them from disassembling actin microfilaments (left image). MBP binds to PIP_2 on the OL membrane, releasing cofilin/gelsolin and triggering actin disassembly (right image). Adapted from Zuchero *et al*. (2015).

A similar study (Nawaz et al., 2015) showed that, by depolymerizing the actin cytoskeleton, leaving F-actin only at the outer rim, OL create heterogeneous tension across the membrane. At the outer rim, tension is greater, generating a force that may be able to push the edge further. On the other hand, areas closer to OL soma have lower tension, which may allow them to spread out, creating a large myelin sheet. This model suggests two steps: first, actin polymerization drives the leading edge forward and subsequent depolymerization allows lateral spreading of the myelin sheet. Successive cycles of actin polymerization and depolymerization may drive the leading edge forward while allowing the spreading of the outer layers **(Figure 5)**. The authors identified actin depolymerizing factor (ADF) and cofilin as responsible molecules for the regulation of this process. Double knockout OL for ADF and cofilin-1 showed an increase in F-actin at the leading edge and a smaller surface area, which was partially recovered by actin depolymerizing drugs. *In vivo*, these animals showed higher amounts of F-actin in spinal cord OL. This was accompanied by motor deficits, inner tongue enlargement of OL and thinner compact myelin. However, myelin production was not completely impaired, which may be due to compensation by other actin depolymerizing factors like gelsolin and cofilin-2.

The close relationship between MBP production and cytoskeleton rearrangements shown by the studies of Nawaz et al., 2015 and Zuchero et al., 2015 clearly demonstrates how difficult it is to decouple the two mechanisms, myelination and process outgrowth of OL.

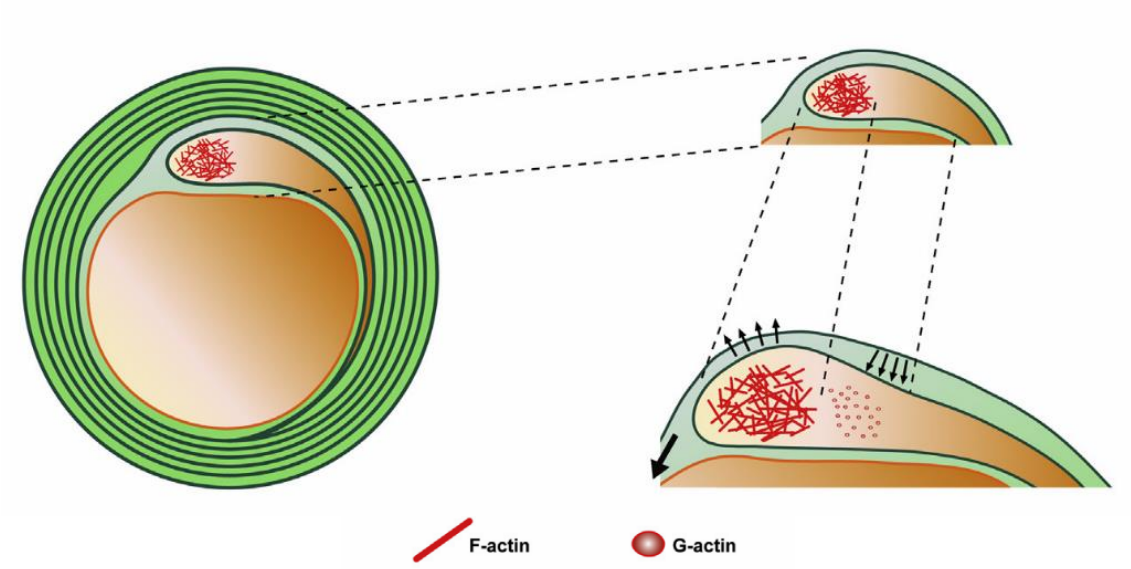

Figure 5 Model of actin-driven OL process wrapping. Polymerizing F-actin creates a force that pushes out membrane protrusions, squeezing in between the axon and the myelin sheath. Subsequent disassembly of F-actin promotes adhesion and spreading of the inner tongue. Successive cycles of actin polymerization and depolymerization inflate and deflate the inner tongue (arrows), driving OL process wrapping and myelin membrane formation. Adapted from Nawaz *et al*. (2015)

By wrapping membranous protrusions around axons, OL make axonal membranes impervious to the passage of ions, which are necessary for the conduction of action potentials. Voltage-gated sodium channels are thus relocated to the unmyelinated sites (nodes of Ranvier), enabling saltatory (“jumping”) conduction **(Figure 6)** (Kaplan et al., 1997; mikeclaffey.com). Saltatory conduction is faster and more energy efficient than continuous conduction because the area of membrane to be depolarized is very small. However, despite these advantages not all axons are myelinated in the CNS. In fact, it is observed that only large caliber axons (greater than 1.3μm in diameter) are myelinated, suggesting axon diameter is a selecting factor for OL myelination (Windebank et al., 1985). On the other hand, it is also observed that OL promote an increase in axonal diameter once myelination is initiated (Colello et al., 1994). This evidence shows that the relationship between axons and OL is bidirectional, complex and that there is still much to learn about OL differentiation and axonal myelination.

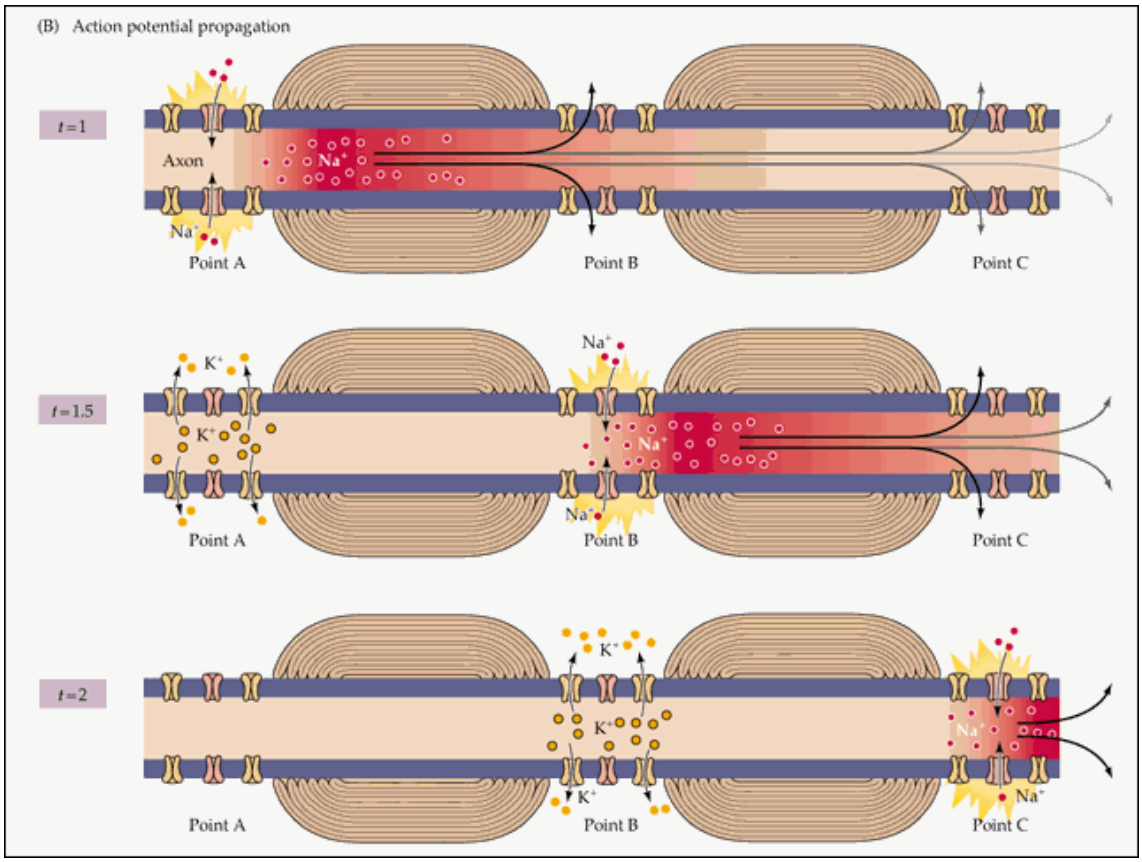

Figure 6 **Saltatory conduction in nerve fibers.** When a nervous impulse reaches a node of Ranvier, voltage-gated sodium (Na^+) channels open and Na^+ ions enter the cell, depolarizing the membrane and pushing pre-existing ions inside the cell forward. Then, voltage-gated potassium (K+) channels open, allowing K+ ions to leave the cell, repolarizing the membrane. When the flow of ions reaches the next node of Ranvier, voltage-gated Na+ ions open and the impulse is propagated. Adapted from mikeclaffey.com

Besides the nodes of Ranvier, there are other important regions in axon-OL interaction such as the paranodes (Bhat et al., 2001) – promote adhesion between the axon and myelin sheath, and limit ion diffusion between the node of Ranvier and the internode – and the juxtaparanodes (Poliak et al., 2003) – regions enriched in voltage-gated potassium (K^+) channels, necessary for membrane repolarization **(Figure 7)** (Buttermore et al., 2013) .

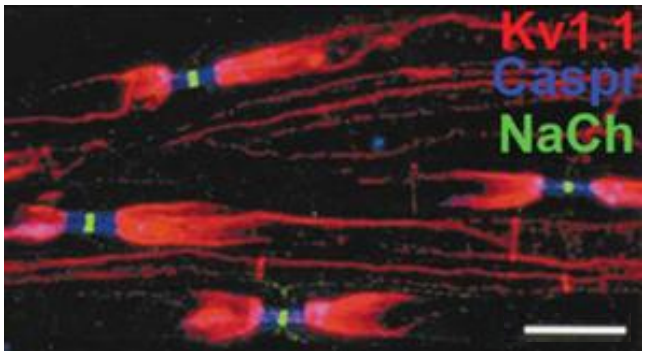

Figure 7 **Structure of the nodal, paranodal and juxtaparanodal regions of axons.** Sciatic nerve of a wild-type mouse stained for sodium channels, located at the node of Ranvier in green, Caspr adhesion molecule, located at the paranode in blue and potassium channels located at the juxtaparanode in red. Adapted from Buttermore *et al.* (2013).

Myelin’s main components (70-85% dry weight) are membrane lipids such as cerebroside (also known as galactosylceramide), cholesterol and phospholipids like ethanolamine-containing plasmalogen (Quarles and Morell, 1999). Proteins such as myelin basic protein (MBP), proteolipid protein (PLP), myelin-associated glicoprotein (MAG), myelin-oligodendrocyte glycoprotein (MOG) and myelin-associated oligodendrocytic basic protein (MOBP) are essential for the formation and maintenance of myelin membranes and their dysregulation can lead to pathologies **(Figure 8)**.

MBP is a positively charged (basic) protein essential for the compaction of myelin membranes. Knocking out MBP leads to poorly compacted myelin sheaths, hypomyelination and a phenotype characterized by tremors and early death (*shiverer* mouse) (Readhead and Hood, 1990). When injected into an animal, MBP can trigger an autoimmune response mediated by T lymphocytes that induces experimental allergic encephalomyelitis (EAE), a model of multiple sclerosis (Constantinescu et al., 2011). MBP messenger RNA (mRNA) is transcribed early during OPC/OL differentiation but is kept silent through interaction with heterogeneous nuclear ribonucleoproteins (hnRNPs, RNA-binding proteins). Then, it is transported along microtubules to the extremities of OL processes until a signal is received to begin translation (Hoek et al., 1998; Laursen et al., 2011). MBP interacts with membrane lipid $PI(4,5)P_2$ (Nawaz et al., 2009). This interaction with negatively-charged membrane causes MBP to self-assemble into a cytoplasmic lattice, which acts as a sieve, allowing

small molecules to pass through its pores while keeping other larger proteins (like MAG) out of compact myelin (Aggarwal et al., 2013). The formation of a mesh-like structure brings the two cytoplasmic membranes closer, zippering and compacting the myelin membrane (Bakhti et al., 2014).

PLP, as the name indicates, is made of a protein backbone linked to fatty-acids palmitate, oleate and stearate (Bizzozero et al., 1986). PLP knockdown has a mild phenotype, whereas gene duplication and point mutations cause ultrastructural abnormalities of myelin (due to loss of structural support), oligodendrocyte death (caused by disrupted protein trafficking) and axonal pathology (due to alterations in gene dosage) (Yool et al., 2000).

MAG is a member of the immunoglobulin superfamily (Arquint et al., 1987). It is present at the periaxonal oligodendrocyte membrane where it mediates and maintains contact between the two cells (Sternberger et al., 1979). Given its binding affinity to sialic acid, MAG is regarded as an adhesion molecule and may be responsible for cell-cell interactions necessary for myelin sheath formation and maintenance (Kelm et al., 1994).

MOG is also a member of the immunoglobulin superfamily (Gardinier et al., 1992) and is localized on the surface of myelin sheaths and oligodendrocytes (Quarles, 2002). Along with MBP, PLP and MAG it is a target antigen of T lymphocytes in MS patients (de Rosbo et al., 1993). MOBP is a small basic protein found in compact CNS myelin (Yamamoto et al., 1994). MOBP-deficient mice generate normal myelin and do not appear to have any significant phenotype (Yool et al., 2002).

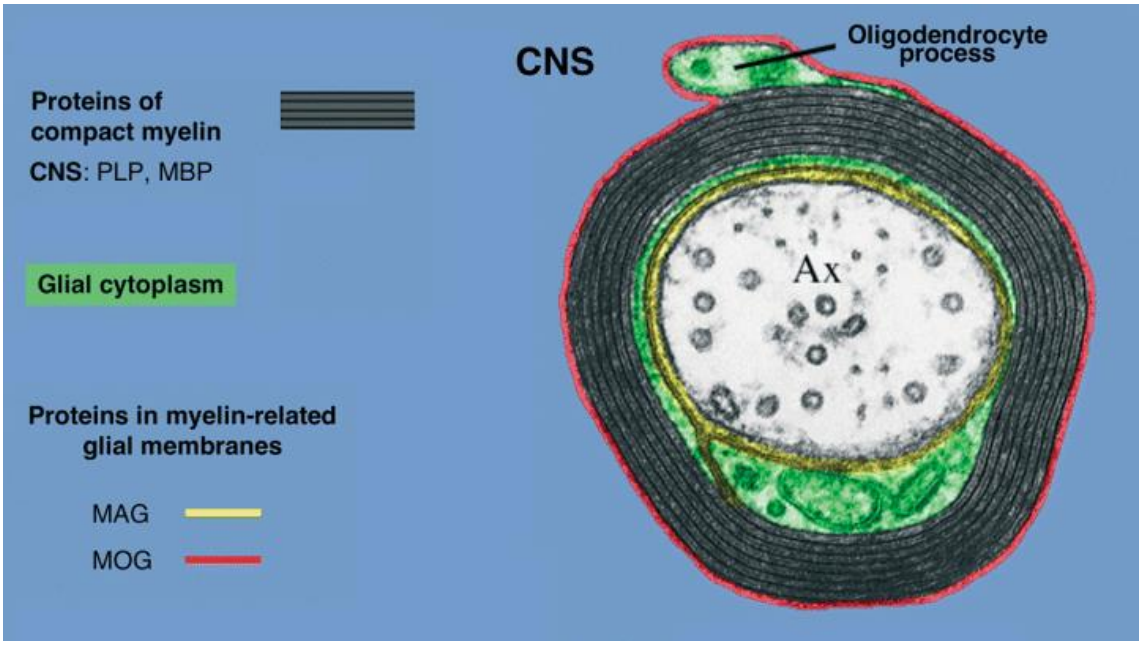

Figure 8 Localization of myelin proteins in the CNS. MBP and PLP are present in compact myelin; MAG is on the axon-glia contact surface and MOG on the outer myelin/OL surface. Adapted from Quarles (2002)

Even though OL have a low turnover rate (0.3% per year) (Yeung et al., 2014), increasing evidence shows that myelin is produced and remodeled throughout life, not just during childhood and adolescence. Additionally, this remodeling seems to be activity dependent. One example is the comparison between professional pianists and same-age control individuals, where it was discovered that pianists had increased white matter in brain regions related to learning, hand coordination and visual and auditory processing (Bengtsson et al., 2005). Learning a new motor skill is also dependent on active myelination and on the adult pool of OPC (8-9% in white matter, 2-3% in grey matter (Dawson et al., 2003)). Inhibiting the formation of new OL, without compromising pre-existing OL and myelin, prevented mice from learning how to run on a complex wheel (McKenzie et al., 2014), which suggests that the formation of new OL during adult life is another important mechanism for neuroplasticity. Adult OPC exist throughout the CNS, namely in the optic nerve (Shi et al., 1998), motor cortex, corpus callosum (Clarke et al., 2012) and cerebellum (Levine et al., 1993). They have characteristics of stem cells such as self-renewal, production of differentiated progeny, multipotency and mitotic quiescence (Alberts et al., 2002b). This means that adult OPC proliferate at a slow rate but are able to become activated in response to stress or injury, giving rise to mature OL and other cell types like astrocytes (Raff et al., 1983) and Schwann cells (Zawadzka et al., 2010).

1.2. The oligodendrocyte (OL) cytoskeleton

In order to exert their functions as myelinating cells, OL need to undergo cytoskeletal rearrangements during the processes of differentiation and myelination. The following section addresses the composition of OL cytoskeleton and the signaling pathways involved in regulating process extension and branching, necessary for morphological differentiation of OL.

1.2.1. Tubulin and Actin

Tubulin is a family of globular proteins involved in the formation of the cytoskeleton. In eukaryotes, α- and β-tubulin form heterodimers that constitute microtubules, whereas γ-tubulin is a component of the microtubule organizing center located at the centrosome (Zheng et al., 1995).

Microtubules are dynamic filamentous structures. They have a fast-growing end (deemed plus (+) end, β subunit is exposed) and a slow-growing end (minus (-) end, α subunit is exposed), where α/β tubulin dimers can be added. The flexural rigidity of microtubules and their high persistence length make them resistant to deformation and, therefore, they are important for maintaining cellular shape (Gittes et al., 1993). Motor proteins like dyneins and kinesins travel along microtubules, carrying molecular cargos from one cellular location to another (Hirokawa et al., 1998).

Actin is a globular protein (G-actin), involved in the formation of microfilaments (F-actin). In most cell types, microfilaments form intracellular networks necessary for maintaining cell shape, extending protrusions and migration (Fukui, 1993). Actin microfilaments give rise to stress fibers (contractile bundles of microfilaments) (Kreis and Birchmeier, 1980), filopodia (spikes at the front of a migrating cell) (Mattila and Lappalainen, 2008) and lamellipodia (flat cytoplasmic extensions necessary for motility) (Small et al., 2002).

In oligodendrocytes, actin microfilaments can be found throughout the cell but are enriched at the tips of extending processes and in branching sites, especially in younger OL relatively to mature ones (Song et al., 2001). Microtubules also exist in the cell body and processes, but they do not reach the leading edge of extending processes **(Figure 9)**.

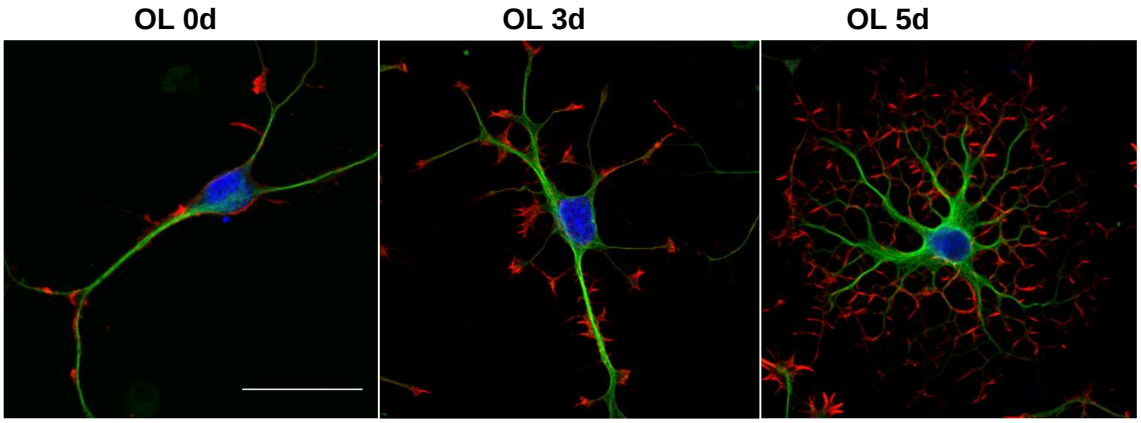

Figure 9 **Oligodendrocyte cytoskeleton.** α-tubulin (green) and actin (red) cytoskeleton during *in vitro* OL differentiation (DAPI in blue). Scale bar: 30μm.

It has been concluded that actin microfilaments open the way for microtubules to later invade and stabilize newly formed processes. The same was observed for the formation of connections between processes during OL maturation – at first these connections are established by actin microfilaments and later filled by microtubules. Another characteristic of OL cytoskeleton is that microtubules in the cell body and in primary processes are rich in acetylated tubulin, which is associated with more stable microtubules, while microtubules invading leading edges are enriched in more dynamic tyrosinated tubulin (Song et al., 2001).

In oligodendrocytes, cytoskeleton dynamics is regulated by various signaling pathways, of which β1-integrin, Rho GTPases and mitogen-activated protein kinases (MAPKs) will be addressed in this thesis.

1.2.2. β1-Integrin signaling

Integrins are transmembranar proteins that act as adhesion molecules and receptors for extracellular matrix (ECM)-based stimuli (Alberts et al., 2002a).

An integrin receptor is composed of two transmembranar subunits called α and β, for which there are many isoforms. Different combinations of α and β subunits interact with different ECM components and trigger specific signaling pathways. For example, α6β1 integrin interacts with ECM laminin whereas α5β1 integrin interacts with fibronectin.

The cytoplasmic tail of β subunits interacts with the cytoskeleton through anchor proteins like talin, α-actinin, filamin and vinculin, which in turn interact with actin microfilaments **(Figure 10)**. This interaction can lead to the formation of focal adhesions – macromolecular complexes associated with clusters of integrins that increase the strength of cell-ECM adhesion. Integrins can activate signaling pathways within the cell by recruiting focal adhesion kinase (FAK) and integrin-linked kinase (ILK)

(Legate et al., 2006), which will then recruit and activate other proteins such as members of the Src family, PI3K/Akt and MAPK (Alberts et al., 2002a).

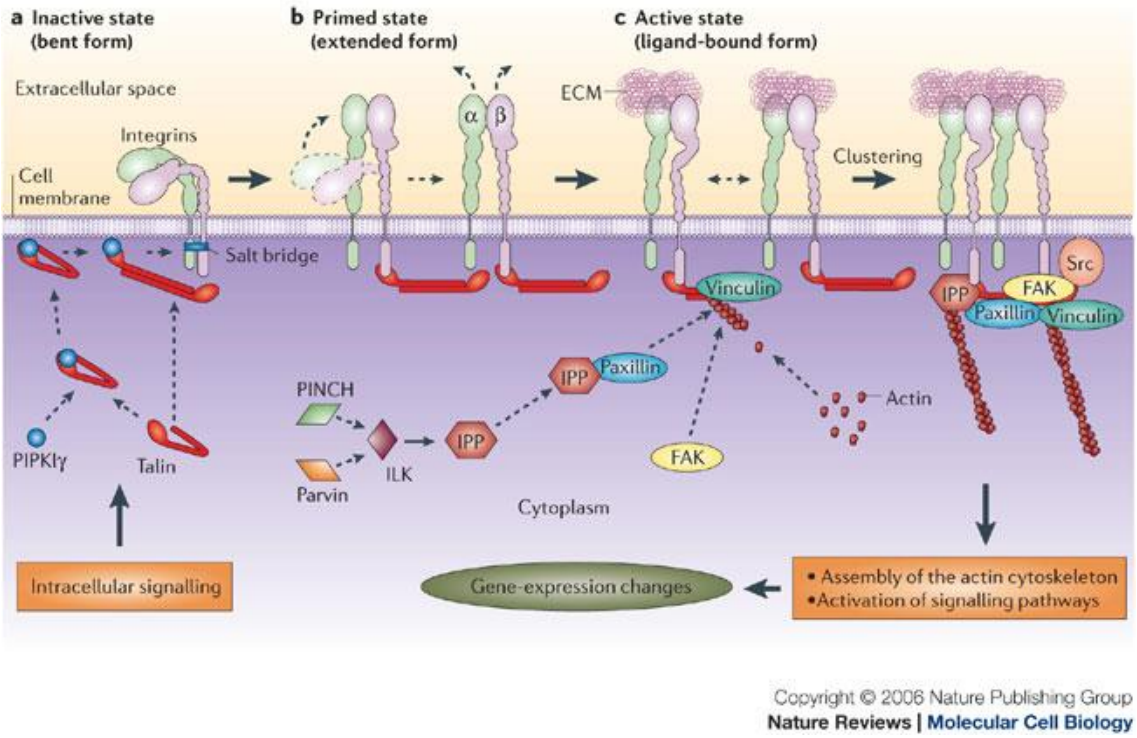

Figure 10 Integrin activation and interaction with actin cytoskeleton. Both intracellular and extracellular stimuli can trigger integrin signaling. Integrin interaction with anchor proteins (talin and vinculin), IPP complex (ILK, Parvin and PINCH) and Src Kinases is necessary for actin cytoskeleton remodeling. Adapted from Legate *et al.* (2006).

In OL, integrin expression is temporally coordinated: the first to be expressed, αvβ1, contributes to cellular migration during OPC stage. Over-expression of αvβ3 stimulates cell proliferation and inhibits differentiation, while antibody blockage of αvβ5 inhibits process extension (Blaschuk et al., 2000; Milner and ffrench-Constant, 1994). Finally, α6β1 is essential for myelination through interaction with laminin-2 (Buttery and ffrench-Constant, 1999). *In vitro*, laminin-2-coated surfaces stimulate the formation of flat myelin membranes spreading across the plate and, *in vivo*, laminin-2 at the axonal surface induces OL process wrapping (Buttery and ffrench-Constant, 1999; Colognato et al., 2002).

In OPC stage, Src family kinase Lyn is associated with the αvβ3 integrin-PDGFαR complex, activating signaling pathways that promote proliferation **(Figure 11, 1)**. However, once axonal contact is established, interaction of α6β1 integrin with laminin-2 induces dissociation of Lyn and activation of Src family kinase Fyn. Fyn-α6β1 complexes can interact with PDGFαR or ErBb2/4 receptors and promote OL survival, differentiation and myelin formation **(Figure 11, 2)** (Colognato et al., 2004). Additionally, laminin-2-deficient mice present an accumulation of cells in OPC stage,

accompanied by an increase of Fyn inhibitory proteins (like Csk shown in figure 11) and increased phosphorylation of Fyn at an inhibitory site (Relucio et al., 2009).

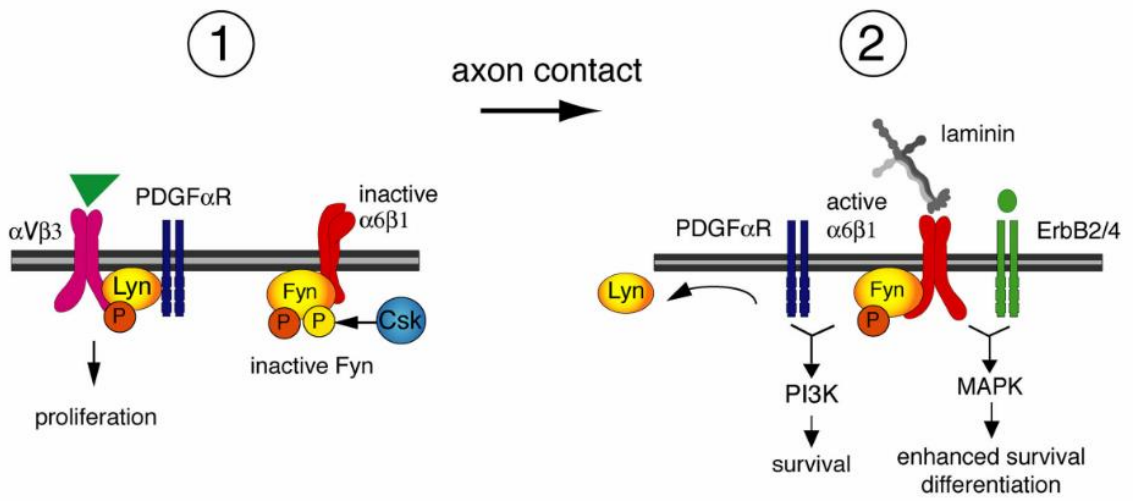

Figure 11 Switch between proliferation and differentiation in OL is mediated by integrin signaling. Axonal contact induces down-regulation of Lyn kinase interaction with αvβ3 and up-regulation of Fyn kinase interaction with α6β1 Adapted from Colognato *et al.* (2004).

A dominant negative (DN) chimera of β1 integrin, comprised of the extracellular and transmembranar domains of the interleukin-2 receptor and the cytoplasmic tail of β1 integrin (delivered to OL via retroviral infection), reduces the formation of myelin membranes on laminin-2 substrates, but does not interfere with MBP expression timing nor with the percentage of MBP^+ cells in culture (Relvas et al., 2001). This suggests that β1 integrin signaling is necessary for myelination but not for cell survival.

A conditional knockout experiment in which β1 integrin was excised from OL genome (Cre recombinase expressed under 2',3'-Cyclic-nucleotide 3'-phosphodiesterase (CNPase) promoter) gave conflicting results (Benninger et al., 2006). In these conditions, myelination appeared to be normal in the optic nerve, spinal cord and corpus callosum, at 2 and 3 months of age. In addition, re-myelination at 5 weeks after lysolecithin-induced spinal cord injury was not impaired in the absence of β1 integrin. However, it was observed that premyelinating OL in the cerebellar periphery were undergoing increased apoptosis at P5, relative to control animals. Despite this, myelination was unaffected in this region at 2 months of age. This conflict may be due to the fact that CNPase is expressed in premyelinating OL (Pfeiffer et al., 1993), leading to an early deletion of β1 integrin and possibly allowing a compensation by other integrins.

A different DN approach in which mice expressed a β1 integrin lacking the C-terminal cytoplasmic tail (β1ΔC) in oligodendrocytes (under PLP promoter) (Lee et al., 2006) showed region-specific hypomyelination in optic nerve and spinal cord but an absence

of myelination abnormalities in the corpus callosum. The construct used would bind laminin and compete with other receptors on OL surface but would be unable to trigger a signaling cascade.

To try and reconcile these conflicting results regarding β1 integrin function, a third DN study was made (Câmara et al., 2009). Here, the construct used only had the intracellular domain of β1 integrin. It would not be able to bind its ligand, and consequently no signaling would occur. In addition, the authors expressed this construct under MBP promoter, thus evaluating only the role of β1 integrin during active myelination. In these conditions, it was observed that OL were less efficient in myelinating small-caliber axons than wild type or OL over expressing dominant-negative β3 integrin. However, the thickness and length of myelinated axon tracts was normal. Therefore, it was suggested that inhibition of β1 integrin signaling impaired initiation but not completion of myelination. This is consistent with the observations made by Colognato *et al.* (Colognato et al., 2002; Colognato et al., 2004).

Also consistent with these results, conditional ablation of β1 integrin in the CNS (Cre recombinase expressed under nestin promoter) and in OL solely (Cre recombinase expressed under NG2 promoter) leads to a reduction in myelin sheath thickness in the spinal cord, optic nerves and cerebellum **(Figure 12)** (Barros et al., 2009). This phenotype is not due to defects in oligodendrocyte differentiation or survival. When these mutant OL are cultured on laminin-2-coated plates and treated with neuregulin-1 (activator of Akt), Akt is not significantly activated, suggesting β1 integrin is an upstream activator of the Akt pathway.

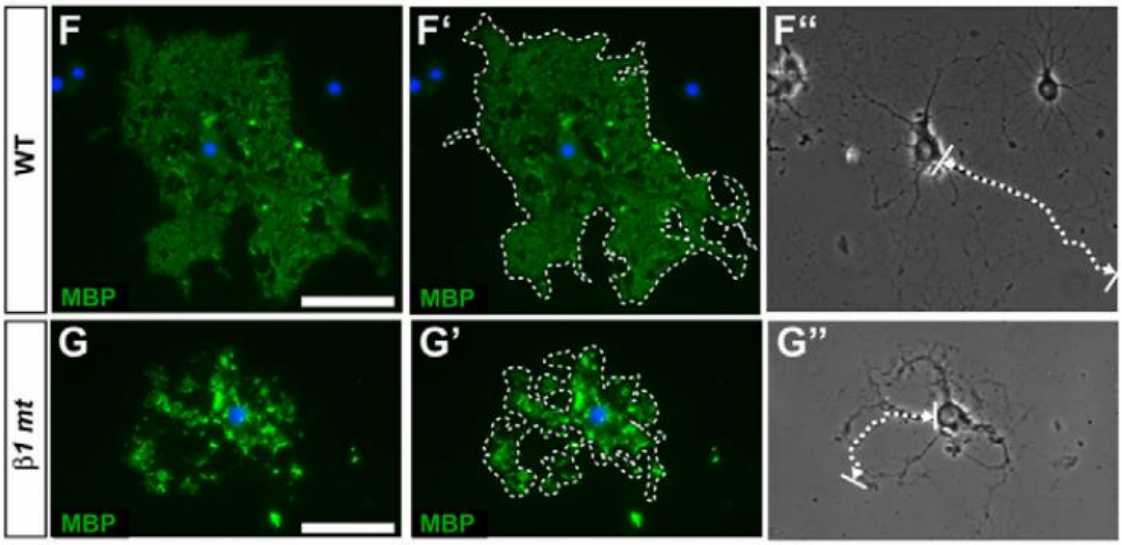

Figure 12 **OL lacking β1 integrin produce smaller myelin sheets.** Morphometric analysis of wild-type (F-F'') and nestinCre-Itgb1-flox (G-G'') oligodendrocytes showing a smaller area of MBP staining and a shorter process length for the knockout. Adapted from Barros *et al.* (2009).

Over-expression of constitutively active Akt in OPC and OL (under PLP promoter) does not alter the number of oligodendrocytes produced, but causes a dramatic increase in the amount of myelin produced and sustains active myelination in the adult mouse (Flores et al., 2008). In β1 integrin-deficient OL, over-expression of constitutively active Akt is able to rescue the defect in myelin sheet outgrowth (Barros et al., 2009).
It can be concluded from these studies that β1 integrin is important for different signaling pathways, which need to be temporally coordinated to ensure appropriate OL maturation.

1.2.3. Rho GTPases

Other downstream effectors of β1 integrins are Rho GTPases: a family of small GTP-hydrolyzing proteins that act as molecular switches: when bound to GTP they become active (“on” state) and, after hydrolysis of GTP to GDP, they become inactive (“off” state). Guanine nucleotide exchange factors (GEFs) stimulate exchange of GDP for GTP to generate the active form and GTPase-activating proteins (GAPs) enhance the intrinsic GTPase activity to inactivate the switch (Alberts et al., 2002d). There are several members in this family, of which RhoA, Cdc42 and Rac1 are the most studied Rho GTPases in mammals. Their function is closely related to actin cytoskeleton rearrangements: in fibroblasts, activation of RhoA promotes stress fiber formation (Ridley and Hall, 1992), activation of Cdc42 induces filopodia (Nobes and Hall, 1995) and activation of Rac1 induces lamellipodia (Ridley et al., 1992).
During oligodendrocyte differentiation, total levels of RhoA are reduced two- to threefold and levels of active (GTP-bound) RhoA are reduced four- to fivefold (Liang et al., 2004). Oppositely, both the expression levels and activity of Rac1 and Cdc42 increase more than twofold throughout differentiation. Consistent with this regulation, over-expression of constitutively active (CA) RhoA inhibited OL process extension and ramification whereas over-expression of a dominant-negative (DN) form promoted it. Again, the opposite was observed when over-expressing CA and DN Rac1 and Cdc42 **(Figure 13)**.

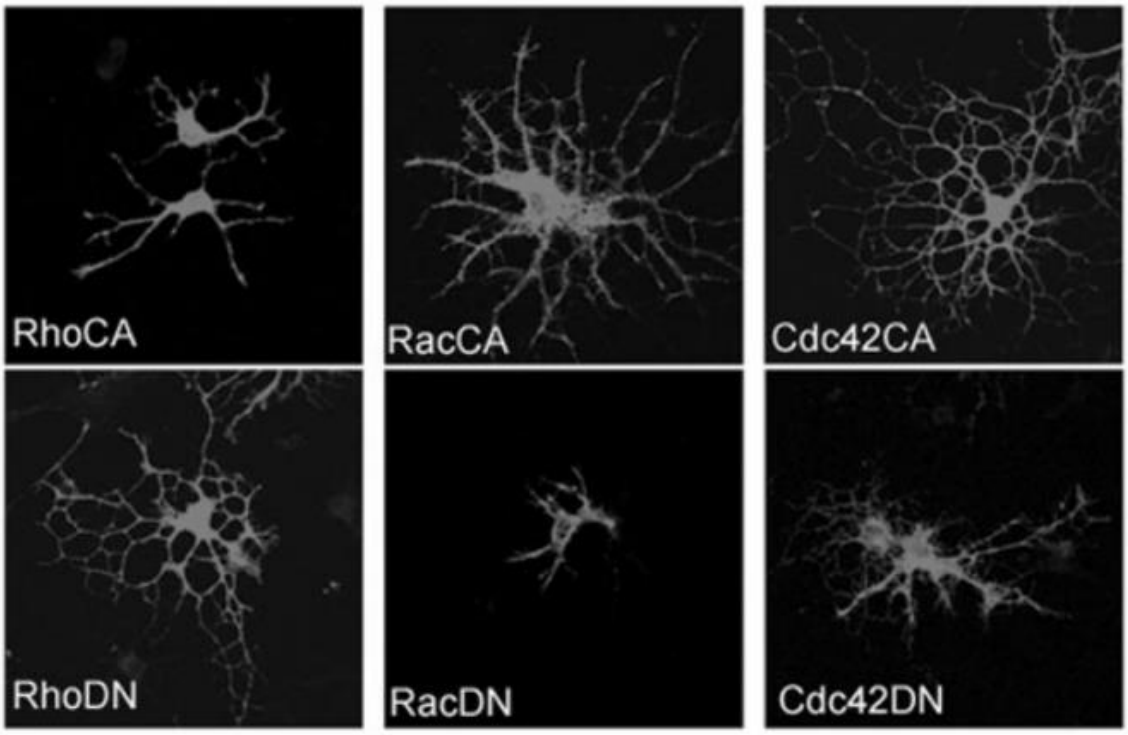

Figure 13 Over-expression of constitutively active (CA) and dominant-negative (DN) forms of Rho, Rac and Cdc42 GTPases. Opposite roles of Rho and Rac/Cdc42 can be observed by the different morphology attained by OL. Adapted from Liang *et al.* (2004).

This switch of Rho GTPases is made by integrin-Fyn signaling: upon Fyn activation, p190RhoGAP is phosphorylated and activated, inducing RhoA to “switch off” by hydrolyzing GTP to GDP. Simultaneously, Fyn activates FAK and leads to activation of Rac1 and Cdc42 (Hoshina et al., 2007; Liang et al., 2004; Wolf et al., 2001).

In vivo, conditional ablation of Cdc42 in OL (Cre recombinase expressed under CNP promoter) yielded conflicting results: it led to formation of aberrant myelin outfoldings in the spinal cord, optic nerve and corpus callosum (indicative of an important role in proper ensheathment and myelination of axons) but had no effect in OPC proliferation, directed migration or morphological differentiation (Thurnherr et al., 2006). The same method was used to knockout Rac1. Like Cdc42 mutants, Rac1 mutants presented myelin outfoldings. Then, it was hypothesized that these two Rho GTPases could have synergistic effects in regulating myelination. Therefore, double knockouts with different gene-dosage were created (single heterozygous, double heterozygous, single homozygous, double homozygous and Rac1 homozygous/Cdc42 heterozygous). It was found that single Cdc42 homozygous mice had more myelin outfoldings than single Rac1 homozygous mice, Rac1 homozygous/Cdc42 heterozygous had more myelin outfoldings than single Rac1 homozygous and that double homozygous had the greatest amount of outfoldings of all. These results suggest that Rac1 and Cdc42 cooperate but are not interchangeable in regulating myelination.

The conflicting results observed for Cdc42 are due to the nature of the methods used. Dominant negative mutants of Rho GTPases bind their corresponding GEFs with higher affinity than endogenous Rho GTPases, sequestering them. However, they do not interact with their downstream targets, making this an unspecific way to “turn off” just one Rho GTPase. There may be some contribution of other Rho GTPases to the observed phenotype. In the conditional knockout, only one gene is excised from the genome, thanks to the loxP sites that flank its sequence. In this situation, one can assume with greater certainty that the observed phenotype is related to the genetic alteration made.

Another mediator of integrin-Rho GTPase signal transduction is integrin-linked kinase (ILK). ILK is an important component of the macromolecular complex formed at focal adhesion sites, which connects extracellular signals to the cytoskeleton and other downstream effectors (Brakebusch and Fässler, 2003). Conditional knockdown of ILK specifically in OL leads to a delay in both the production of molecular markers of maturation (such as myelin-associated glycoprotein, MAG) and in process extension, which is accompanied by an increase in active RhoA. This phenotype is partially recovered by inhibition of ROCK, an effector kinase of RhoA (O'Meara et al., 2013).

In summary, RhoA inhibits OL process extension, branching and myelination, whereas Cdc42 and Rac1 are necessary to ensure proper formation of myelin layers during OL wrapping of axons.

1.2.4. Mitogen-activated protein kinases (MAPK) – JNK pathway

Many stimuli received by cells are relayed by a cascade of kinases called the mitogen-activated protein kinase (MAPK) pathway. In this pathway, MAPKs like c-Jun NH_2-terminal kinase (JNK), ERK and p38 are activated by MAPK kinases (MAPKK or MKK) and these, in their turn, are activated by MAPKK kinases (MAPKKK) (Schaeffer and Weber, 1999). MAPKs have an activation domain called T-loop that consists of threonine-X-tyrosine tripeptide, where X can be any amino acid. The threonine (Thr) and tyrosine (Tyr) residues must be phosphorylated by MAPKKs for MAPKs to be fully activated. MAPK activity is regulated by several proteins including dual-specificity phosphatases (DSPs or Dusps), which are able to dephosphorylate both threonine and tyrosine residues (Camps et al., 2000).

JNKs are coded by three genes, Jnk1, Jnk2 and Jnk3, which can be alternatively spliced and originate 10 JNK isoforms (Gupta et al., 1996). In JNK, the T-loop has a phosphorylation motif Threonine-Proline-Tyrosine and it is phosphorylated by MKK4

and MKK7 (preferentially on Tyr and Thr, respectively) (Lawler et al., 1998) **(Figure 14)**.

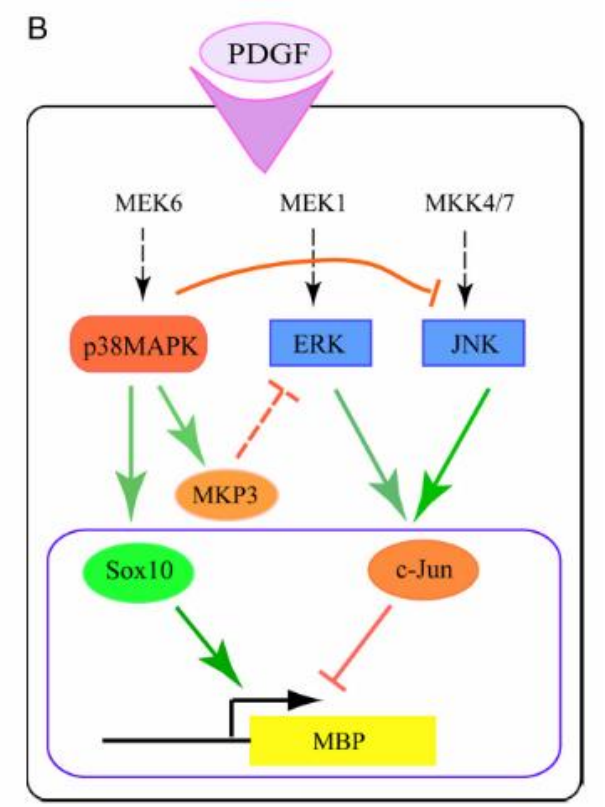

Figure 14 **The MAPK/JNK pathway in oligodendrocytes.** Mitogens like PDGF activate the MAPK signaling cascade. Both positive and negative regulators of myelin gene expression are activated: p38MAPK stimulates MBP transcription through activation of Sox10 and inhibition of ERK and JNK. ERK and JNK repress MBP transcription through c-Jun. Adapted from Chew *et al.* (2010).

Inhibition of JNK phosphorylation prevents OPC proliferation induced by B104 neuroblastoma cells-conditioned medium *in vitro* (Zhang et al., 2014a). c-Jun, a target and effector of JNK, suppresses transcription of the MBP gene. However, in Schwann cells (the myelinating cells of the peripheral nervous system), this seems to be dependent on c-Jun protein levels and not its activation (Parkinson et al., 2008). In any case, JNK can regulate the levels of c-Jun as well as its activation (Besirli et al., 2005), so repressing the JNK pathway could increase MBP production. A dominant-negative form of c-Jun effectively recovers some MBP production after Mitogen/Extracellular signal-regulated kinase (MEK)-induced repression of myelin promoter activity, suggesting that MEK acts on MBP through c-Jun (Chew et al., 2010).

Inhibition of JNK also leads to a decrease in microtubule-associated protein 1B (MAP1B) phosphorylation in *in vitro* cultured cortical neurons (Kawauchi et al., 2005). MAP1B is a phosphoprotein that interacts with microtubules to regulate their dynamics and enable microtubule bundling and elongation. MAP1B can be phosphorylated in two

modes: mode I makes microtubules more dynamic and can be found in growth cones(Goold et al., 1999), whereas mode II leads to the stabilization of microtubules and can be found in the proximal regions of growing neurites (Ulloa et al., 1994). In neurons, MKK7 mRNA is found at the growth cone of neurites where it can be locally translated and activate the JNK pathway (Feltrin et al., 2012). This finding is accompanied by a high level of phospho-MKK7, phospho-JNK and phospho-MAP1B at the neurites. Knockdown of MKK7 leads to an inability to form microtubule bundles in neurites. These findings identify this pathway to be important for axonal outgrowth.

In oligodendrocytes, MAP1B is expressed during development and precedes the formation of flat myelin membranes *in vitro* (Vouyioukiis and Brophy, 1993). MAP1B phosphorylation by JNK is a separate pathway from the one that activates c-Jun. It is possible that coordinated activation of c-Jun and MAP1B leads to process outgrowth and suppression of MBP translation in earlier stages of OL development.

1.3. Local mRNA translation in OL

Proteins are the building blocks of cells. Whether they are structural or catalytic, they are essential for cellular homeostasis and to respond to environmental cues. In all types of cells, but especially in highly polarized cells like neurons and oligodendrocytes, proteins or their precursor mRNAs must be transported to the location where they will exert their functions, such as cytoplasmic extensions (Holt and Schuman, 2013).

mRNAs are produced from the splicing of nuclear pre-mRNAs (Alberts et al., 2002c). They are then exported to the cytoplasm where they can either be immediately translated into proteins, by interaction with ribosomes, or packaged into ribonucleoprotein particles (RNPs) along with specialized RNA-binding proteins (RBPs) (Anderson and Kedersha, 2009). These RNPs form granules that are transported along microtubules until they reach their final destination. There, RNPs are disassembled and mRNAs are translated into proteins.

The information needed to indicate an mRNA’s destination is contained in its 5’ or 3’ untranslated regions (UTRs): non-coding regulatory regions immediately before the coding sequence (5’UTR) or between the stop codon and the polyA tail (3’UTR) (Wilkie et al., 2003). These sequences must be recognized and bound by RBPs, which keep mRNAs protected from translation and degradation as well as mediate interactions with molecular motors that transport RNPs (Mangus et al., 2003). The regulatory RNA sequences contained in the UTRs can be considered *cis*-acting factors of RNA transport and translation, whereas the proteins that bind them can be considered *trans*-acting factors (Shahbabian and Chartrand, 2012). Different combinations of RBPs and their relative ratios are important for appropriate targeting and timely unfolding of RNPs (Skabkin et al., 2004). This may be a way for cells to coordinate gene expression in a cost-effective manner (Keene and Tenenbaum, 2002): all the machinery needed for protein synthesis is placed at the site where it will be used, waiting for the appropriate signal to begin translation (Willis et al., 2007).

In OL, MBP is the archetype of a locally synthesized protein (Müller et al., 2013) **(Figure 15)**. After transcription and splicing, MBP mRNA is packaged into RNPs containing a large number of regulatory and transport proteins, making up RNA granules. Proteins such as heterogeneous nuclear ribonucleoproteins (hnRNPs) are involved in stabilizing the mRNA, keeping it silenced until it reaches its final destination. MBP mRNA contains an A2 responsive element (A2RE) in its 3’UTR, which binds to hnRNP A2. This protein seems to have a structural role in assembling RNA granules (Han et al., 2010). hnRNP A2 also associates with hnRNP E1 and K (Kosturko et al.,

2006; Laursen et al., 2011): hnRNP E1 is responsible for maintaining the mRNA silenced during transport and hnRNKP K is necessary for the transport of MBP mRNA along processes. Knocking-down hnRNP K leads to an accumulation of MBP mRNA at branching points in OL processes (Laursen et al., 2011). De-repression of MBP mRNA translation seems to be triggered by integrin binding to axonal laminin and activation of Fyn kinase. During OL differentiation, hnRNP K associates with transmembranar α6β1 integrin (Laursen et al., 2011), becomes phosphorylated and releases the mRNA to allow translation to occur. Also, Fyn appears to phosphorylate hnRNP A2, stimulating the translation of MBP mRNA (White et al., 2008).

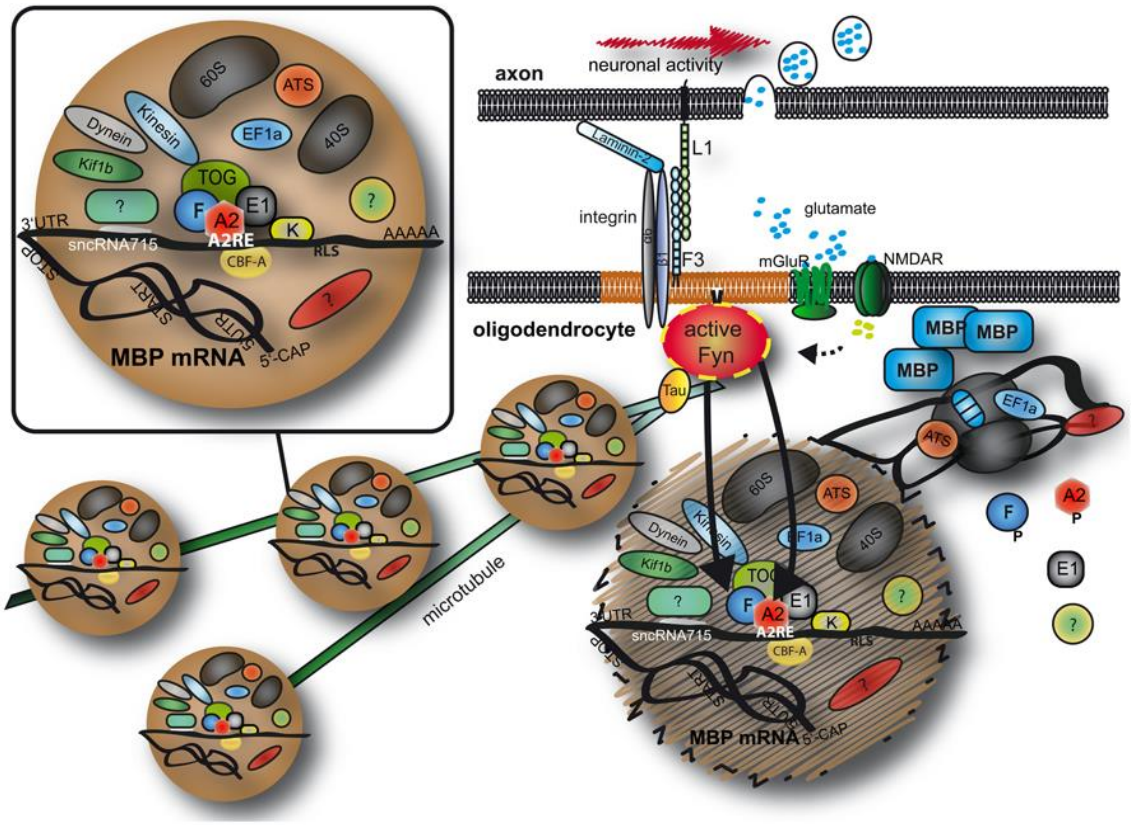

Figure 15 Transport and local translation of MBP mRNA. MBP mRNA is packaged into RNA granules with RNA binding proteins, motor proteins and parts of the protein synthesis machinery. Then it is transported along microtubules towards the OL plasma membrane where Fyn kinase receives axonal signals to locally induce MBP translation. MBP, myelin basic protein; A2, F, E1, K, heterogeneous nuclear ribonucleoproteins A2, F, E1, and K; CBF-A, CArG-box binding factor A; TOG, tumor over expressed gene; mGluR, metabolic glutamate receptor; NMDAR, NMDA receptor; EF1a, elongation factor 1a; ATS, arginyl-tRNA synthetase; 60S/40S, large/small ribosomal subunit; 5’-CAP , 5’ 7-methylguanylate CAP; UTR, untranslated region; AAAAA, Poly A tail. Adapted from Müller *et al.* (2013).

The spatial and temporal coordination of the production of myelin components is essential for proper myelination of axons. Defects in this process lead to hypomyelination or abnormal myelin sheaths (Song et al., 2003), which can cause motor impairments, as in the taiep (tremor, ataxia, immobility, epilepsy and paralysis) rat mutant (Holmgren et al., 1989).

1.4. Transcriptomics of CNS resident cells

Transcriptomics is the study of cellular mRNA composition (Brent, 2000). It differs from genomics, which aims to identify the genetic composition of an organism, and proteomics, which looks at cellular protein composition. Like the proteome, the transcriptome varies among cell types, changes during the differentiation process and can be altered according to changes in environmental context. However, changes in transcription can be found prior to changes in protein synthesis. It is therefore important to identify which mRNAs are more highly expressed in a given cell type in order to understand their function, distinguish subpopulations and anticipate developmental or pathological behavior.

Several studies have compared the transcriptome of the different CNS resident cells: neurons, astrocytes, oligodendrocytes, microglia and vascular endothelium. These have allowed the identification of novel specific markers to distinguish cell types, as well as the demotion of others, found to be less specific than previously thought (Cahoy et al., 2008). These studies also allowed the identification of cell type-specific or enriched transcription factors and post-transcriptional regulators, such as RBPs, that may help us understand how different cell types express their specific differentiation programs. Transcriptomics also allows the identification of similarities between cell types. For example, pathways involved in axonal guiding, integrin signaling, ERK/MAPK, stress-activated protein kinase (SAPK)/JNK and actin cytoskeleton signaling are commonly enriched in astrocytes, neurons and OL. Not surprisingly, this suggests conserved mechanisms for process extension in all three cell types (Cahoy et al., 2008).

In the particular case of OL, transcriptomic studies have allowed the identification of distinct phases of cell differentiation (Dugas et al., 2006). In each of these phases, a specific pool of myelin genes and transcription factors is expressed, with tight temporal regulation. In OPC stage, most up-regulated genes are related to cell cycle progression, DNA synthesis and cytoskeleton. This is to be expected because OPC are highly proliferative and migratory cells. As OL mature, these proliferation-related genes are down regulated and a different set of genes becomes activated. For example, transcription factor Sox10 is up-regulated at early stages of differentiation, inducing the production of early myelin protein MBP, whereas zinc-finger protein 536 (Zfp536) (a putative transcription factor identified by the authors) is up-regulated in later stages, contributing to the production of late myelin protein MOG. Consistently, depletion of Sox10 does not alter the levels of MOG, and depletion of Zfp536 does not cause any

change in the levels of MBP. This suggests that each step of the differentiation process is independently controlled.

During OPC/OL differentiation process, simultaneously with the up-regulation of myelin genes, there is a significant down-regulation of cytoskeletal and matrix genes, as well as an up-regulation of genes related to cytoskeleton depolymerization (like gelsolin), which are important for myelin compaction (Cahoy et al., 2008; Zuchero et al., 2015). Metabolic pathways enriched in oligodendrocytes are 3-phosphoinositide biosynthesis and degradation (involved in calcium signaling) (Cahoy et al., 2008). Several derivatives of phosphatidylinositol are important for the formation of plasma membranes and for intracellular signaling. In the case of OPC, Phosphoinositol 3-kinase (PI3K) is an important mediator of proliferation, cell survival and prevention of differentiation (Ebner and Dunbar, 2000). Additionally, calcium signaling is induced by inositol 3-phosphate (IP3) upon activation of muscarinic receptors at the OPC membrane (Haak et al., 2002). This may be a mechanism by which neuron activity influences OPC migration and differentiation. In OL, phosphatidylinositol-4,5-bisphosphate ($PI(4,5)P_2$) seems to be necessary for myelin membrane formation (Zuchero et al., 2015), as mentioned in a previous section.

This identification of distinct sets of genes responsible for different steps during OL maturation could be useful to study the processes of myelination and re-myelination, and to understand why this process fails in the context of demyelinating diseases.

1.5. Demyelination and remyelination in Multiple Sclerosis (MS)

Multiple Sclerosis (MS) is an early onset inflammatory neurodegenerative disease with unknown causes (Compston and Coles, 2008; Nave, 2010). It is thought to be autoimmune in nature: myelin-specific auto-reactive T-lymphocytes and macrophages cross the blood–brain barrier and invade the brain parenchyma accompanied by an activation of resident microglia. Inflammation and immune attacks destroy oligodendrocytes and myelin sheaths originating lesions in the white matter. These are detectable by magnetic resonance imaging and turn into oedematous plaques (*sclerae*, hence the name Multiple Sclerosis) **(Figure 16)** (Intermountain Medical Imaging).

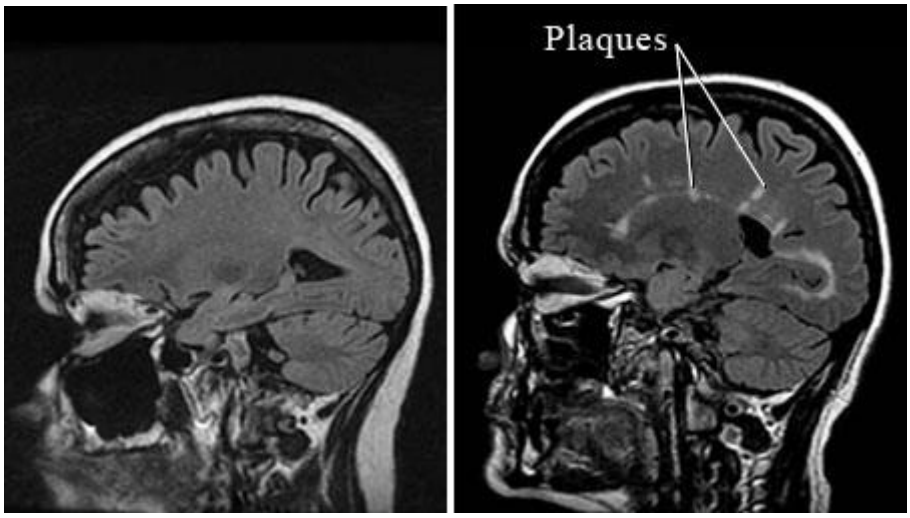

Figure 16 **MRI comparing a healthy and an MS patient’s brains.** In the picture on the right it is possible to see white plaques of demyelination which do not exist in the healthy brain (left). Adapted from www.webmd.com – Magnetic Resonance Imaging (MRI) of Multiple Sclerosis.

Most patients (80%) (Compston and Coles, 2008) suffer acute attacks, accompanied by an aggravation of symptoms (relapse) and followed by a recovery (remission), which characterizes the relapsing-remitting form of MS (RRMS). The relapse is due to the loss of myelin sheaths at internodes, which blocks impulse conduction along the axon (McDonald and Sears, 1969), and the remission can be due to the appearance of sodium channels along the demyelinated axon (England et al., 1996), remyelination by newly recruited OPC (Prineas and Connell, 1979) and resolution of inflammation (Redford et al., 1997). The disease can then evolve into a secondary progressive phase (SPMS) in which there is a decrease in axonal conduction recovery and an irreversibility of symptoms caused by axonal degeneration and inflammation (Compston and Coles, 2008). The microenvironment involving the lesion, rich in myelin debris, inflammatory cytokines and chemokines, inhibits the differentiation of adult OPC and demyelination is accentuated (Brück and Stadelmann, 2003; Kotter et al., 2006). A

minority of patients (20%) (Compston and Coles, 2008) experience a primary progressive form of MS (PPMS) which does not have acute attacks but a progressive loss of motor and cognitive abilities.

OPC and mature OL can be found around the border of active demyelinating lesions, but not in inactive, chronic lesions (Kuhlmann et al., 2008). This localization of OPC/OL is accompanied by changes in the expression of guiding molecules for OPC migration and ECM components (Gutowski et al., 1999; Sobel et al., 1995; Williams et al., 2007). These seem to promote OPC recruitment, however, their pattern of expression shifts as lesions become chronic, and OPC/OL become unable to repair lesion sites (Chang et al., 2002). There is clearly an early attempt to repair demyelinating lesions, but somehow the pro-myelinating cues are exchanged by inhibitory signals as the disease progresses (Charles et al., 2002; John et al., 2002).

All therapeutic strategies for MS that have so far been approved by the United States Food and Drug Administration are immunomodulatory (Goodin et al., 2002; NMSS). They rely on glucocorticoids, interferons (IFNβ), neutralizing antibodies against T-lymphocytes (alemtuzumab) and inhibitors of DNA synthesis (mitoxantrone and teriflunomide) to accelerate recovery and reduce the rate of attacks during the RR phase. There are no approved drugs so far that stimulate OPC proliferation and myelination. Trials are being conducted to test an anti-LINGO1 antibody (Biogen): LINGO1 is a membrane receptor expressed in neurons and OL whose inhibition leads to OL differentiation *in vitro* and *in vivo* (Mi et al., 2005), as well as remyelination in animal models (Zhang et al., 2015).

Thus, studying OPC/OL normal development can lead to the discovery of novel molecules essential for myelination and, therefore to the development of new therapies for MS.

1.6. RNA Sequencing of Oligodendrocyte soma *versus* processes

In order to develop better therapies for treating demyelinating diseases, it is fundamental to understand the mechanisms underlying OL differentiation and myelination. In our lab, we hypothesized that mRNA molecules enriched in the processes of OL could have a higher probability of being important for the regulation of OL process extension, differentiation and myelination. Therefore, the total mRNA of OPC processes and soma was sequenced and compared. To collect the two fractions of mRNA, the OPC processes were physically separated from soma using a modified Boyden chamber system with chemotactic (PDGF and netrin) and haptotactic (laminin-2) gradients (Thomsen and Nielsen, 2011) **(Figure 17)**.

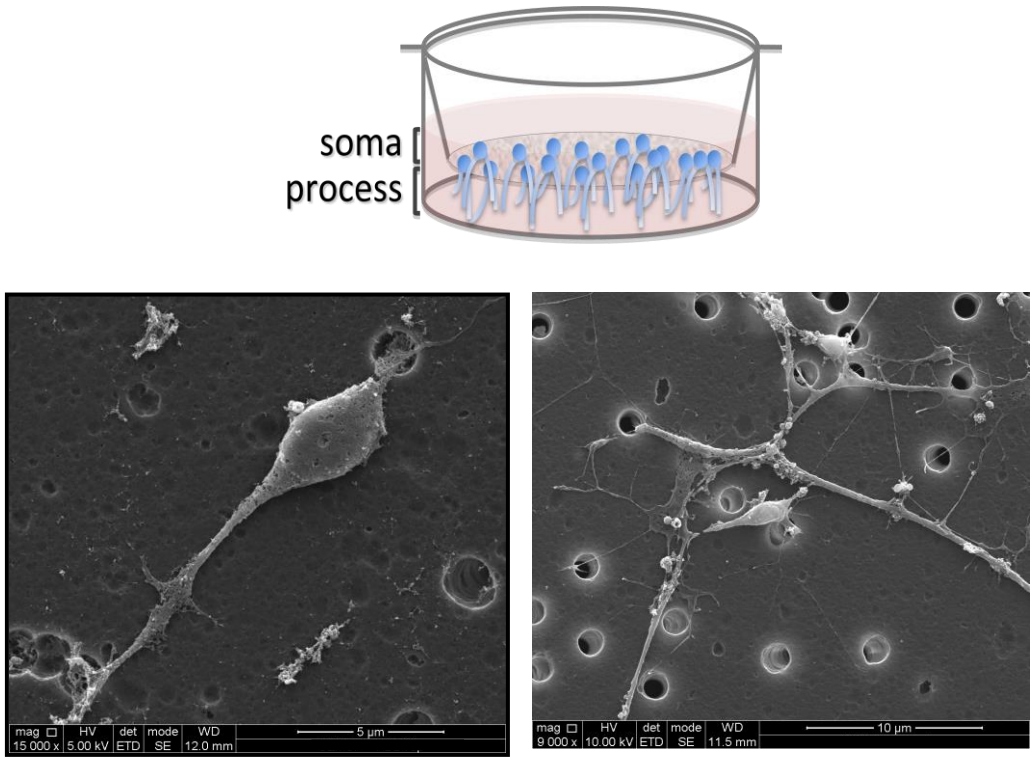

Figure 17 **Physical separation of OPC soma and processes.** Schematic representation of the modified Boyden chamber system used to separate OPC soma from processes (top). Scanning electron microscopy images of OPC cultured on Boyden chamber membranes: OPC soma on the upper side of the membrane (left) and OPC processes on the lower side of the membrane (right) (Domingues, H. S., unpublished data).

Bioinformatics analysis of the two transcriptomes showed an asymmetric distribution, with a larger number of transcripts being significantly more expressed in the OPC processes than in the soma, which was named "processsome" **(Figure 18)**. Importantly, two main categories stood out: transcripts related to cytoskeleton rearrangements and protein synthesis (Domingues, H.S, unpublished data, not shown).

This reinforced the idea that one of the main events occurring during OPC process extension is local protein translation, in particular of mRNAs involved in cytoskeleton rearrangements. (Domingues, H. S., unpublished data).

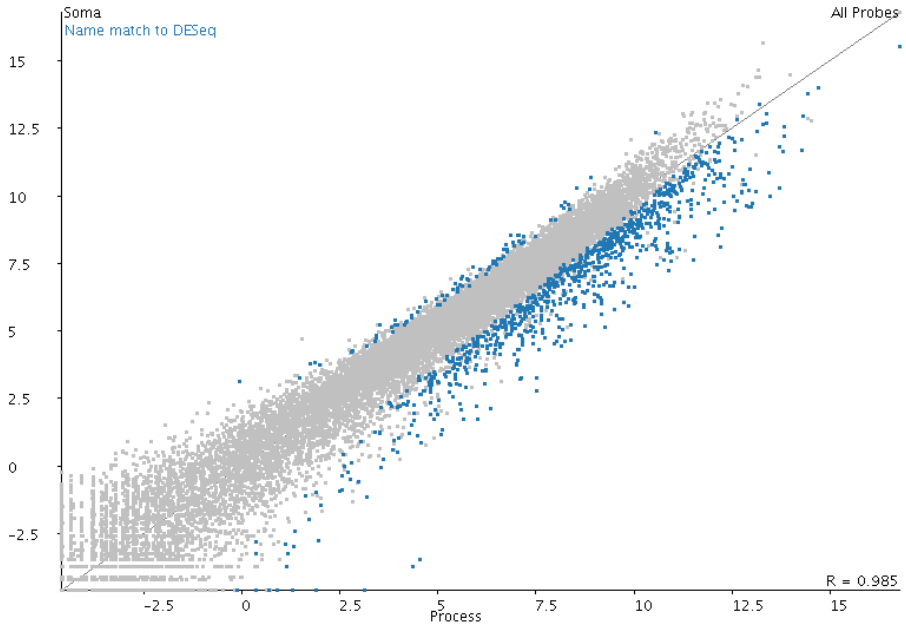

Figure 18 RNA sequencing of OPC soma vs. process. Each dot represents the expression of each transcript, with blue dots indicating molecules significantly enriched in the process or soma fractions. The majority of significantly enriched transcripts are found in the process fraction (Domingues, H.S., unpublished data).

After thorough literature reviewing, four candidate genes were selected for functional studies in OL differentiation: Kank2, Dusp19, PABPC1 and YBX1. These were chosen based on current knowledge, functionality related to cytoskeleton rearrangements and protein translation, availability of commercial reagents such as antibodies and differential expression in OPC process vs. soma, expression profile during *in vitro* OPC/OL differentiation and *in vivo* CNS myelin development (Domingues, H.S. and Cruz, A., unpublished data, not shown). Moreover, PABPC1 and YBX1 were identified in an *in silico* screen searching for proteins that bind the 3’ UTRs of mRNAs important in OL differentiation. This screen was done using an in-house developed software called Protein Binding Site Finder (PBS-Finder http://ilp.fe.up.pt/pbsfinder/) (Cruz, A., unpublished data, not shown). PBS-Finder is a user-friendly bioinformatics tool for rapid identification and analysis of putative binding sites for RNA-binding proteins (RBPs) in mRNAs derived from genome wide studies.

1.6.1. Kank N-motif and ankyrin repeat domain-containing protein 2 or Kidney ankyrin repeat domain-containing protein 2 – Kank2

Kank2, also known as ankyrin repeat domain-containing protein 25 (ANKRD25), matrix-remodeling-associated protein 3 (MXRA3) and SRC-1-interacting protein (SIP), is an 851 amino acid protein containing an ankyrin-repeat domain. Ankyrin-repeat domains are thought to be involved in protein-protein interactions (Sedgwick and Smerdon, 1999). The Kank N-motif is conserved in all Kank proteins and contains a leucine-rich region and an arginine-rich region (Zhu et al., 2008). There are four members of the Kank family, Kank1 to Kank4, with high structural similarities **(Figure 19)** (Zhu et al., 2008).

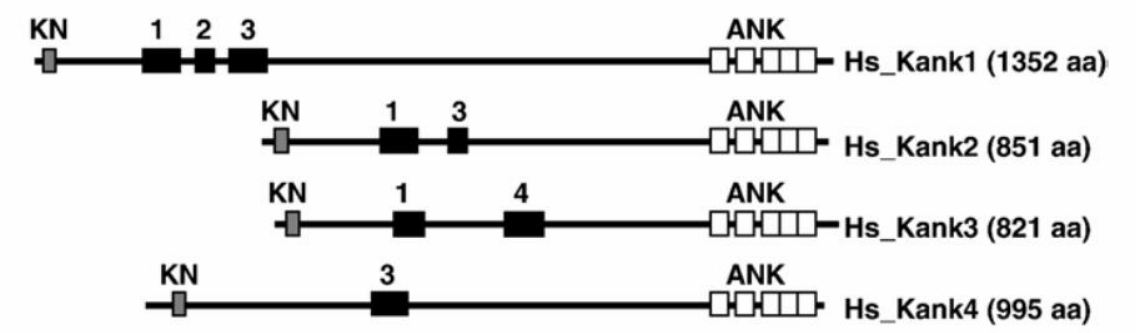

Figure 19 **Schematic representations of the structure of human Kank family proteins.** Black boxes indicate coiled-coil motifs, white boxes indicate motifs of the ankyrin-repeats (ANK), and gray boxes indicate the Kank N-terminal (KN) motif. Numbers indicate variations of the coiled-coil motifs. Adapted from Zhu *et al.* (2008).

Kank1 is the best characterized Kank isoform. It was originally identified in renal cell carcinoma (Sarkar et al., 2002) and is responsible for shuttling β-catenin between the nucleus and the cytoplasm to induce β-catenin-dependent transcription (Wang et al., 2006). In the cytoplasm, Kank1 regulates actin polymerization by inhibiting PI3K/Akt activation of RhoA through binding to 14-3-3 protein, thus controlling cytoskeleton remodeling (Kakinuma et al., 2008). Over-expression of Kank1 in NIH3T3 cells significantly reduces the amount of active RhoA. This effect is mediated by interaction of Kank1 with 14-3-3 after phosphorylation of Kank1 by PI3K/Akt signaling pathway. The reduction in active RhoA levels leads to a decrease in actin polymerization and formation of stress fibers. This phenotype can be recovered by over-expression of 14-3-3, which may saturate Kank1 and possibly leave the remaining 14-3-3 free to interact with RhoA activators such as p190RhoGEF (Zhai et al., 2001). Kank1 also inhibits Rac1 from interacting with IRSp53 and, consequently, prevents the formation of lamellipodia, but doesn't interfere with the formation of filopodia, in NIH3T3 cells (Roy et al., 2009). It also inhibits insulin induced membrane ruffling (NIH3T3 cells), integrin-mediated cell spreading (NIH3T3 cells) and IRSp53-induced neurite elongation in

N1E115 (mouse neuroblastoma) cells. Over-expression of all other Kank isoforms (in NIH3T3 cells) leads to a reduction in the formation of actin stress fibers, suggesting a similar role in regulation of actin polymerization for Kank2, 3 and 4 as observed for Kank1 (Zhu et al., 2008) **(Figure 20)**.

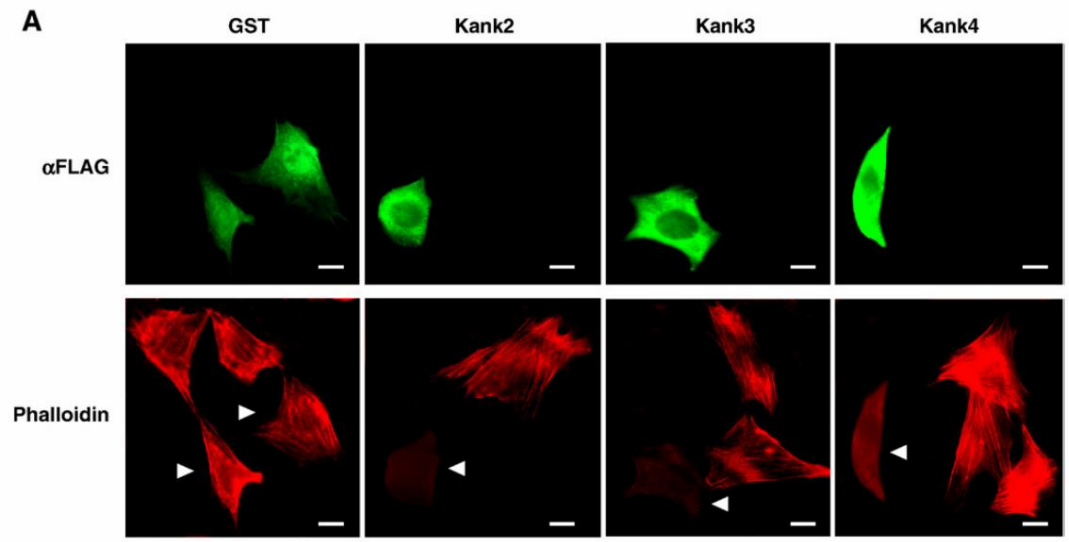

Figure 20 **Over-expression of Kank2-4 reduces the formation of actin stress fibers.** NIH3T3 cells over-expressing Kank2-4 (green) present lower staining of actin cytoskeleton (red). Scale bar: 20μm. Adapted from Zhu *et. al* (2008).

Much less is known about Kank2. Its mRNA has been found to be enriched in the protrusions of different cell types such as astrocytes processes (Thomsen and Nielsen, 2011) and NIH3T3 cells pseudopodia (Mili et al., 2008). It has been shown to be involved in palmoplantar keratoderma and woolly hair syndrome (Ramot et al., 2014). In this disorder, alanine 670 is replaced by valine. This mutation may make Kank2 unable to sequester steroid receptor co-activators in the cytoplasm, leading to an increase in vitamin D receptor signaling. Recently, Kank2 was found to be involved in steroid resistant nephrotic syndrome. In this disease, serine 181 is substituted by a glycine residue (Gee et al., 2015). A co-immunoprecipitation assay showed that wild-type Kank2 interacts with RhoGDI (Rho GDP-dissociation inhibitor) in human podocytes, and that a mutated form increases the binding of RhoGDI to small RhoGTPases like RhoA, Cdc42 and Rac1. On the other hand, knockdown of Kank2 led to an increase in active RhoA, but not Rac1 nor Cdc42, and a decreased migratory phenotype in mouse podocytes. Given the role of RhoA in modulating actin cytoskeleton dynamics in OL, Kank2 could be an important regulator of OL process extension and/or myelination.

1.6.2. Dual specificity phosphatase 19 – Dusp19

Dual-specificity phosphatase 19 (DUSP19) also known as stress-activated protein kinase pathway-regulating phosphatase 1 (SKRP1) and low molecular weight dual specificity phosphatase 3 (LMW-DSP3) (Cheng et al., 2003), is a 217-amino acid protein able to dephosphorylate both tyrosine and serine/threonine residues. Not much is known about Dusp19. It is a MAPK phosphatase involved in the JNK pathway (Zama et al., 2002a). Dusp19 interacts directly with MKK7, an activator of JNK, in order to dephosphorylate its biological substrate JNK and thus inhibiting the pathway. Dusp19 may also act as a scaffold protein (Zama et al., 2002b): expression of Dusp19 within a defined range inhibited the activation of MKK7, but the over-expression promoted the activation of the pathway. In neurons, MKK7 mRNA localizes to neurite growth cones and its localized translation enables the activation of JNK/MAP1B signaling (Feltrin et al., 2012). Active MAP1B promotes microtubule bundling and neurite elongation. Considering the role of JNK in OPC proliferation (Zhang et al., 2014a), MBP production (Chew et al., 2010) and modulation of microtubule dynamics (Feltrin et al., 2012), it is possible that Dusp19 plays a role in OL differentiation and myelination via the signaling complex assembly of ASK1/MKK7/JNK as a scaffold protein and/or in the dephosphorylation of JNK **(Figure 21)**.

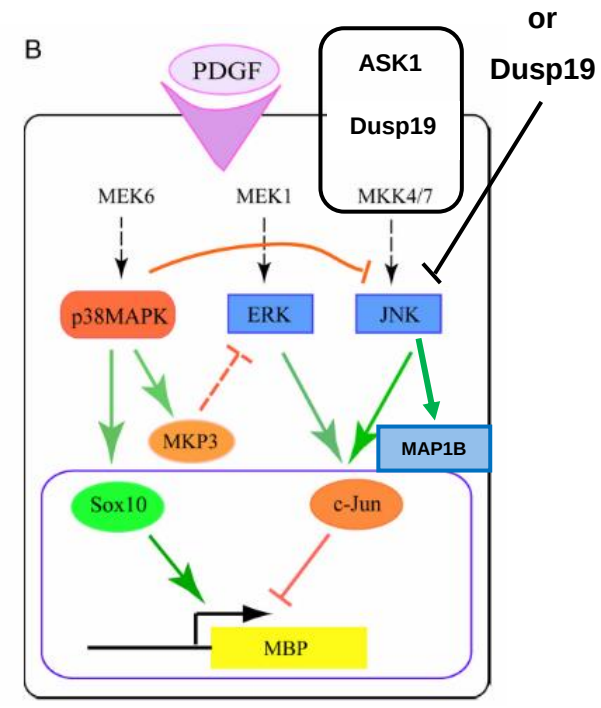

Figure 21 **Possible roles of Dusp19 in JNK pathway.** Dusp19 may regulate the JNK pathway by direct dephosphorylation of JNK or by interfering with the assembly of signaling complexes involving MKK7 and ASK1. Adapted from Chew *et al.* (2010).

1.6.3. PolyA-Binding Protein Cytoplasmic 1 – PABPC1

PolyA-Binding Protein Cytoplasmic 1 (PABPC1) is a 636 amino acid protein that binds to all polyA tails of mRNAs in the cytoplasm. Its function is to protect mRNAs and regulate their translation/degradation (Mangus et al., 2003). PABPC1 also binds to the 3’ UTRs of many mRNAs, independently of binding to PolyA tails. It stimulates translation by recruiting ribosome subunits (Kahvejian et al., 2005) and prevents mRNA degradation by protecting the PolyA tail and impeding deadenylation (Ford et al., 1997). PABPC1 is necessary for the formation of RNPs, which transport mRNAs along microtubules to the location where they will be translated (Dai et al., 2012). It is also part of the machinery behind microRNA-mediated regulation of translation and nonsense-mediated mRNA decay (Nicholson and Mhlemann, 2010). PABPC1 is necessary for the expression of other RBPs like YBX1 (Skabkina et al., 2003). Depletion of PABPC1 mRNA in HeLa cells led to inhibition of mRNA translation but not transcription nor transport (Zannat et al., 2011). Cells showed no changes in mRNA levels but protein synthesis was so strongly impaired that cells eventually underwent apoptosis. Over-expression of PABPC1 reduced the levels of several mRNAs, including MAP Kinase MKK2, by altering their stability (Ma et al., 2006). As a result, MKK2/ERK-mediated phosphorylation of PABPC1 was down-regulated and this acted as a feedback mechanism to prevent deleterious effects of excess PABPC1. In OL, PABPC1 can bind to the 3’UTR region of most early and late markers of differentiation such as NG2, Olig1 and 2, PDGFRα, CNP, MBP, MOBP, MOG, MAG and PLP1 (Cruz, A., *in silico* analysis, unpublished data). Therefore, it could be an important regulator of OL process extension, branching and myelination.

1.6.4. Y-Box binding protein 1 – YBX1

Y-Box binding protein 1 (YBX1) is a 323 amino acid protein that binds to promoter regions containing a Y-box sequence (5'-CTGATTGGCCAA-3'). It binds both DNA and RNA molecules and is involved in processes such as DNA replication, transcription and repair, pre-mRNA splicing and translation. In the cytoplasm, YBX1 can act as a packaging protein of RNPs and it regulates translation in a dose-dependent manner – at high YBX1-mRNA ratios it inhibits translation and at low ratios it promotes translation, by unfolding RNPs and making the mRNA accessible to translation initiation factors and ribosomes (Minich and Ovchinnikov, 1992; Skabkin et al., 2004). In OL, YBX1 can bind to the 3’UTR region of early markers of differentiation such as Olig1 and 2, PDGFRα and CNP, and to late markers MBP and MOBP (Cruz, A., *in silico* analysis, unpublished data). YBX1 may act as a promoter of translation of the

early markers and an inhibitor of the later ones, until the cell receives an appropriate signal to begin myelination.

1.7. Image analysis for morphological studies

Studies of cellular morphology require visualization of their architecture. This can be achieved by immunostaining of cytoskeletal components such as microtubules and actin microfilaments followed by microscopy. These microphotographs then have to be analyzed for morphological features and any differences found relative to the control phenotype can then be used as evidence to support or discredit a hypothesis.

1.7.1. Manual Categorization

One possible method to characterize cell morphology is by categorization (Thurnherr et al., 2006). An arbitrary number of morphological categories can be established and the criteria used to create these categories must be adapted to the model and reflect the different phenotypes or behaviors observed. It is a simple and low-tech method. All that is needed are pictures of the cells in the sample and a spreadsheet to count the number of cells assigned to each category for each experiment. However, despite being easy, this method is not without limitations. It is time consuming and biased to the user’s observation skills, opinion and experience. It is a method that takes training – a more experienced user will have a different opinion of what he is observing and he will have a different result than a less experienced user. Another limitation is that cells don’t have defined phenotypes: they lie on a spectrum that can range from less differentiated immature cells to fully differentiated and complex mature ones (taking OPC/OL as an example, **Figure 22**). This type of analysis is qualitative rather than quantitative and the information obtained depends on the categories created.

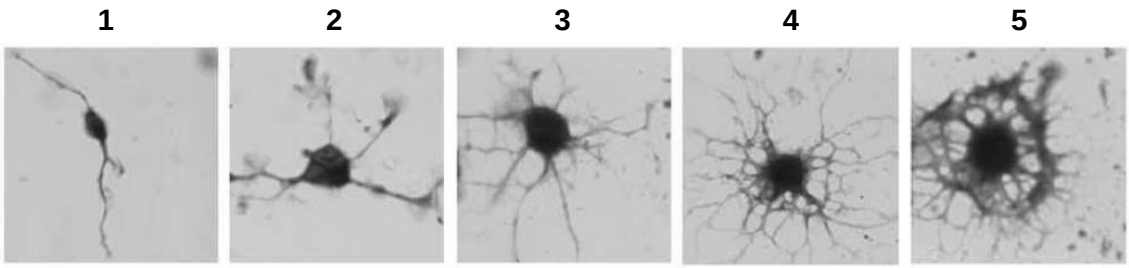

Figure 22 **Branching categorization of OPC/OL.** OPC/OL increasing morphological complexity throughout differentiation can be analyzed by assigning cells to different stages of development. Adapted from Thurnherr *et al.* (2006).

1.7.2. Sholl Analysis

Sholl Analysis is a quantitative method used to analyze highly polarized cells like neurons and oligodendrocytes. First published by D. A. Sholl in 1953 (Sholl, 1953), it consists in overlapping a series of equidistant, concentric circles with an image of a branched cell **(Figure 23)** (Binley et al., 2014). The circles should be centered at the cell body and the number of intersections between each circle and the processes are quantified.

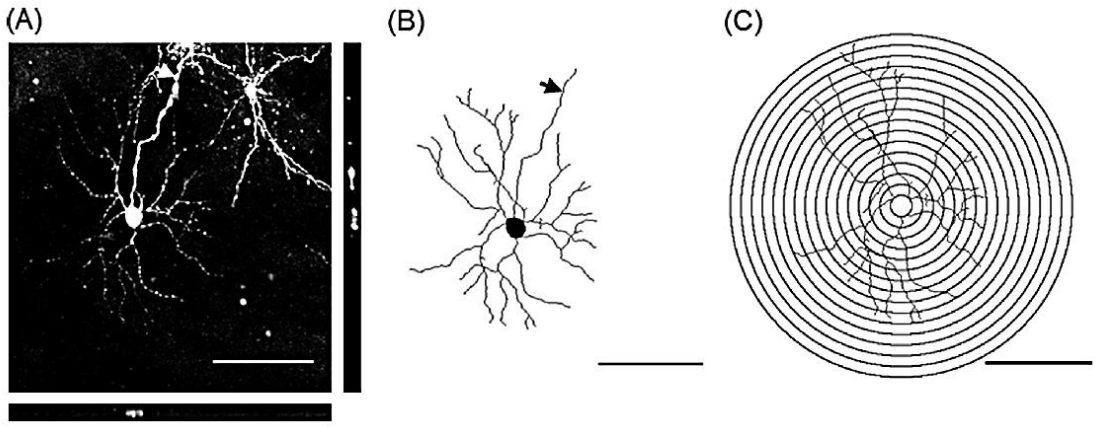

Figure 23 **Sholl Analysis of a neuron.** A fluorescence image of a neuron (A) is traced over to outline the dendrites and the axon (arrow) (B). Then, regularly spaced circles are superimposed with the traced pictures, centered at the cell body, and the number of intersections between the circles and the dendrites is determined (C). Adapted from Binley *et al*. 2014

The average number of intersections for each circle is further plotted against the distance from the soma. This originates a curve with a peak representing the critical value (radius at which there is a maximum number of intersections) and the maximum number of processes. The first point in the graph represents the number of primary processes and the ratio between the maximum number and this primary number gives a measure of the branching degree (Schoenen Ramification Index). A shift in the position of the peak along the x-axis (Sholl Ring radius) indicates an earlier (shorter distance) or later (longer distance) production of branches, whereas a shift along the y-axis (average number of intersections) indicates an increase or decrease of branching **(Figure 24)**.

Nowadays, there is software which can semi-automate this technique, like FIJI’s Sholl Analysis plugin (Ferreira et al., 2014; Schindelin et al., 2012).

Sholl Analysis is an accurate way to achieve quantitative data from samples. However, it is a very time consuming technique, since it can only analyze one cell at a time, and it can be biased because it depends on the user’s choice of which cells to analyze.

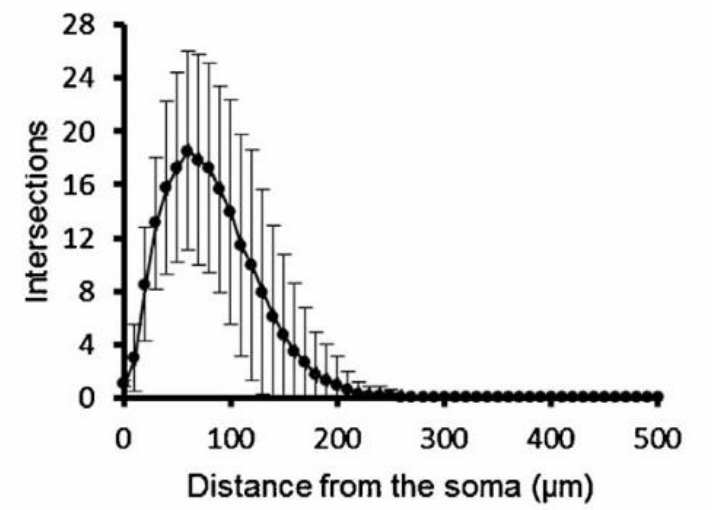

Figure 24 **Sholl Profile of neurons.** 62 cells were analyzed using the Simple Neurite Tracer plugin of FIJI. Adapted from Binley *et al.* (2014).

1.7.3. High-throughput Image Analysis

The two methods previously described are time consuming, reducing the number of cells analyzed in a useful time frame, and biased to the user’s observations and choice of which cells to analyze and which to ignore. To solve these limitations, some companies have developed automated image analysis software to enable a high throughput image analysis.

The INCell Developer Toolbox software (GE Healthcare) was used in this thesis (Healthcare, 2008a). It is associated to the INCell Analyzer fluorescence microscope and it is designed to obtain a great amount of information from images acquired with the microscope. This microscope has several acquisition modes, like 2D (separate files for each individual plane along the z-axis, which must later be projected together) and 3D (a single file including all the planes acquired along the z-axis) (Healthcare, 2008b). In addition, it also has a 2.5D mode: it is an intermediate between 2D acquisition (low quality, low file size but requires post-processing) and 3D (high quality but large file size and lower acquisition speed). It acquires a “thick slice” that begins above and ends below the focus point, projects it onto a single plane and outputs a deconvoluted image **(Figure 25)**.

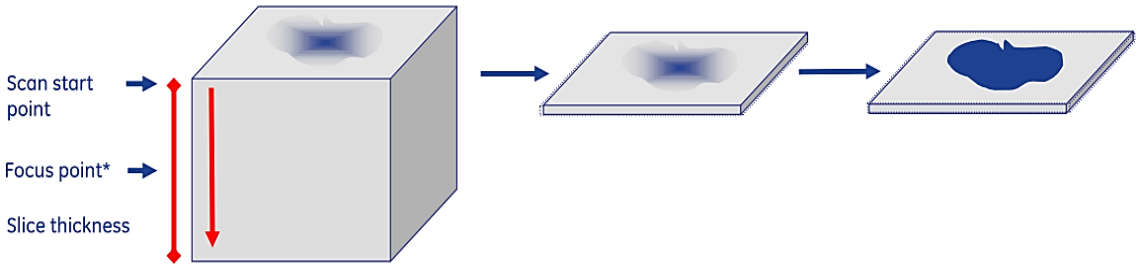

Figure 25 **2.5D image acquisition mode.** Image acquisition begins above the focus point and ends below. Then, the image is projected onto a single plane and deconvoluted (Healthcare, 2008b)

In order to reduce the file size even further, camera binning can be used (Healthcare, 2008b). For example, a 2x2 binning converts each set of 4 pixels in the original image created by the camera to a single pixel in the saved image (resolution is reduced to one-fourth).

The INCell Developer Toolbox software comes with pre-established analysis modules for common studies such as cell cycle progression, membrane trafficking and neurite outgrowth. INCell Developer Toolbox also allows the user to define his own protocol to answer questions that may not be covered by the analysis modules. In this situation, the user can explore the many tools offered by the software to manipulate fluorescent images in order to make cells and their features more “visible” to the software **(Table 1)**. After pre-processing, grey-scale images can be segmented based on a single thresholding operation (object segmentation) or multiple operations (intensity segmentation), depending on the target’s characteristics. The targets can be nuclei, vesicles, processes, etc. During segmentation, the user can define exclusion parameters such as minimum intensity and form factor (circularity of the target).

After segmentation, targets can be further processed to enhance their characteristics. For example, if cells are in very close proximity they can clump together, making it difficult to identify intercellular boundaries. A “clump breaking” operation can be used to separate adjacent cells. The software also includes a series of macros the user can apply to process and combine different targets. A macro is a set of program commands that is performed automatically, simplifying complex or repetitive tasks. For example, it is possible to use a macro to take a total cell and subtract the cell body in order to keep only the processes for further processing or analysis.

Table 1 Some image processing tools available in INCell Developer Toolbox software.

Tool Name	Function
Pre-processing	
Denoising (gradient)	A higher degree of smoothing is applied to areas of the image where the gradient is small (e.g., in background) than in areas where the gradient is steep (e.g., across edges).
Segmentation	
Intensity segmentation	Segments pixels within a defined range of fluorescence intensities, set by the user
Object segmentation	Uses kernels: sets of at least 9 pixels (3x3) in which the center pixel is replaced by the value computed using the eight pixels that surround it.
Post-processing	
Sieve	Filter that removes objects that are too big or too small and do not correspond to real targets
Dilation	Enlarges boundaries of regions of foreground pixels increasing their size while holes within those areas become smaller
Erosion	Shrinks a region's outer boundary whilst at the same time enlarging any holes within it
Clump breaking	Uses a secondary target, such as the nucleus, to identify cellular borders. The boundaries between neighboring cells are calculated at the equidistance from each nucleus, and then imposed onto the cell segmentation image

After segmentation and post-processing, the user can link several targets together. For branched cells, for example, it makes sense to link one cell body to many processes but only one nucleus to one cell body. Then it is possible to define which measurements the software should make from the data. There are many pre-established measurements such as density levels (mean pixel intensity within a target), target area, target length, number of branch nodes and end nodes (for fibrous shapes like cellular processes), etc. The user can also create classifiers to organize the data in a manner easier to interpret, for example GFP^+/GFP^- cells, according to an arbitrary fluorescence intensity threshold. Finally, all the data obtained from the image analysis can be exported in a spreadsheet-type file, such as an Excel file for later statistical analysis of results. This software is an example of a high-throughput image analysis system given the short amount of time needed to obtain a large amount of information.

1.8 Aim

The specific aims of this Master thesis are the following:

1. Develop an automated high-throughput protocol for image analysis to study OL morphology and myelin production
2. Study the functional role of Kank2, Dusp19, PABPC1 and YBX1 in *in vitro* OPC/OL differentiation and myelination. In particular, evaluate the role of these molecules in OL process extension and myelin production

2. Materials and Methods

2.1. Reagents

Buffers:

Phosphate Buffer Saline (PBS): 137mM NaCl (VWR), 2.7mM KCl (Merck Millipore), 10mM $Na_2PO_4 \cdot 7H2O$ (Merck Millipore), 1.7mM KH_2PO_4 (Alfa Aesar), pH 7.3-7.4.

Microtubules-protecting (MP) buffer: 65mM PIPES (Millipore), 25mM HEPES (Sigma), 10mM EGTA (brand), 3mM $MgCl_2$ (Sigma), pH 6.9.

MP-PFA 4%: 40g paraformaldehyde (Sigma) in 1L MP buffer.

Cell culture media:

Complete Dulbecco’s Modified Eagle Medium (cDMEM): DMEM high glucose GlutaMAX™ Supplement (Gibco) supplemented with 10% Fetal Bovine Serum (FBS, Sigma) and 1% penicillin/streptomycin 10000U/mL (Gibco).

SATO medium: 1 mg/mL human apo-transferrin (Sigma), 1 mg/mL bovine serum albumin (NZYtech), 0.16 mg/mL putrescin dihydrochloride (Sigma), 0.0012 µg/mL progesterone (Sigma), 0.008 µg/mL sodium selenite (Sigma), 0.008 µg/mL L-thyroxine (Sigma), 0.006 µg/mL triiodothyronine sodium salt (Sigma) in DMEM high glucose GlutaMAX™ Supplement (Gibco).

OPC SATO medium: SATO medium supplemented with 1% penicillin/streptomycin 10000U/mL, 10 ng/mL recombinant human fibroblast growth factor-basic (Peprotech), 10 ng/ml recombinant human platelet-derived growth factor AA (Peprotech) and 5µg/mL recombinant human insulin solution (Sigma).

OL SATO medium: SATO medium supplemented with 1% penicillin/streptomycin 10000U/mL, 0.5% FBS and 5µg/mL recombinant human insulin solution (Sigma).

Blocking Solution for Immunocytochemistry (ICC)

5% Normal Goat Serum (Invitrogen) in PBS.

2.2. Mixed Glial Cell Cultures

This protocol was based on the works of Chen *et. al* (2007) and McCarthy and de Vellis (1980) with adaptations (Chen et al., 2007; McCarthy and de Vellis, 1980).

Mixed glial cell cultures were obtained from isolating the brain cortices of P1-P2 (1-2 post-natal days) Wistar rats. Pups were euthanized by decapitation using a pair of scissors. Then, the skull was cut open, starting at the foramen magnum, forward along the sagittal suture and then towards either side of the skull to expose the brain. Afterwards, brains were scooped out using a pair of curved tweezers into chilled Hank’s Balanced Salt Solution (HBSS, Gibco) supplemented with 1% penicillin/streptomycin 10000U/mL. Next, brains were dissected to remove the meninges and isolate the cortex. Isolated cortices were first mechanically homogenized by pipetting up and down using a serological pipette and a syringe with a 25G needle. Then, the cells were enzymatically treated with 0.1mg/mL DNAse I (Sigma) and 0.0025% trypsin (Gibco) in HBSS for 15 minutes at 37ºC. Reaction was stopped with serum-containing DMEM and cells were then centrifuged (Heraeus Megafuge 1.0) at 500g for 10 minutes. The supernatant was discarded and the cells were re-suspended in complete DMEM and filtered through a 100µm nylon cell strainer (BD Falcon) into 50mL sterile centrifuge tubes (Fisher). Finally, the cell suspension was plated on poly-D-lysine (PDL)-coated (Sigma) T75 flasks (Sarstedt) at a concentration of 2 brains per flask. Flasks were cultured in complete DMEM medium at 37ºC in 5% CO_2 for approximately 10 days. Medium was replaced every 2-3 days.

2.3. Oligodendrocyte Progenitor Cells isolation and culture

After approximately 10 days, a mixed glial cell culture consists of a confluent layer of astrocytes on top of which OPC and microglia grow. OPC do not differentiate because astrocytes produce large amounts of PDGF (Moore et al., 2011). At this time, culture flasks were pre-shaken at 200 rpm and 37ºC for 2 hours (INFORS HT Minitron incubator shaker) to remove microglia cells. Afterwards, flasks were shaken at 220 rpm overnight to collect OPC. Depending on the intended analysis, OPC were plated in PDL and laminin-2 (human merosin, Milipore)-coated 6-well plates (Thermo Scientific); 60mm Ø Petri dishes (Orange Scientific) or 18 mm Ø HCl-treated glass coverslips (Thermo Scientific) (day -2). OPC were cultured in OPC SATO medium for 2 days to enable cell synchronization and promote proliferation. OL differentiation was induced by replacing the medium with OL SATO (day 0). In general, cells were collected for

analysis at day 0 (OPC stage, OL 0d), 3 (immature OL, OL 3d) and 5 (myelinating mature OL, OL 5d) post-differentiation.

2.4. Lentivirus production and OPC infection

This protocol was based on the protocol by Tiscornia *et al.* (2006) with adaptations (Tiscornia et al., 2006). Lentiviral vector particles were produced using packaging HEK293T cells. Cells were transfected with three different plasmids: lentiviral pSicoR plasmids (Addgene plasmid # 11579 (Ventura et al., 2004)) carrying shRNA sequences and a green fluorescent protein (GFP) reporter tag, psPAX2 plasmid (Addgene plasmid # 12260, Didier Trono) carrying genes coding for lentiviral packaging proteins and pCMV-VSV-G plasmid (Addgene plasmid # 8454 (Stewart et al., 2003)) containing genes coding for envelope proteins. The transfection reagent used was jetPRIME (Polyplus). Lentiviral particles were collected from the cell culture supernatants 2 days post-transfection and the viral titer was determined by Fluorescence-activated cell sorting (FACS): HEK293T cells were infected with 10 fold dilutions of virus suspension and the percentage of GFP positive (GFP^+) cells was determined by flow cytometry using FACSCalibur (BD Biosciences). The viral titer was calculated by

$$TU/\mu L = \frac{P \times N}{100 \times V} \times \frac{1}{F}$$

where:

TU=transducing units

P =% GFP^+ cells

N= number of cells at time of transduction

V=volume of supernatant added to each well

F= dilution factor

OPC were infected with shRNA-loaded virus for the depletion of Kank2 and Dusp19 on the same day that they were plated (day -2). OPC were transduced with the shRNAs for the depletion of PABPC1 and YBX1 on the day of OL induced differentiation (day 0). A shRNA against dsRED fluorescent protein was used as infection control. Cells were infected using a multiplicity of infection (MOI, ratio of virus particles to cells) of 1:1.

The Kank2, YBX1 and PABPC1 shRNA sequences **(Table 2)** were designed by pSicoOligomaker 1.5 software (http://jacks-lab.mit.edu/protocol/psico). The shRNA sequence for Dusp19 was validated by Sigma (Clone Number: TRCN0000081192).

The shRNA sequences were cloned into the lentiviral pSicoR vector (Addgene) using HpaI-XhoI cleavage sites (Domingues, H.S and Cruz, A., unpublished data).

Table 2 shRNA sequences for mRNA knockdown.

Gene	shRNA Sequence (5’ – 3’)
dsRED	AGTTCCAGTACGGCTCCAA
Kank2	GCTTGGCCCTGGAGAAATA
Dusp19	GACCACGCTAACTGGAAAGAA
PABPC1	GTAACATCCTTTCATGTAA
YBX1	GAGAACCCTAAACCACAAGAT

2.5. RNA isolation and cDNA synthesis

RNA was isolated from OL cultures using Quick-RNA MicroPrep kit (Zymo Research) or TRIzol reagent (Invitrogen). Briefly, cells were lysed using Quick-RNA MicroPrep RNA Lysis buffer and a cell scraper. Then, RNA was purified by mixing with an equal volume of ethanol, placing the mixture in a purification column and centrifuging with RNA Prep buffer, followed by RNA Wash buffer (twice). Finally, RNA was eluted from the column using RNAse-free water. Afterwards, RNA concentration was determined by spectrophotometry (NanoDrop 1000, Agilent).

RNA extraction using TRIzol was performed as follows: cells were lysed in 500µL TRIzol, let at room temperature for 5 minutes and frozen at -80°C. Afterwards, samples were thawed at room temperature, mixed with 100µL chloroform and vortexed. The mixture was allowed to incubate for 3 minutes at room temperature and then centrifuged at 12000g, 4°C for 15 minutes. The aqueous phase was transferred to a new tube (on ice) and 1µL Glycoblue (15mg/mL) was added to each sample. Then, an equal volume of isopropanol was added, the mixture was vortexed and frozen at -80°C. Samples were thawed at room temperature, centrifuged at 12000g, 4°C for 20 minutes and the supernatant was removed. The pellet was washed with 500µL chilled ethanol 75% and centrifuged at 12000g, 4°C for 10 minutes. Ethanol was removed and the RNA pellet was re-suspended in 15µL nuclease-free water. The solutions were incubated on ice for 3 min, pipetting up-and-down every 30s. An aliquot was taken from each sample to quantify and the remainder was stored at -80°C.

cDNA synthesis was then performed using SuperScript III First-Strand Synthesis Supermix for quantitative real-time PCR Kit (Invitrogen) following the manufacturer’s

instructions and using C1000 Thermal Cycler (Bio-Rad). Up to 1µg of RNA was mixed with 10µL RT reaction mix, 2µL RT Enzyme mix and diethylpyrocarbonate (DEPC)-treated water, up to a final volume of 20µL. The mixture was incubated at 25°C for 10min, followed by 50°C for 30min and 85°C for 5min. Then, the reaction mixture was cooled, 1µL of RNAse H was added and the mixture was incubated for 20min at 37°C.

2.6. Quantitative Real-Time Polymerase Chain Reaction

Quantitative real-time PCR (qPCR) was performed using iQ SYBR Green Supermix (Bio-Rad) and iCycler iQ5 Real-Time PCR machine (Bio-Rad). The supermix contains deoxynucleotides (dNTPs), iTaq DNA polymerase, $MgCl_2$ and SYBR Green dye. For each gene, reaction mixtures were prepared as follows: 0.5µL of forward and reverse primer solutions (10µM) were mixed with 10µL iQ SYBR Green Supermix 2X, 1µL of cDNA (pre-diluted 1:3) and 8µL of nuclease-free water to a final volume of 20µL. YWHAZ or GAPDH were used as reference genes and 9µL of pure water were used as no-template control. qPCR was performed using iCycler iQ5 and consisted in 3 minute incubation at 94°C for polymerase activation and DNA denaturation followed by 40 cycles of amplification – 15s at 94°C, 20s at 60°C and 15s at 75°C. Melting curve was obtained by heating the sample from 55°C to 95.5° (step 0.5°C, 81 cycles) to confirm PCR product specificity.

Primer sequences are shown in

Table 3.

Table 3 **Primer sequences used for qPCR.**

Gene	Primer Forward	Primer Reverse
Kank2	GGAGGAAATTCGGATGGATCTG	ACTTTCAGTTCTCGCTCTGTGA
Dusp19	ACCTGCAAGTTGGCGTTATTA	TGGTTTCAGGCACATCCAGTAT
PABPC1	AACCGTGCTGCATACTATCCT	GCATATTCTGGAATGGATGAGGTC
YBX1	GAAGGAGAAAAGGGTGCGGA	TGGTAATTGCGTGGAGGACC
YWHAZ	GATGAAGCCATTGCTGAACTTG	GTCTCCTTGGGTATCCGATGTC
GAPDH	TGGAGTCTACTGGCGTCTT	TGTCATATTTCTCGTGGTTCA
MBP	GCTCCCTGCCCCAGAAGT	TGTCACAATGTTCTTGAAGAAATGG

2.7. Immunocytochemistry (ICC)

OL were collected on days 0, 3 and 5 post-induction of differentiation (OL 0d, OL 3d and OL 5d). Cells were fixed with 4% paraformaldehyde in MP buffer for the preservation of the cytoskeleton integrity. Afterwards, cells were permeabilized in 0.1% Triton X-100 in PBS for 10 minutes at room temperature and incubated in blocking solution for 1h at room temperature. Then, samples were incubated with primary antibodies **(Table 4)** diluted in blocking solution overnight at 4ºC, washed 3 times in PBS for 5 minutes each, followed by 1h incubation at room temperature with fluorescent-conjugated secondary antibodies **(Table 4)** and/or Alexa Fluor 594 Phalloidin (Molecular Probes). Finally, samples were washed 3 times in PBS for 5 minutes, the nuclei were counterstained with DAPI (1:20000) (Invitrogen) for 10 minutes, washed again twice in PBS and mounted on glass slides using Immu-Mount mounting medium (Thermo Scientific). Olig2, an oligodendrocyte-specific transcription factor, was used as a marker of OPC/OL, to analyze exclusively OPC/OL and not contaminating cells such as microglia and astrocytes. For morphological analysis, samples were stained with anti-Olig2 and anti-α-tubulin antibodies. For MBP analysis, samples were stained with anti-Olig2 and anti-MBP antibodies.

Table 4 **List of primary antibodies, secondary antibodies and stains used for immunocytochemistry.**

Primary Antibodies				
Antigen	**Animal of origin**	**Dilution**	**Product reference**	
α-tubulin	Mouse, mAb	1:2000	T5168, Sigma	
Olig2	Rabbit, pAb	1:500	AB9610, Chemicon International	
MBP	Rat, mAb	1:100	MCA4095, AbD Serotec	
Secondary Antibodies				
Antigen	**Conjugated fluorophore**	**Animal of origin**	**Dilution**	**Product reference**
Mouse IgG	Alexa Fluor® 647	Goat, pAb	1:1000	A-21236, Life Technologies
Rabbit IgG	Alexa Fluor® 568	Goat, pAb	1:1000	A-11036, Life Technologies
Rabbit IgG	Alexa Fluor® 647	Goat, pAb	1:1000	A-21236, Life Technologies
Rat IgG	Alexa Fluor® 568	Goat, pAb	1:1000	A-11077, Life Technologies

Stains		
	Dilution	**Product reference**
4',6-diamidino-2-phenylindole (DAPI)	1:20000	D1306, Life Technologies
Alexa Fluor® 594 Phalloidin	1:100	A12381, Life Technologies

2.8. Image acquisition

For morphological and MBP analysis of OL, fluorescent images (four channels – DAPI, FITC, Texas Red and Cy5) were obtained using In Cell Analyzer 2000 widefield microscope (General Electric), a 20X objective and 2.5D acquisition mode.

Between 36 and 100 fields were obtained per sample, corresponding to the analysis of at least 1000 cells. Exposure times were adjusted for each experiment, but maintained for all samples within experiments, to allow comparison of results.

Images representative of quantitative results were obtained using the Laser Scanning confocal microscope Leica TCS SP5 II (Leica Microsystems, Germany) or the wide-field fluorescent microscope Leica DMI 6000B (Leica Microsystems, Germany).

Images representative of results were edited using ImageJ. Fluorescence intensity was adjusted to increase contrast and avoid overexposure and the image stack was merged using a maximum projection of each plane. Planes that were out of focus were rejected.

2.9. Image Analysis using INCell Developer Toolbox software

The INCell Developer Toolbox software was used to perform high-throughput image analysis of pictures obtained using the INCell Analyzer 2000 microscope. Several protocols were produced to study OL morphology and the production of MBP in the context of shRNA-mediated knockdown of Kank2, Dusp19, PABPC1 and YBX1. These protocols were under optimization and will be, therefore, further described in detail in Section 3.

2.10. Morphological Categorization by Manual Image Analysis

Images obtained using INCell Analyzer 2000 were also manually analyzed for morphological categorization. As previously, Olig2 staining was used to identify OL and GFP signal was used as reporter of infection. α-Tubulin staining was used to visualize the cytoskeleton.

Four morphological stages were established based on the number of primary processes, branching degree and cell symmetry (Thurnherr et al., 2006):

- **Stage 1:** bipolar cell, long unbranched processes;
- **Stage 2:** three or more processes, few branches, asymmetrical process distribution;
- **Stage 3:** five or more processes, symmetrically distributed, few branches, “star-shaped” cell;
- **Stage 4:** five or more processes, symmetrically distributed, highly branched and interconnected, “spider-web”-like shaped cell or large, highly ramified “crochet”-like process network.

Images representative of these morphologies can be seen in Section 3. At least 200 cells were counted per condition, per experiment with this technique.

2.11. Sholl Analysis

Sholl Analysis plugin in FIJI software was used as following (Ferreira et al., 2014; Schindelin et al., 2012): images were thresholded for signal intensity using α-tubulin staining (labels all cells) and scale was corrected. Then, $Olig2^{+}$, GFP^{+} cells were selected and a straight line was traced from the cell body to the end of the longest process (without intersecting with neighboring cells). Finally, Sholl Analysis plugin was run, with an interval between Sholl Ring radii of 5μm and 3 samples per radius.

At least 30 cells were analyzed per condition, per experiment with this method.

2.12. Statistical Analysis

Statistical analysis of results was done using Graph Pad Prism 6. Unpaired t-test, one sample t-test, one-way ANOVA and two-way ANOVA (with Bonferroni’s multiple comparisons test) statistical tests were applied to evaluate significance, as indicated in results graphs.

3. Results and Discussion

3.1 Development of high-throughput protocols for image analysis using INCell Developer Toolbox

The first aim of this thesis was to develop automated protocols to analyze OL morphology and myelin production in a large scale – high-throughput analysis – using the INCell Developer Toolbox software. The goal is to quantitatively analyze thousands of cells in a short period of time and in an unbiased manner, circumventing qualitative and biased analyses like categorization, which rely on users’ opinion and experience in recognizing different morphologies. Three different approaches were attempted for OL morphological analysis and one for myelin production quantification.

3.1.1. Development of an automated protocol for morphological analysis of OL

To do a morphological analysis, OL in an immature stage (OL3d), which had been previously knocked down with a specific lentiviral-delivered shRNA carrying GFP as a reporter gene, were immunostained for α-tubulin and counter-stained with DAPI. Then, fluorescence images were acquired using the INCell Analyzer 2000 wide-field microscope and analyzed using the INCell Developer Toolbox software.

First, we analyzed the images in a context module for the analysis of neurite outgrowth, already included in the software. We tried to adapt this protocol to oligodendrocytes due to morphological similarities with neurons. Briefly, a series of segmentations based on fluorescent signal intensity were applied to grey level images, resulting in binary images (black pixels – background, white pixels – foreground targets). DAPI signal was used to segment nuclei and α-tubulin signal was used to segment cell bodies and process networks **(Figure 26)**. Then, images were processed to exclude targets that were too big or too small to be real cells and processes. Afterwards, a “clump breaking” step was used to separate adjacent cells and targets were linked so that one cell would have multiple processes. Finally, mean pixel intensity (density levels) for GFP (reporter of infection) was measured for each cell and cells were classified as GFP positive or negative based on arbitrary thresholds. The smaller size of OL, their thinner processes and the necessity for high confluency in cell culture led to many errors in the automatic segmentation **(Figure 27)**. Another challenge encountered during the preparation of this protocol was related to fluorescence intensity along processes. The fluorescent signal for α-tubulin used in these samples was stronger in the cell body than in the processes and much dimmer at the tip of the processes. This required overexposure of the cell bodies in order to view the process tips. However, this also increased the

background signal, which made it more difficult for the analysis software to distinguish background from cells.

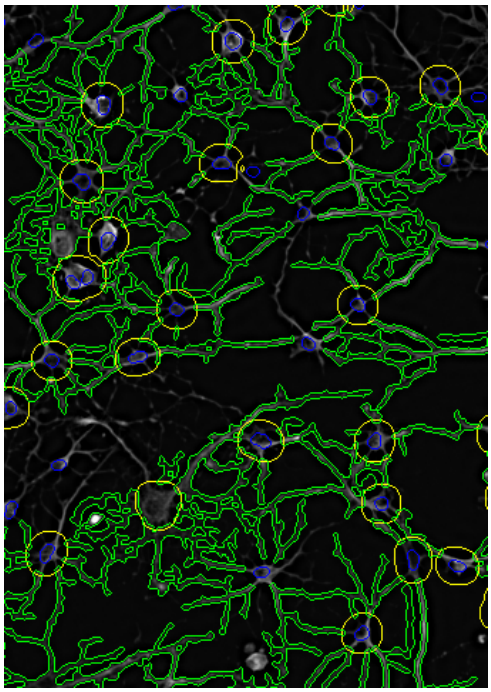

Figure 26 **Image segmentation.** Blue – nuclei (segmented using DAPI signal); Yellow – cell bodies and Green – processes (segmented using α-tubulin signal).

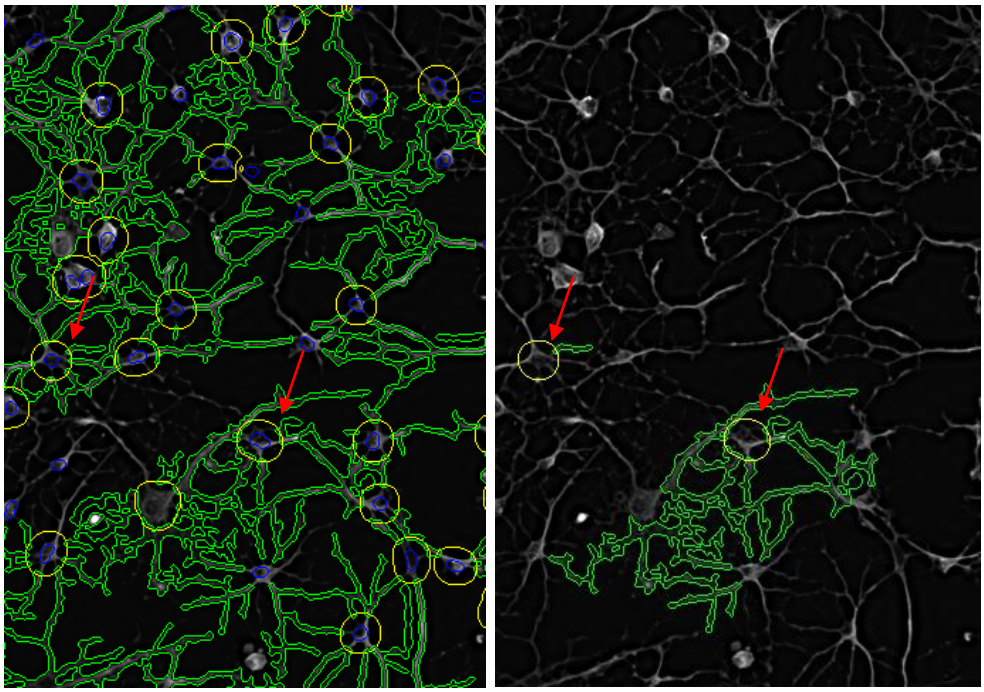

Figure 27 **Image analysis of oligodendrocytes at OL3d.** Images represent the result of image analysis using a protocol based on a context module for neurite outgrowth. Red arrows indicate the same cells with segmentation errors. dsRED-transduced cells stained for α-tubulin.

Due to the high occurrence of segmentation errors and taking into account what we had learned while exploring the context module for neurons, we decided to create a new protocol. We included an immunostaining against an OL-specific marker, Olig2, to exclude the possible analysis of “contaminating cells” such as astrocytes and microglia. Olig2 is a transcription factor and localizes preferentially in the nucleus. First, DAPI signal was segmented based on signal intensity and eroded to leave a small “seed” within the nucleus. This small area within the nucleus was later used to discriminate adjacent cells. Then, segmentations were used to identify nuclei (DAPI), cell bodies (α-tubulin) and processes (α-tubulin). Several intermediate “clump breaking” steps were used to separate adjacent cells and to divide processes between them. Finally, cells were classified according to their signal intensity as Olig2 and GFP positive or negative. The quantitative measurements made included number of processes, process length, number of branch points and number of end nodes. At first glance, this protocol seemed to work very well but, when cells were very confluent, many processes were attributed to one cell only, originating giant cells with huge process networks while others would had their processes reduced to 1-2μm long **(Figure 28**, left**)**. However, where cells were less confluent, process segmentation was perfect, indicating that further optimization was needed **(Figure 28**, right**)**. It was expected that, in the overall analysis, these segmentation errors would cancel each other out and any differences between conditions would be observed. Unfortunately this was not the case **(Graph 1)**. The analysis of the number of primary processes, branch points and end nodes did not show a significant difference between the control (dsRED shRNA) and the two knockdowns, Kank2 and Dusp19. Nevertheless, the data sets represented in red show that the knockdown of Kank2 slightly increases the percentage of cells with fewer processes, branch points and end nodes, relative to control, indicating a delay in OL differentiation. At present time, we were unable to optimize this protocol.

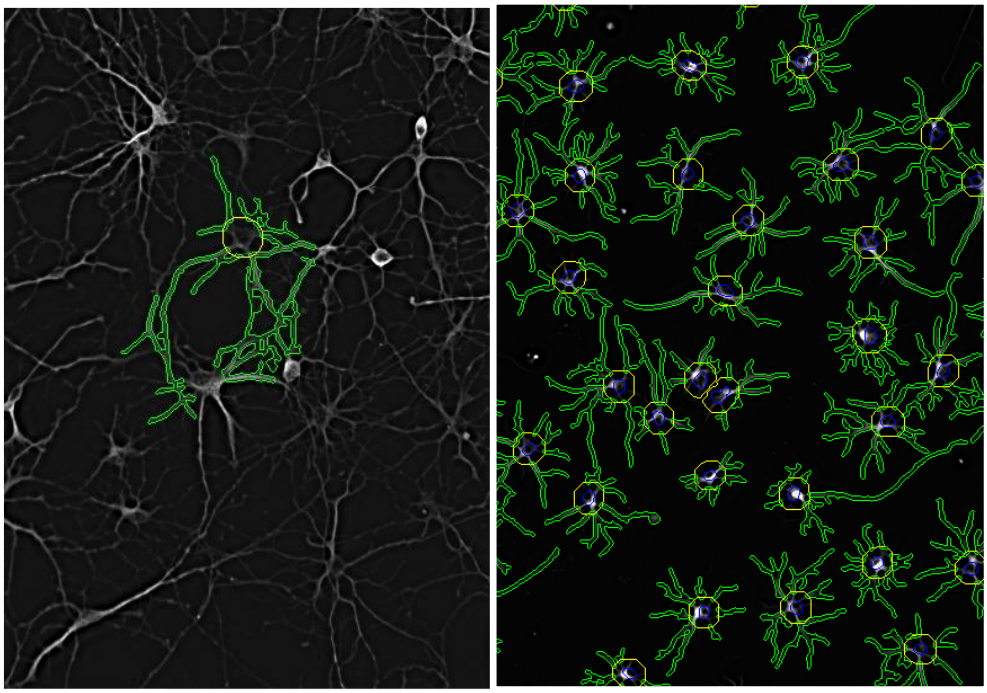

Figure 28 **Image analysis of oligodendrocytes.** Segmentation errors occur frequently when cells are highly confluent (left), but not at lower confluency (right). Staining: α-tubulin.

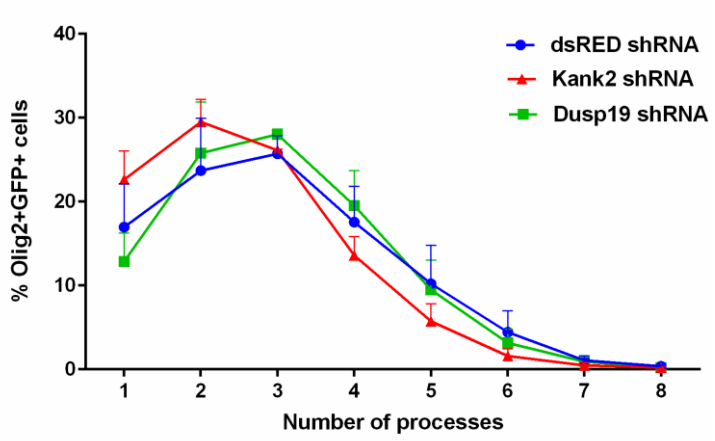

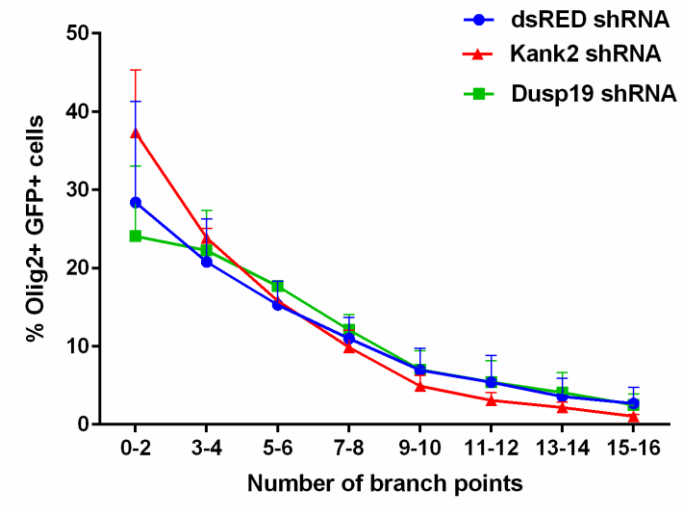

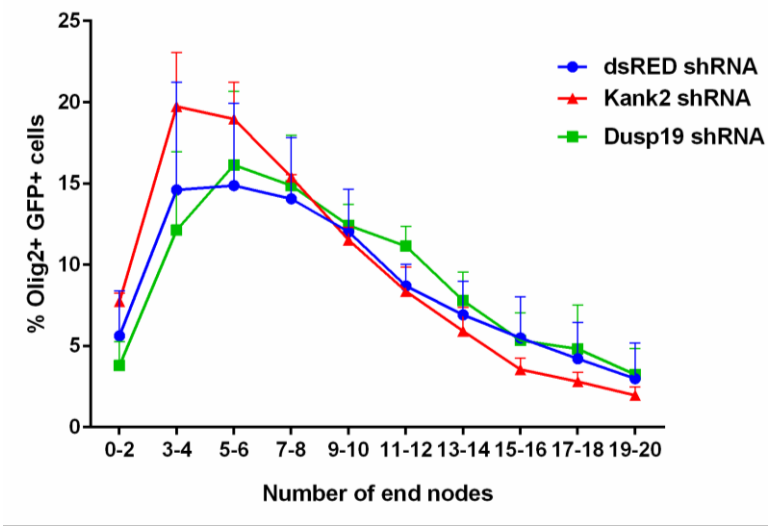

Graph 1 **Graphical representations of number of processes, branch points and end nodes of OL at OL3d.** Results obtained by automated high-throughput analysis using INCell Developer Toolbox. There appears to be an increase in the percentage of cells with lower numbers of processes, branch points and end nodes when we knockdown Kank2 relative to control. No differences are seen between Dusp19 knockdown and control (n=3).

Finally, with the collaboration of a GE technical expert, a third protocol was recently developed following a different approach. After segmenting nuclei, cell bodies and process networks, the area that belonged to the cell body was dilated until a neighboring cell was encountered **(Figure 29)**. Instead of outlining whole processes from soma to tip, only the processes included inside this large area (the collar, in yellow in **Figure 29**) were counted and measured for length. This prevented process overlapping with neighboring cells but did not allow us to measure whole process length. Within this area it was possible to quantify total process length within the collar and the ratio of process area to total area. Therefore, the greater these measurements, the higher the branching and more differentiated the cells were. At present time, this is a work in progress and, therefore, we do not have quantitative results to present.

Overall, the three protocols tested consist in an effort to develop high-throughput image analysis methods for morphological studies of OL. These are already in use for neuronal cells but have not yet been developed for OL, probably due to technical difficulties similar to the ones previously described. It is an innovative approach that we believe will be of great relevance and impact in the field of OL. Therefore, we intend to dedicate ourselves to the optimization of at least one of these protocols and apply it to future studies as well.

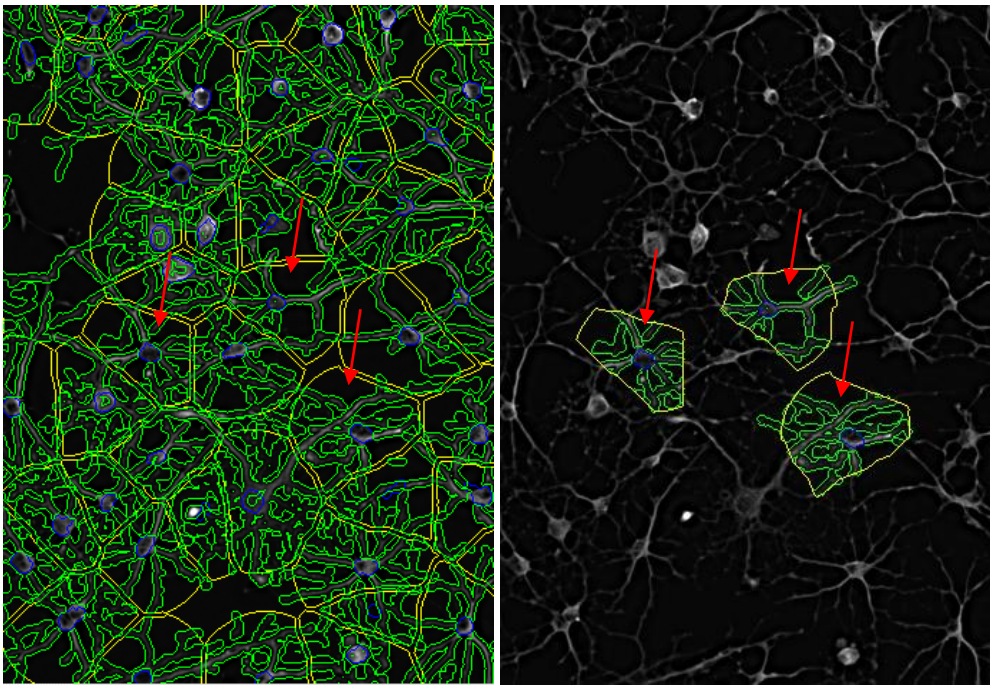

Figure 29 Image analysis of oligodendrocytes. After expanding the cell body until reaching a neighbouring cell it is possible to define an area that encases a single OL and its primary processes. Red arrows indicate the same cells in both images. dsRED-transduced cells at OL3d, staining α-tubulin.

3.1.2. Development of an automated protocol for quantification of myelin production

To quantify OL myelin production, samples of mature OL (OL5d), which had previously been transduced with lentiviral-mediated shRNA and GFP reporter, were immunostained for MBP and Olig2, and counter-stained with DAPI. The protocol was specifically designed to identify MBP positive cells and was the following:

Step 1 – Seed: DAPI signal was segmented based on signal intensity and eroded to leave a small "seed" within the nucleus: small area within the nucleus which is later used to differentiate between adjacent cells **(Figure 30)**.

Step 2 – Nuclei: DAPI signal was segmented based on signal intensity. Adjacent cells were separated using a "clump breaking" function with seed as secondary target. Targets that were too big, too small or that did not meet the requirement for approximately circular shape were excluded **(Figure 30)**.

Step 3 – Measurements: mean pixel intensity within the cells area (density levels) was measured for GFP (FITC channel), MBP (Texas Red channel) and Olig2 (Cy5 channel) **(Figure 31)**.

Step 4 – Classifiers: cells were classified as Olig2 positive or negative ($Olig2^+/Olig2^-$) to exclude contaminating cells such as astrocytes and microglia, GFP positive or negative (GFP^+/GFP^-) to distinguish between transduced and untransduced cells and MBP positive or negative (MBP^+/MBP^-), all based on arbitrary thresholds for density levels.

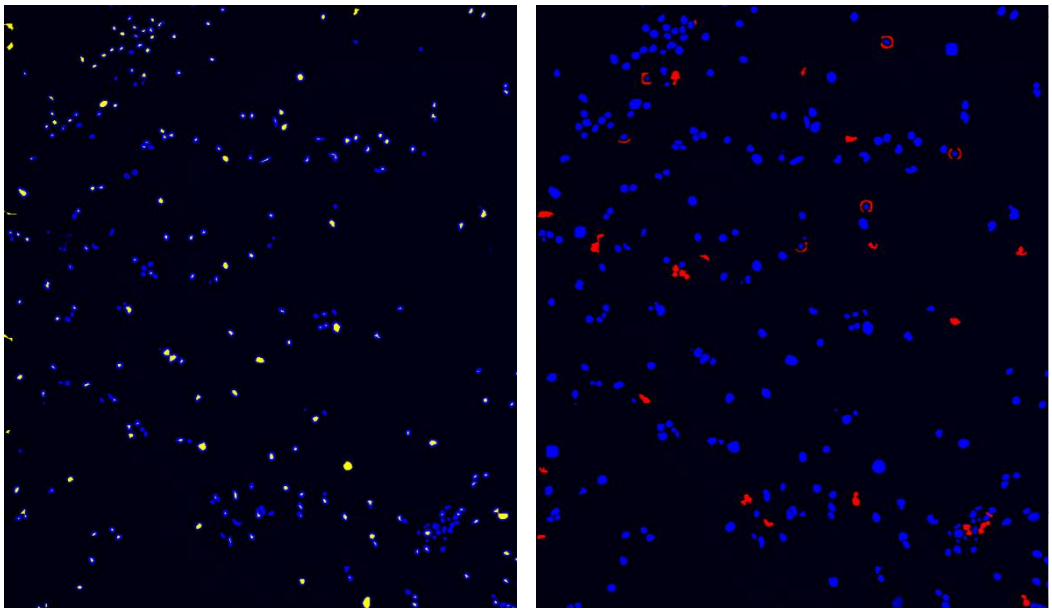

Figure 30 **Segmentation steps used in the automated protocol for analysis of MBP^+ cells.** Image on the left: example of segmentation of seed. Image on the right: example of segmentation of nuclei. Blue – DAPI, yellow – seed, red – targets excluded from segmentation.

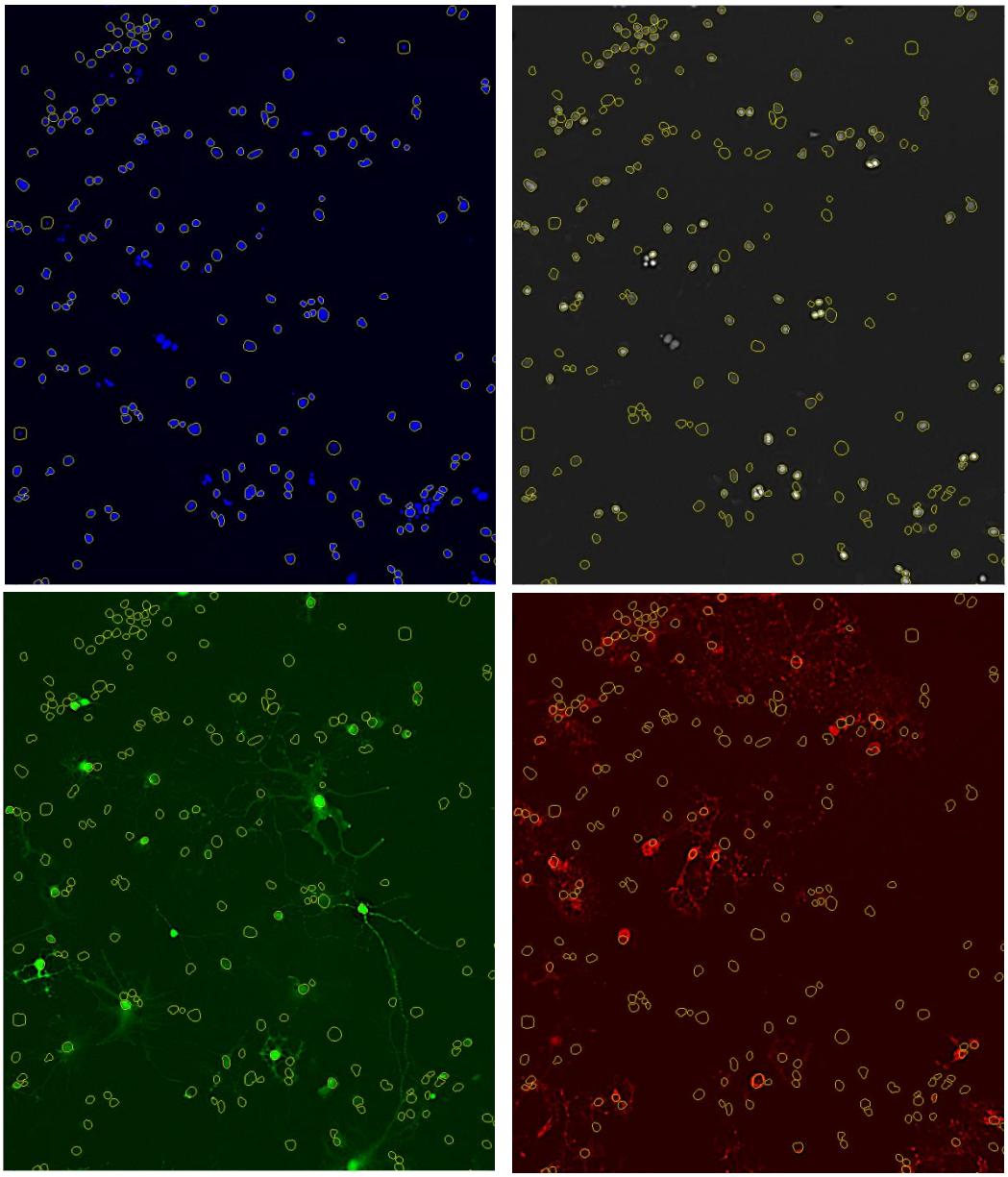

Figure 31 Result of the analysis using the automated protocol for MBP+ cells. Yellow circles outline the nuclei segmented using the DAPI signal. Density levels of Cy5 (grey, Olig2), FITC (green, GFP) and Texas Red (red, MBP) can then be measured within each circle to determine if cells are $Olig2^{+/-}$, $GFP^{+/-}$ and $MBP^{+/-}$.

After running the analysis protocol, the results were opened on Spotfire Decision Site software to verify if the applied intensity thresholds were appropriate to the sample. For example, if a cell appeared to have a high fluorescence intensity of Olig2 staining (classified as $Olig2^{+}$) but its morphology did not resemble that of an oligodendrocyte, then it was concluded that the threshold was too low and should be raised in order to exclude background or unspecific staining. After identifying the suitable thresholds for each channel, the protocol was run again. A table of results was further exported as an Excel file containing all fields analyzed, the number of identified targets, the density levels measured for each channel for every target and the classification of targets as

Olig2, GFP and MBP positive or negative. Only $Olig2^+$ targets were considered for quantification and, of these, the percentage of GFP^+/MBP^+ cells was determined. At least 1000 cells were analyzed per condition, per experiment using this method. The results obtained using this protocol are shown in the next section.

Overall, this analysis protocol was very successful in discriminating MBP positive from MBP negative cells, which is a reliable way to assess the degree of myelin production. It is ready to be used in other studies of OL where the percentage of MBP positive cells is an important parameter for the characterization of a phenotype.

3.2. Functional study of Kank2, Dusp19, PABPC1 and YBX1 in OL differentiation and myelination

An RNASeq analysis of the mRNA pools of OPC processes and soma previously done in the laboratory (Domingues, H. S., unpublished data) showed a differential expression of many transcripts between the two fractions. Most of the identified transcripts were enriched in the OPC processes and many of these were found to be related to cytoskeleton rearrangements and protein synthesis. In parallel, an *in silico* analysis searched for RNA binding proteins that could, putatively, interact with the 3’UTR of markers of OL differentiation and identified some molecules in common with the RNASeq (Cruz, A. unpublished data). Of these two data sets, 4 candidates were selected for functional validation in OPC/OL differentiation and myelin production: Kank2, Dusp19, PABPC1 and YBX1.

3.2.1. Kank2

Very little is known about the function of Kank2. Its mRNA has been found to be enriched in the protrusions of different cell types such as astrocytes processes (Thomsen and Nielsen, 2011) and NIH3T3 cells pseudopodia (Mili et al., 2008). Kank1 is known to inhibit RhoA activation by interaction with 14-3-3 proteins after phosphorylation of Kank1 by Akt (Kakinuma et al., 2008). This leads to a decrease in actin polymerization and formation of stress fibers. Kank1 also inhibits the formation of lamellipodia by preventing the interaction between Rac1 and IRSp53 (Roy et al., 2009). Over-expression of all other Kank isoforms (Kank2, Kank3 and Kank4) also inhibits the formation of actin stress fibers in NIH3T3 cells (Zhu et al., 2008). Very recently, Kank2 was identified as an interactor of RhoGDI in podocytes, enhancing RhoGDI-mediated inhibition of RhoA (Gee et al., 2015). When Kank2 is knocked-down, levels of active RhoA rise, possibly due to a lower interaction with RhoGDI. In OL, RhoA is an inhibitor of process extension and branching. When RhoA (Liang et al., 2004) or its effector kinase ROCK (O'Meara et al., 2013) is inhibited, OL become more differentiated. With this in mind, we hypothesize that Kank2 may be a regulator of RhoA in OL.

We have previously observed that Kank2 mRNA expression increases during *in vitro* OL differentiation and is enriched in the OPC processes. Moreover, Kank2 protein is found in CNS white matter regions such as optic nerve, cerebellum and spinal cord and it co-localizes with α-tubulin but not actin in all stages of OL differentiation *in vitro* (Domingues, H.S., unpublished data, not shown).

Next, to address the functional role of Kank2 in OL differentiation and myelination, a shRNA was designed and cloned into a lentiviral plasmid to deplete the mRNA expression. The knockdown efficiency of this shRNA was evaluated by quantitative real

time PCR at OL0d, 2 days post-infection (dpi). It was found that the shRNA for Kank2 had a knockdown efficiency of 60% **(Graph 2)**. However, taking into account the fact that the infection efficiency was never 100% but mostly between 40-50%, we predict an effective higher efficiency of this shRNA per infected cell.

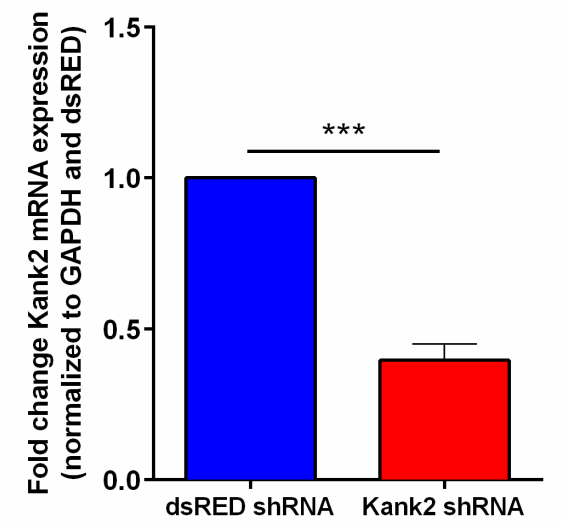

Graph 2 **Knockdown efficiency of Kank2 shRNA.** qPCR shows a reduction of Kank2 mRNA levels of 60% relative to GAPDH (reference gene) and to control cells infected with dsRED shRNA, at OL0d. N=5, bars represent mean plus SEM, one sample t-test, P<0.001(***).

In order to assess the effect of Kank2 knockdown in OL process extension and branching, we immunostained samples of OL3d (5 dpi) against the OL lineage-specific marker Olig2 and α-tubulin, and counter-stained with DAPI. GFP was used as a reporter of infection (dsRED shRNA or Kank2 shRNA). Fluorescence images were obtained using the INCell Analyzer 2000 microscope and manually analyzed by morphological categorization, as previously described by Thurnherr et al. (2006). Four stages of classification were established based on number of processes, degree of branching and cell symmetry **(Figure 32)**.

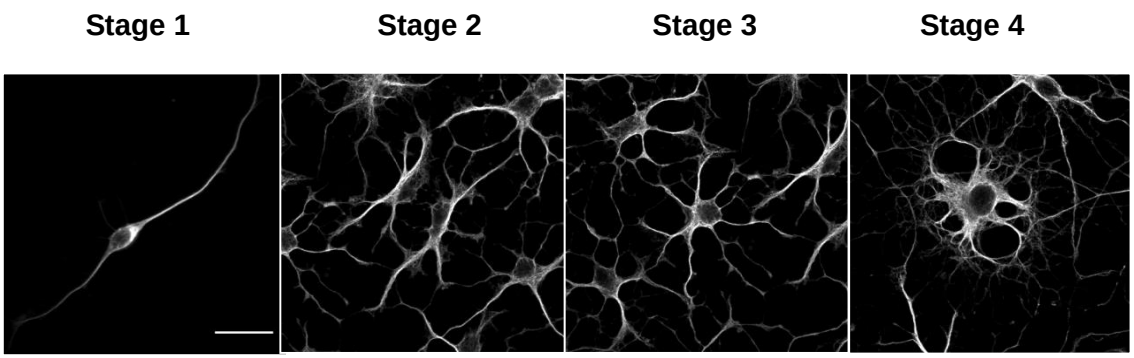

Figure 32 **Morphological categorization of OL development.** OL morphology was classified in four stages of increasing complexity. Staining: α-tubulin. Scale bar: 20μm.

Manual analysis by morphological categorization showed a delay in OL process extension and branching at OL3d (5 dpi) when Kank2 is knocked-down by shRNA, relative to control **(Figure 33, Graph 3)**. Although we only achieved statistical significance for stage 3, it can be observed an increased percentage of mutant cells in stages 1 and 2 and a reduction of the percentage of cells in stage 4, when compared with the control dsRED.

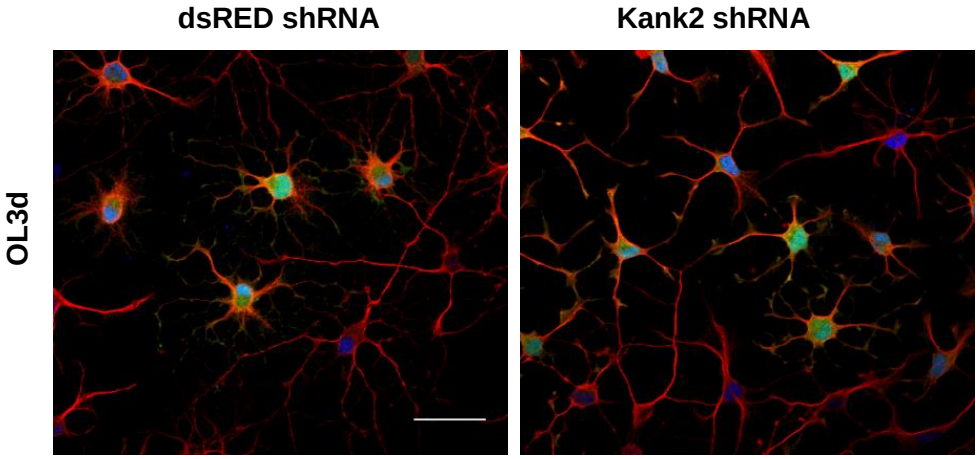

Figure 33 **Representative picture of control and Kank2 knockdown cells at OL3d.** Knockdown of Kank2 leads to less differentiated cells, relative to control. Green: GFP (reporter of infection), blue: Olig2 (marker for OL), red: α-tubulin. Scale bar: 30μm.

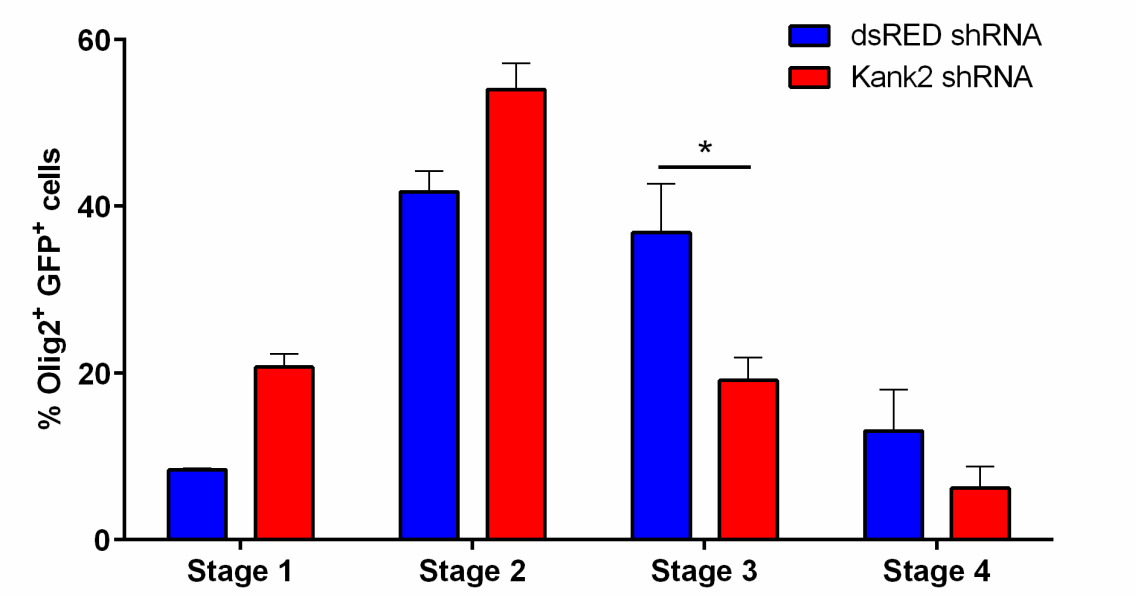

Graph 3 **Distribution of Olig2$^+$GFP$^+$ cells in four morphological stages.** Knockdown of Kank2 delays OL differentiation: cells accumulate in stages 1 and 2, leading to a reduction in the percentage of cells in stages 3 and 4 at OL3d, relative to control. N=3, bars represent mean plus SEM, two-way ANOVA, $P<0.05$ (*).

Afterwards, we performed immunostaining on samples of OL5d (7 dpi) to visualize myelin production. Cells were stained for Olig2 and MBP, and counter-stained with DAPI. GFP was used as a reporter of infection (dsRED shRNA or Kank2 shRNA). Fluorescence images were obtained using the INCell Analyzer 2000 microscope and analyzed using the automated protocol we developed with INCell Developer Toolbox software. We determined the percentage of MBP^+ cells and we observed that knocking down Kank2 significantly reduced the percentage of MBP^+ cells at OL5d (7dpi), relative to control **(Figure 34, Graph 4)**.

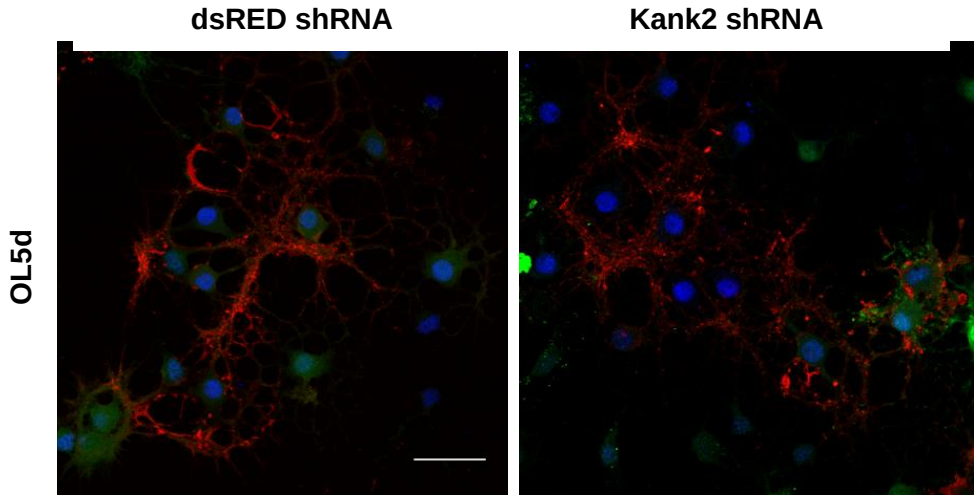

Figure 34 Representative picture of control and Kank2 knockdown cells at OL5d. Knockdown of Kank2 leads to less MBP^+ cells, relative to control. Green: GFP (reporter of infection), blue: Olig2 (marker for OL), red: MBP. Scale bar: 30µm.

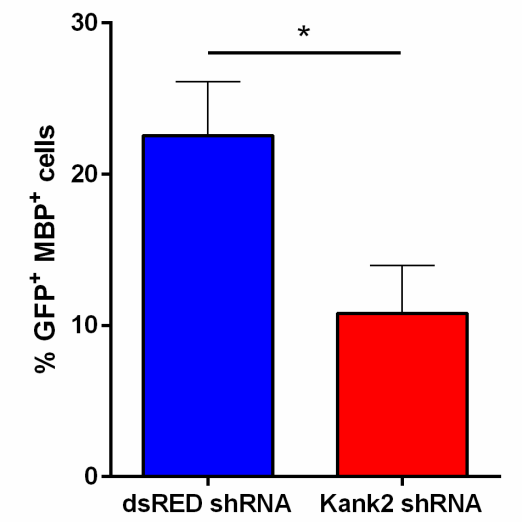

Graph 4 MBP production of control and Kank2 knockdown cells. Knockdown of Kank2 significantly impairs the percentage of MBP^+ cells at OL5d, relative to control. N=5, bars represent mean plus SEM, unpaired t-test, $P<0.05$ (*).

To verify if this reduction in MBP production was occurring also at mRNA level, we performed qPCR of OL at OL5d. This analysis showed, however, a non-significant reduction in the levels of MBP mRNA **(Graph 5)**.

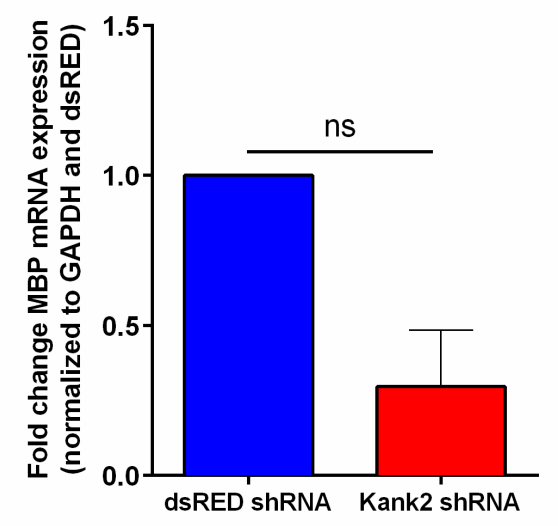

Graph 5 **Knockdown of Kank2 leads to a reduction of MBP mRNA levels.** qPCR shows a reduction of MBP mRNA relative to GAPDH (reference gene) and to control cells infected with dsRED shRNA, at OL5d. N=3, bars represent mean plus SEM, one sample t-test, ns – not significant.

These results suggest that knockdown of Kank2 delays OL differentiation and may inhibit the production of markers of myelination, in this case MBP. We hypothesize that Kank2 may play these roles through the modulation of RhoA signaling. If Kank2 is an interactor of RhoGDI in OL as in other models, the lack of Kank2 may lead to a down-regulation of RhoGDI and an up-regulation of RhoA, causing a delay in OL differentiation (Gee et al., 2015; Liang et al., 2004). To better understand the role of Kank2 in OL process extension, its relationship with RhoA must be addressed. By pulldown assay, we will soon investigate if the depletion of Kank2 causes any changes in the levels of active RhoA. If the pathway is conserved in OL as it has been described in NIH3T3 cells and podocytes(Gee et al., 2015; Zhu et al., 2008), then we expect to observe an activation of RhoA when Kank2 is depleted. Moreover, it would also be interesting to analyze the expression of other Kank isoforms (Kank1, Kank3 and Kank4) during OL differentiation and address if these are modulated in Kank2-depleted OL. Finally, R. Kyiama and co-workers have suggested that Kank isoforms may share similar functions after observing that over expression of all four Kanks had similar effect in stress fiber formation in NIH3T3 cells (Kakinuma et al., 2008; Zhu et al., 2008). These authors have recently provided us these constructs for all Kank isoforms and it will be interesting to address in the future if the different Kank isoforms play similar roles in OL process extension.

3.2.2. Dusp19

Dusp19 is a serine/threonine and tyrosine phosphatase involved in the regulation of ASK1/MKK7/JNK signaling (Zama et al., 2002b). However, it is not clear whether the function of Dusp19 in this pathway is as a phosphatase or as a scaffold protein (Zama et al., 2002a; Zama et al., 2002b). In OL, JNK/c-Jun signaling pathway is a known regulator of MBP production (Parkinson et al., 2008) and in neurons JNK/MAP1B signaling pathway is important for microtubule bundling and neurite elongation (Feltrin et al., 2012). This suggests a possible role of Dusp19 in OL process extension and myelination.

It has been previously observed that Dusp19 mRNA expression increases during *in vitro* OL differentiation and is enriched in the OPC processes. Also, Dusp19 protein is found in CNS white matter regions such as optic nerve, cerebellum and spinal cord and co-localizes with α-tubulin but not actin in all stages of OL differentiation *in vitro* (Domingues, H.S., unpublished data, not shown)

To evaluate the functional role of Dusp19 in OL differentiation and myelination, as done for Kank2, a shRNA was previously designed and cloned into a lentiviral plasmid to deplete the mRNA expression. It was found by qPCR that the shRNA for Dusp19 had a knockdown efficiency of 66% at OL0d (2dpi) **(Graph 6)**. As described for Kank2, the efficiency of Dusp19 shRNA per infected cell is expected to be higher.

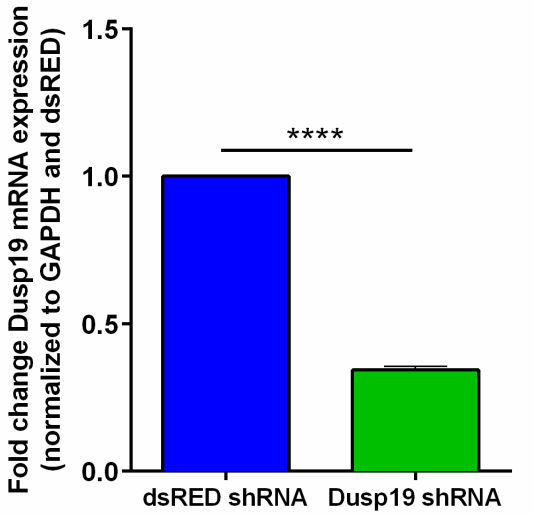

Graph 6 **Knockdown efficiency of Dusp19 shRNA.** qPCR shows a reduction of Dusp19 mRNA levels of 66% relative to GAPDH (reference gene) and to control cells infected with dsRED shRNA, at OL0d. N=4, bars represent mean plus SEM, one sample t-test, P<0.0001(****).

In order to assess the effect of Dusp19 knockdown in OL process extension and branching, we performed immunocytochemistry on samples at OL3d (5 dpi). As described for Kank2, cells were immunostained against Olig2 and α-tubulin, and counter-stained with DAPI **(Figure 32)**. Categorization analysis showed a delay in OL

differentiation when Dusp19 is knocked down by shRNA **(Figure 35, Graph 7)**. Similarly to Kank2 knockdown, we only achieved statistical significance for stage 3, but it can be observed there is an increase of the percentage of mutant cells in stages 1 and 2 and a reduction of the percentage of cells in stage 4, when compared with dsRED control.

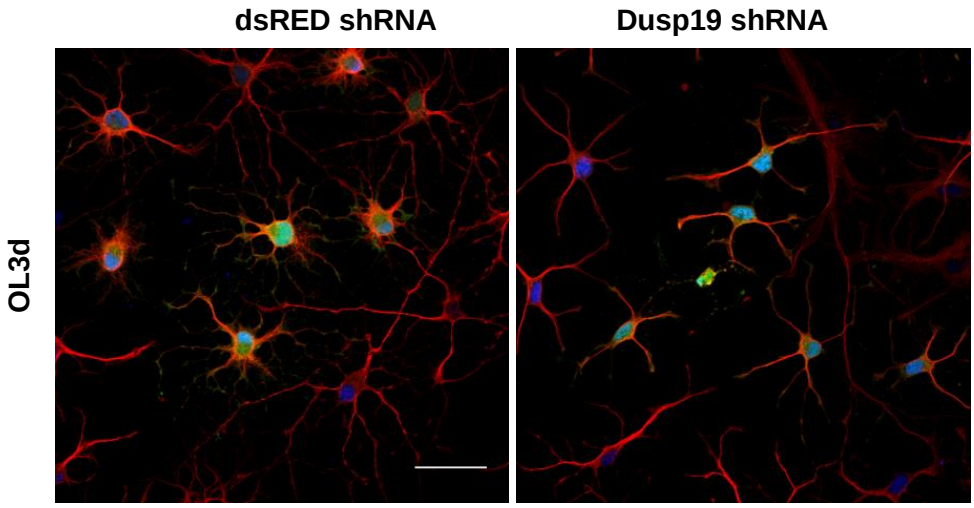

Figure 35 **Representative picture of control and Dusp19 knockdown cells at OL3d.** Knockdown of Dusp19 leads to less differentiated cells, relative to control. Green: GFP (reporter of infection), blue: Olig2 (marker for OL), red: α-tubulin. Scale bar: 30μm.

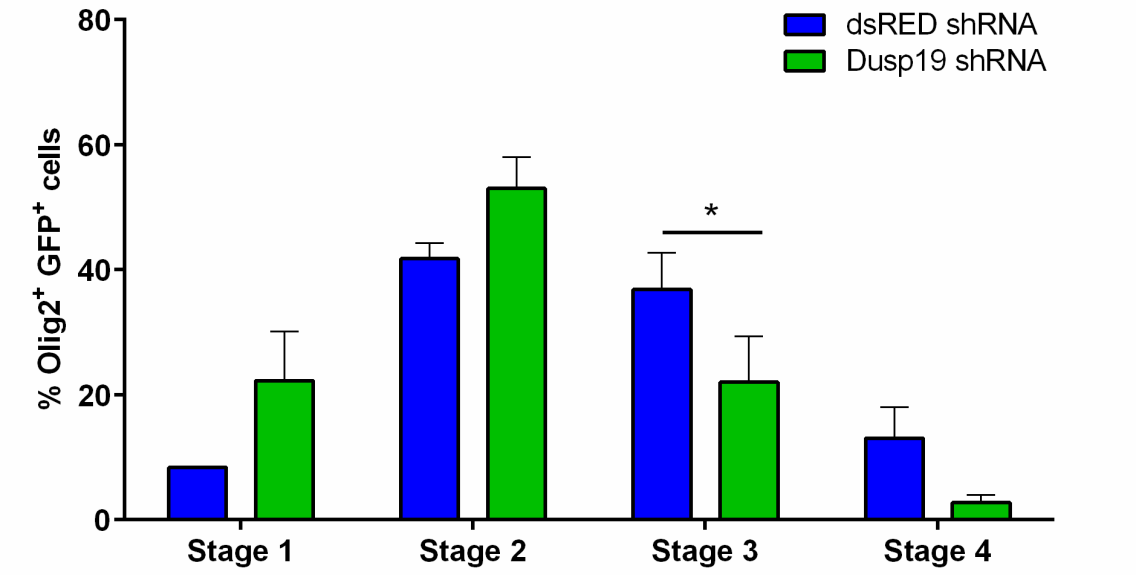

Graph 7 **Distribution of Olig2$^+$GFP$^+$ cells in four morphological stages.** Knockdown of Dusp19 delays OL differentiation: cells accumulate in stages 1 and 2, leading to a reduction in the percentage of cells in stages 3 and 4 at OL3d, relative to control. N=3, bars represent mean plus SEM, two-way ANOVA, P<0.05 (*).

Afterwards, we analyzed samples of OL5d (7 dpi) to quantify the percentage of infected OL producing myelin. Likewise, cells were immunostained against Olig2 and MBP, and counter-stained with DAPI. Interestingly. the quantification of infected MBP^+ OL using the automated analysis protocol we developed (described in section 3.1) showed the absence of Dusp19 significantly decreased the percentage of MBP^+ cells at OL5d, relative to the control **(Figure 36, Graph 8)**.

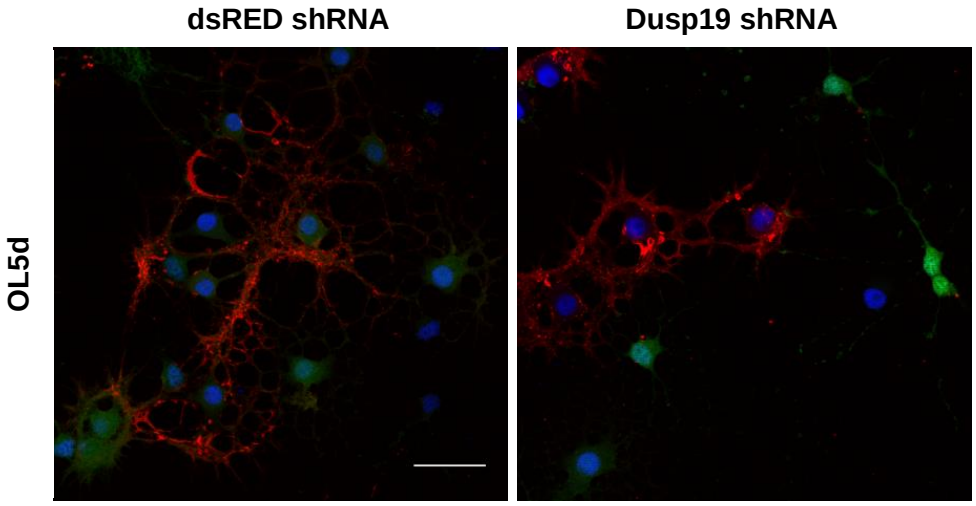

Figure 36 **Representative picture of control and Dusp19 knockdown cells at OL5d.** Knockdown of Dusp19 leads to less MBP^+ cells, relative to control. Green: GFP (reporter of infection), blue: Olig2 (marker for OL), red: MBP. Scale bar: 30µm.

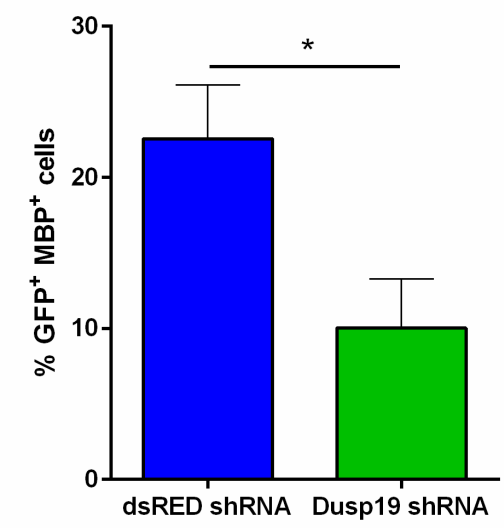

Graph 8 **MBP production of control and Dusp19 knockdown cells.** Knockdown of Dusp19 significantly impairs the percentage of MBP^+ cells at OL5d, relative to control. N=5, bars represent mean plus SEM, unpaired t-test, $P<0.05$ (*).

We also analyzed the expression of MBP by qPCR and observed a significant reduction in the levels of MBP mRNA **(Graph 9)** in the absence of Dusp19, showing a positive correlation between the mRNA and protein levels of MBP.

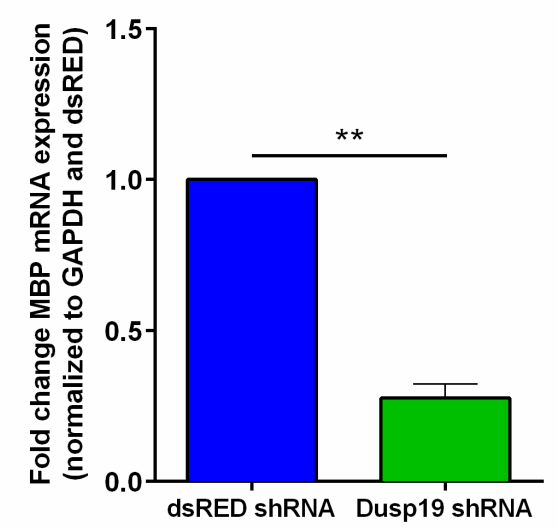

Graph 9 **Knockdown of Dusp19 leads to a reduction of MBP mRNA levels.** qPCR shows a reduction of MBP mRNA relative to GAPDH (reference gene) and to control cells infected with dsRED shRNA, at OL5d. N=3, bars represent mean plus SEM, one sample t-test, $P < 0.01$ (**).

These results suggest that, by knocking down Dusp19, OL differentiation is delayed. We hypothesize that this may be due to an inhibition of ASK1/MKK7/JNK signaling complex assembly or to a direct dephosphorylation of MKK7 by Dusp19. This may lead to a down-regulation of JNK phosphorylation and, consequently, dephosphorylation of MAP1B and disassembly of microtubule bundles inside OL processes as described in neurons (Feltrin et al., 2012). Depletion of Dusp19 also led to a decrease in the percentage of MBP^+ cells and in MBP mRNA levels, relative to control. We have not seen any differences in the levels of phospho-c-Jun in control and Dusp19-depleted OL (Western Blotting, data not shown). It is possible that during OL process extension, Dusp19 works as a scaffold protein and not as a phosphatase. Therefore, knocking down Dusp19 may be affecting the MKK7-JNK-MAP1B pathway without affecting directly myelination through the JNK-c-Jun interaction. Additionally, it is known that OL differentiation is a two-step inter-dependent process: first, processes are extended and ramified and, later, production of myelin components is initiated. Therefore, the inhibition of process extension through the MKK7-JNK-MAP1B pathway by the depletion of Dusp19 may consequently compromise the necessary signals to induce MBP synthesis. This would justify why we observe less myelinated OL when Dusp19 is depleted. To understand if and how Dusp19 knockdown affects the JNK pathway, protein levels and phosphorylation state of JNK pathway molecules, such as MKK7,

JNK and MAP1B will, in the near future, be quantified in control and Dusp19 knockdown cells by Western Blotting.

3.2.3. Sholl Analysis of Kank2 and Dusp19 knockdown

In order to get a quantitative measure of the degree of OL differentiation, the Sholl analysis technique was applied to the images previously analyzed by morphological categorization. This analysis was applied only to cells that were Olig2$^+$, GFP$^+$ and representative of the morphologies previously observed. After thresholding images for signal intensity using α-tubulin staining and correcting the scale, Olig2$^+$/GFP$^+$ cells were selected and a straight line was traced from the cell body to the extremity of the longest process (without intersecting with neighboring cells). Finally, Sholl Analysis plugin was run, with step size between Sholl Ring radii of 5μm and 3 samples per radius. This analysis showed a significant reduction in the number of intersections between processes and a Sholl ring at a distance of 20μm from the cell body when cells were depleted of Kank2. This means that Kank2-depleted cells are less differentiated than control cells. Nevertheless, no differences were observed between control and Dusp19-depleted cells at all distances considered. One of the reasons that may have contributed to these results is the high variability observed in Sholl profiles of control cells **(Graph 10).** This is probably due to the high confluency of these cultures, which made it difficult to find cells that were infected and sufficiently isolated, so that the Sholl rings would not intersect processes of neighboring cells. Because of that, only 30 cells were analyzed per condition per experiment. If we had analyzed a greater number of cells per experiment, we might have reduced the error. Since OL differentiate better *in vitro* when in close proximity, it is possible that the cells selected for Sholl analysis were less differentiated because of the greater distance between them and their neighbors.

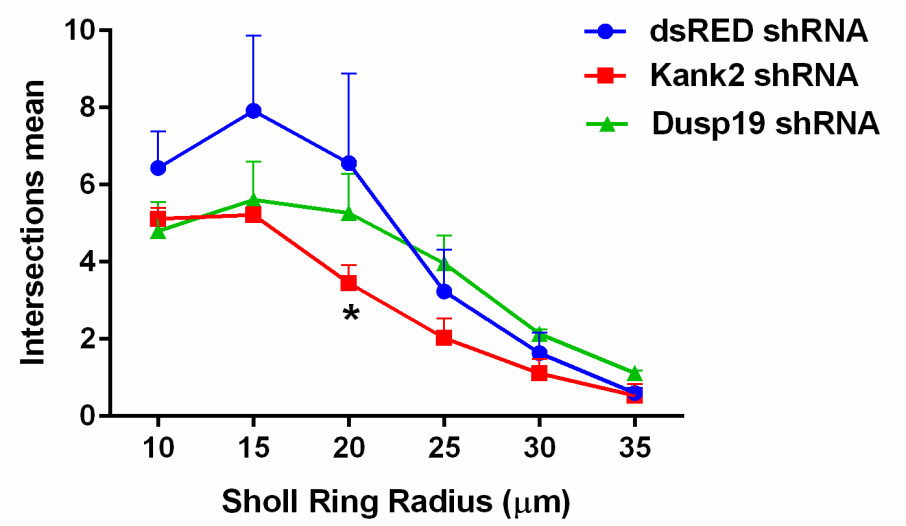

Graph 10 **Sholl Analysis of OL at OL3d.** Graphical representation of the mean number of intersections as a function of Sholl Ring radius. For the control, as Sholl Ring radius increases, the number of intersections peaks indicating an increase in the number of processes and branches, and then decreases because there are fewer cells with longer processes. A lower number of intersections for Kank2 and Dusp19 knock-down indicates these cells are less differentiated. At 20μm in radius, Kank2 knock-down is significantly different from control. N=3, points represent mean plus SEM, two-way ANOVA, Bonferroni's test P<0.05 (*).

3.2.4. PABPC1

PABPC1 is an RNA-binding protein necessary for RNA stability, transport and translation, through binding to PolyA tails. It may also bind regulatory regions in the 3’UTR of many mRNAs, including markers of OL differentiation such as MBP (*in silico* analysis, Cruz, A., unpublished data). In HeLa cells, depletion of PABPC1 impaired mRNA translation, but not transcription, and led to apoptosis (Zannat et al., 2011). Over-expression of PABPC1 caused a decrease in mRNA levels of several genes due to changes in mRNA stability (Ma et al., 2006). This induced a feedback mechanism led by PABPC1 binding to a regulatory region in the 3’UTR of MKK2 mRNA, which destabilized it leading to a decrease in MKK2 mRNA and protein levels. Reduced levels of MKK2 inhibited the phosphorylation of PABPC1, preventing it from binding to mRNAs and causing more adverse effects.

PABPC1 mRNA is significantly enriched in OPC processes and its expression levels decrease during OL differentiation *in vitro*. At the protein level, PABPC1 can be seen in the brain and in cultured OL *in vitro* by immunohistochemistry (Domingues, H.S. and Cruz, A., unpublished data, not shown).

As previously described, to study the functional role of PABPC1 in OL differentiation and myelination, a shRNA was designed and cloned into a lentiviral plasmid to deplete the mRNA expression. By qPCR, it was found that the shRNA for PABPC1 had a knockdown efficiency of 80% at OL3d (3 dpi) **(Graph 11)**.

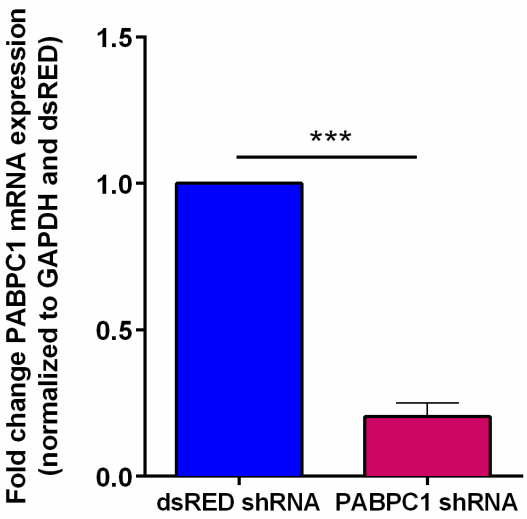

Graph 11 **Knockdown efficiency of PABPC1 shRNA.** qPCR shows a reduction of PABPC1 mRNA levels of 80% relative to GAPDH (reference gene) and to control cells infected with dsRED shRNA, at OL5d. N=4, bars represent mean plus SEM, one sample t-test, P<0.001(***).

Again, to evaluate the effect of PABPC1 knockdown in OL process extension and branching, we performed immunocytochemistry of samples of OL3d (3 dpi).as described for Kank2 and Dusp19 **(Figure 32)**. Manual analysis shows a delay in OL process extension and ramification at OL3d when PABPC1 is knocked-down by shRNA, relative to control. **(Figure 37, Graph 12)**. In this condition, there is a significant difference in the percentage of cells in stage 2 for the knockdown relative to control. Although not statistically significant, it can be observed there is a decrease of the percentage of cells in stages 3 and 4, relative to the control.

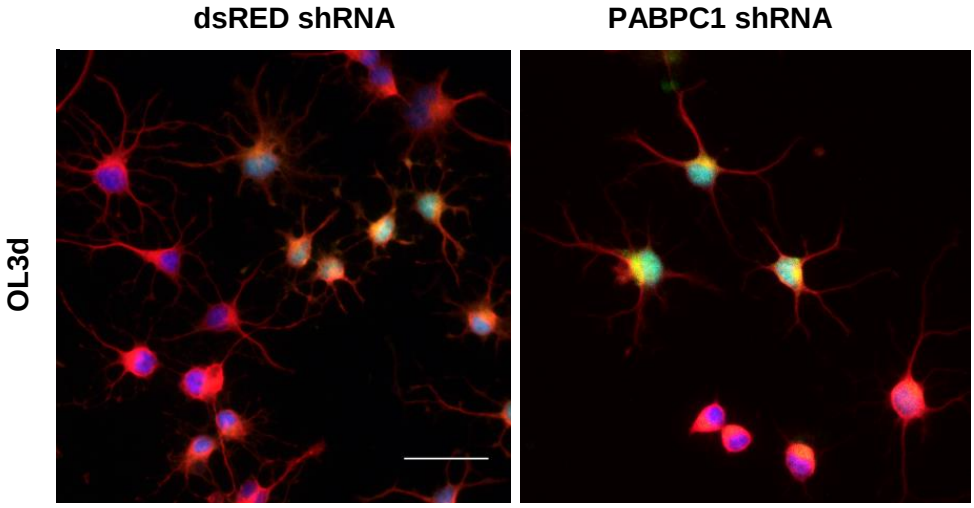

Figure 37 **Representative picture of control and PABPC1 knockdown cells at OL3d.** Knockdown of PABPC1 leads to less differentiated cells, relative to control. Green: GFP (reporter of infection), blue: Olig2 (marker for OL), red: α-tubulin. Scale bar: 30μm.

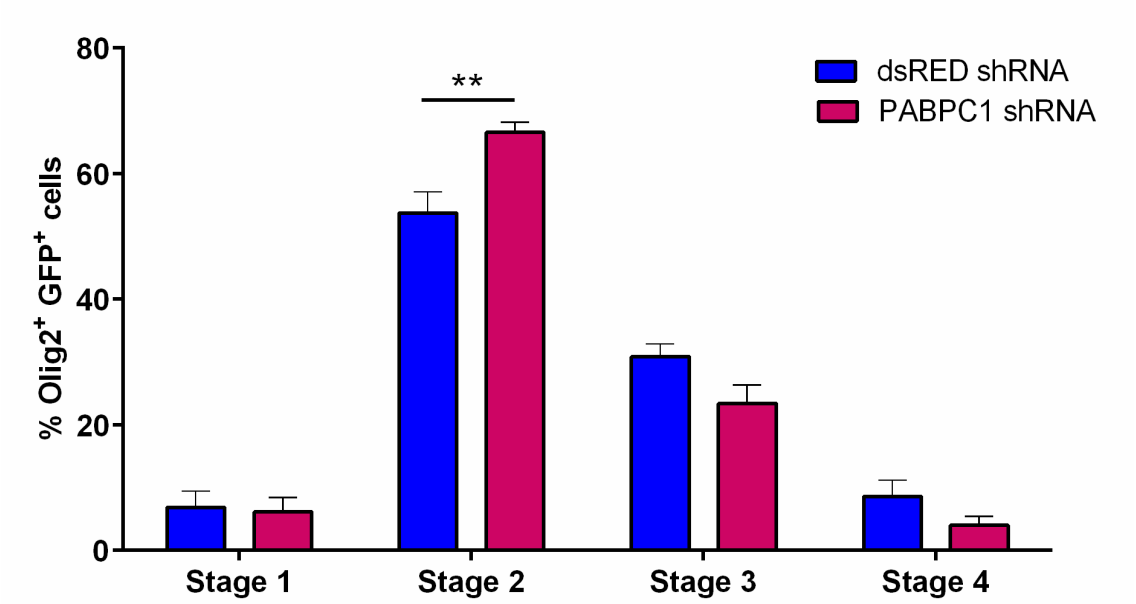

Graph 12 **Distribution of Olig2$^+$GFP$^+$ cells in four morphological stages.** Knockdown of PABPC1 delays OL differentiation: cells accumulate in stage 2, leading to a reduction in the percentage of cells in stages 3 and 4 at OL3d, relative to control. N=5, bars represent mean plus SEM, two-way ANOVA, Bonferroni’s test, P<0.01 (**).

Next, we performed immunostaining of samples of OL5d (5 dpi) to quantify the production of myelin, as done for Kank2 and Dusp19. Similarly, automated analysis of MBP^+ cells using the automated protocol showed that knockdown of PABPC1 impairs MBP production at OL5d **(Figure 38, Graph 13)**. Interestingly, due to the high variability between experiments, this difference is not statistically significant if results are expressed in percentage. However, if they are expressed in fold change relative to control, it becomes highly significant (P<0.01).

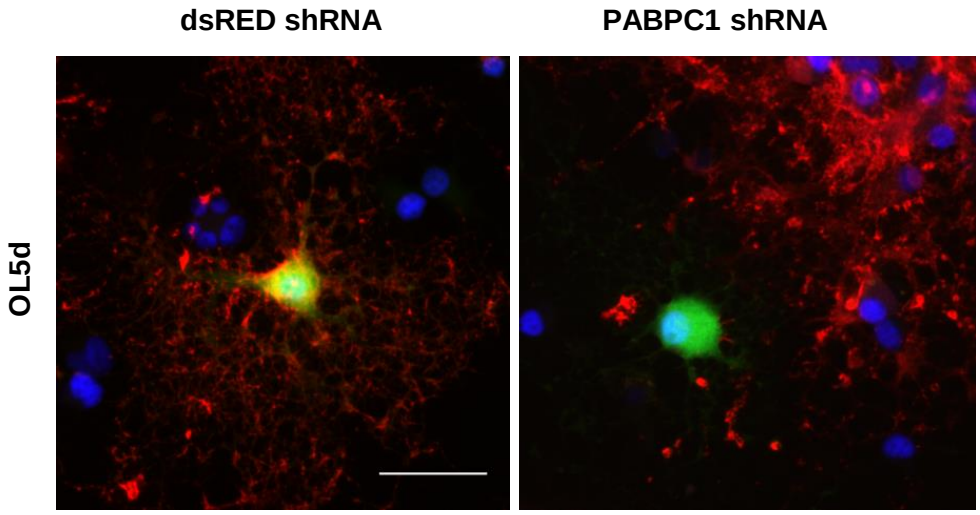

Figure 38 Representative picture of control and PABPC1 knockdown cells at OL5d. Knockdown of PABPC1 leads to less MBP^+ cells when compared to control. Green: GFP (reporter of infection), blue: Olig2 (marker for OL), red: MBP. Scale bar: 30µm.

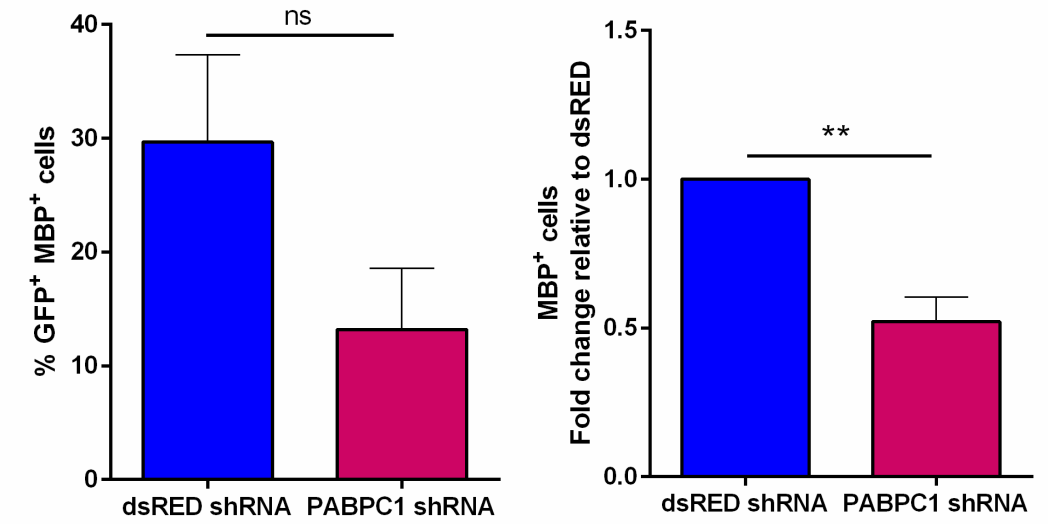

Graph 13 MBP production of control and PABPC1 knockdown cells. Knockdown of PABPC1 significantly impairs the percentage of MBP^+ cells at OL5d, if results are expressed as fold change relative to control. N=5, bars represent mean plus SEM, unpaired t-test, ns – not significant (left graph) and one sample t-test, P<0.01 (**) (right graph).

To confirm the decrease in MBP$^+$ cells by immunocytochemistry, qPCR for MBP was performed. This analysis showed a significant reduction in the levels of MBP mRNA **(Graph 14)**.

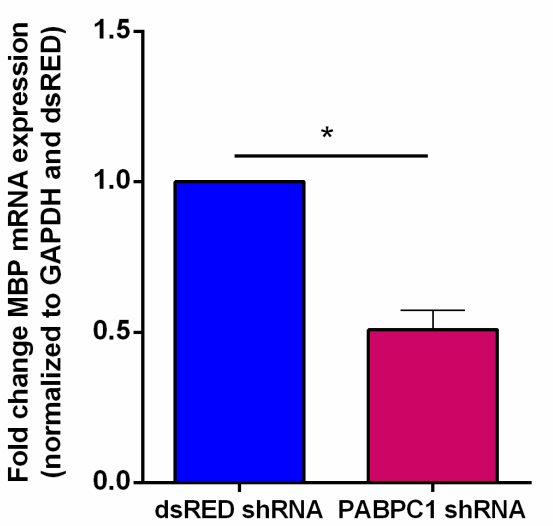

Graph 14 Knockdown of PABPC1 leads to a reduction of MBP mRNA levels. qPCR shows a reduction of MBP mRNA relative to GAPDH (reference gene) and to control cells infected with dsRED shRNA, at OL5d. N=3, bars represent mean plus SEM, one sample t-test, $P < 0.05$ (*).

These results indicate that PABPC1 may act as a promoter of both process extension and myelination in *in vitro* cultured OL. However, we do not know if this is due to the role of PABPC1 as a PolyA-binding protein or as a trans-acting regulator of mRNA stability and translation through 3’UTR sequences.

Further investigation is needed to understand the mechanism by which PABPC1 depletion impairs OL process extension and myelination: it may be due to a general impairment of protein synthesis or a specific regulation of cytoskeleton and myelin genes. The PBS Finder software developed by A. Cruz could be used to identify putative binding sites of PABPC1 to mRNAs of cytoskeleton-related genes, such as integrins, Rho GTPases and molecules in MAPK signaling pathway.

3.2.5. YBX1

YBX1 is an RBP involved in processes such as DNA replication, transcription and translation. In the cytoplasm, it can act as a packaging protein of RNPs (Minich and Ovchinnikov, 1992) and it regulates translation in a dose-dependent manner, inhibiting translation at high YBX1-mRNA ratios and promoting it at low ratios by unfolding RNPs (Skabkin et al., 2004) In OL, YBX1 binds directly to MBP mRNA (RNA immunoprecipitation assay, Cruz, A., unpublished data, not shown) and may bind to other markers of OL differentiation (*in silico* analysis, Cruz, A., unpublished data, not shown).

YBX1 mRNA expression levels peak at OL3d stage of OL differentiation *in vitro*. At the protein level, YBX1 can be seen in the brain and in cultured OL *in vitro* (Domingues, H.S. and Cruz, A., unpublished data, not shown).

As before, to assess the functional role of PABPC1 in OL differentiation and myelination, a shRNA was designed and cloned into a lentiviral plasmid to deplete the mRNA expression By qPCR, it was found that the shRNA for YBX1 had a knockdown efficiency of 56% at OL3d (3 dpi) **(Graph 15)**.

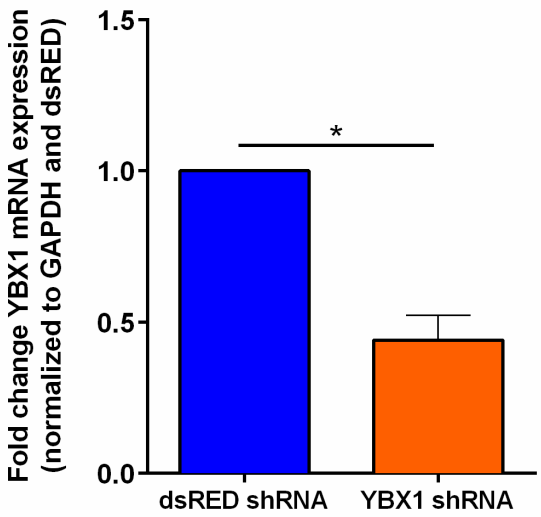

Graph 15 **Knockdown efficiency of YBX1 shRNA.** qPCR shows a reduction of YBX1 mRNA levels of 56% relative to GAPDH (reference gene) and to control cells infected with dsRED shRNA, at OL5d). N=3, bars represent mean plus SEM, one sample t-test, P<0.05(*).

Again, to evaluate the effect of PABPC1 knockdown in OL process extension and branching, we performed immunostaining on samples of OL3d (3 dpi) as previously described **(Figure 32)**. Morphological categorization shows a delay in OL differentiation when YBX1 is knocked-down by shRNA at OL3d **(Figure 39, Graph 16)**. In this condition, there is a statistically significant increase in the percentage of cells in stage 2

and a reduction in the percentage of cells in stage 3, relative to control. Despite the lack of statistical significance, an increase in the percentage of cells in stage 1 and a reduction in stage 4 can be observed as well.

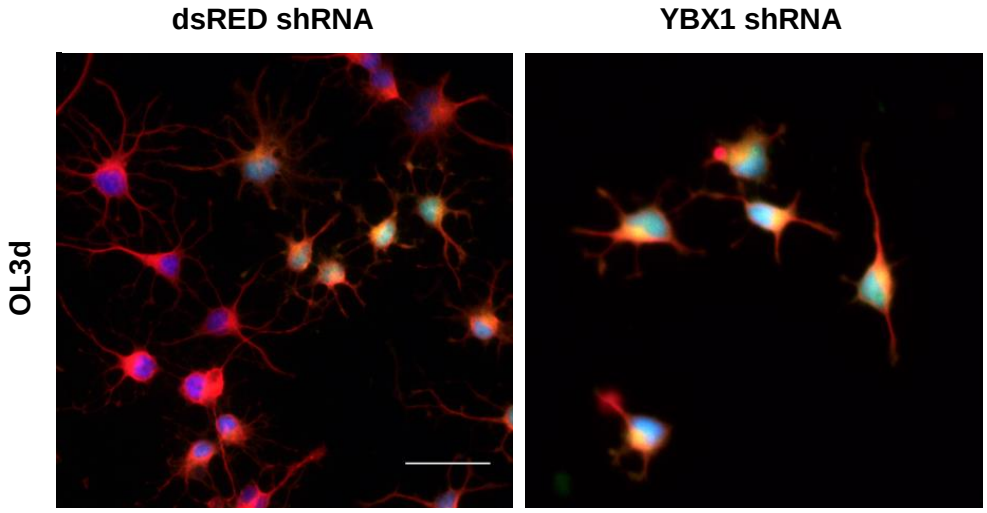

Figure 39 Representative picture of control and YBX1 knockdown cells at OL3d. Knockdown of YBX1 leads to less differentiated cells relative to control. Green: GFP (reporter of infection), blue: Olig2 (marker for OL), red: α-tubulin. Scale bar: 30μm.

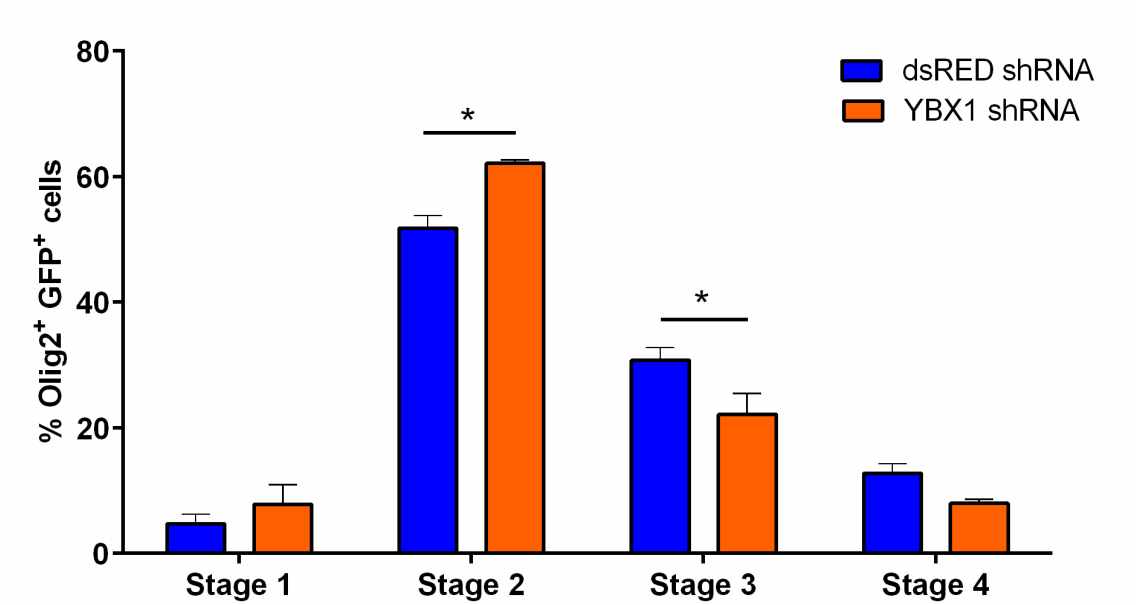

Graph 16 Distribution of Olig2^{+}GFP^{+} cells in four morphological stages. Knockdown of YBX1 delays OL differentiation: cells accumulate significantly in stage 2, leading to a significant reduction in the percentage of cells in stages 3 at OL3d, relative to control. N=3, bars represent mean plus SEM, two-way ANOVA, Bonferroni’s test, P<0.05 (*).

Then, we performed ICC on samples of OL5d (5 dpi) to visualize the production of myelin, as previously. Automated analysis of MBP$^+$ cells using the INCell Developer Toolbox showed a non-significant increase in the percentage of MBP$^+$ cells at OL5d when YBX1 is knocked-down, relative to control **(Figure 40, Graph 17)**.

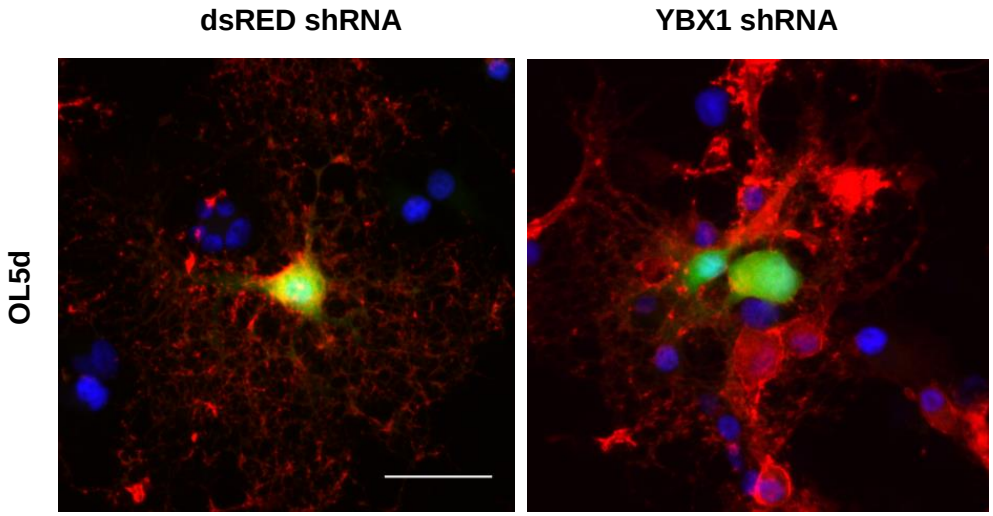

Figure 40 **Representative picture of control and YBX1 knockdown cells at OL5d.** Knockdown of YBX1 does not alter the percentage of MBP$^+$ cells when compared to control. Green: GFP (reporter of infection), blue: Olig2 (marker for OL), red: MBP. Scale bar: 30μm.

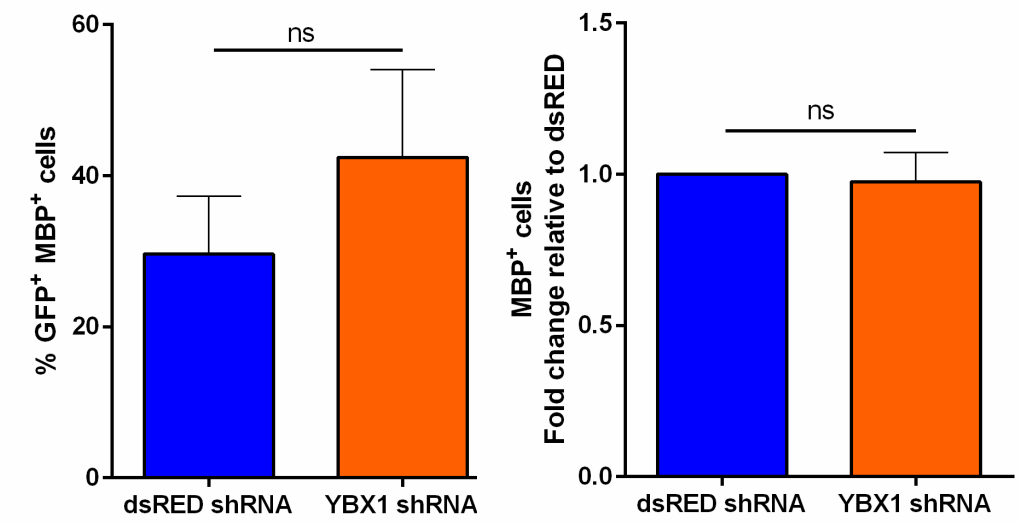

Graph 17 **MBP production of control and YBX1 knockdown cells.** Knockdown of YBX1 causes a non-significant increase in the percentage of MBP$^+$ cells at OL5d. N=3, bars represent mean plus SEM, unpaired t-test (left graph) and one sample t-test (right graph), ns – not significant.

qPCR for MBP was performed to verify the previous result. This showed an increase in the levels of MBP mRNA **(Graph 18)**.

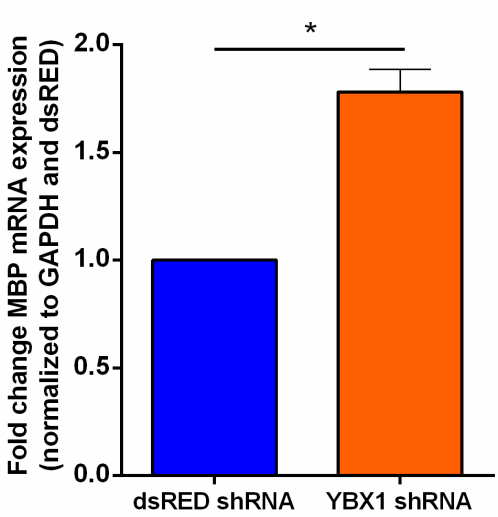

Graph 18 **Knockdown of YBX1 leads to an increase of MBP mRNA levels.** qPCR shows an increase of MBP mRNA relative to GAPDH (reference gene) and to control cells infected with dsRED shRNA, at OL5d. N=3, bars represent mean plus SEM, one sample t-test, $P < 0.05$ (*).

Knockdown of YBX1 has a clear effect in the delay of OL process extension and branching, as shown by the statistically significant increase of the percentage of cells in morphological stage 2 and decrease of the percentage of cells in stage 3. To understand the role of YBX1 in OL process extension we should look for interactions between YBX1 and regulators of cytoskeleton dynamics. Again, the PBS Finder may be a useful tool for the identification of putative candidates for functional studies.

Relatively to MBP, the knockdown of YBX1 presents a very interesting result that suggests a decoupling between process extension and myelin production. The increase in mRNA levels is accompanied by a non-significant increase in the percentage of MBP^+ cells. Despite being transcribed at early stages of OL development, MBP is only translated later on (Laursen et al., 2011). YBX1 binding to MBP mRNA may be necessary to maintain it silenced until the cell receives the appropriate stimulus to initiate translation. By depleting YBX1, we may have promoted MBP translation at an earlier time point, which is why YBX1 knockdown cells have a slightly greater percentage of MBP positive staining than control cells at OL5d. This change in MBP mRNA turnover may also be responsible for the increase in mRNA levels observed. To shed light on this possibility, we are working on determining the percentage of MBP^+ cells at OL3d. This will tell us if MBP production is being anticipated in YBX1-depleted cells, relative to control.

4. Conclusions

The main function of oligodendrocytes is to establish and maintain myelin sheaths around axons. To do so, they must extend cytoplasmic processes, alter their shape to enwrap an axon and produce proteins essential for myelin compaction. These processes demand great cytoskeletal changes and timed protein synthesis in order to ensure efficient myelination.

In this Master thesis, we aimed to characterize the function of four proteins in OL differentiation and myelination *in vitro*. Kank2 and Dusp19 are two novel identified regulators of OL differentiation. These were previously identified in an RNAseq screen that compared mRNA fractions obtained from the soma and processes of OPC, being enriched in the OPC processes (Domingues, H.S., unpublished data). PABPC1 and YBX1 are two known RNA-binding proteins and were also identified to be enriched in the OPC processes. PABPC1 appears to bind to 3’UTR of mRNAs of all known OL differentiation markers, such as NG2, Olig1 and 2, PDGFRα, CNP, MBP, MOBP, MOG, MAG and PLP1, whereas YBX1 appears to bind mostly to earlier ones, such as Olig1 and 2, PDGFRα and CNP, but it may also bind to the late markers MBP and MOBP (Cruz, A., unpublished data).

Our approach to address the function of these proteins in OL differentiation was to deplete their mRNA expression via lentivirus-mediated shRNA delivery. We validated the knockdown efficiency of these shRNAs by qPCR and studied their effect in OL process extension and ramification, as well as production of MBP, by fluorescence microscopy and qPCR.

We found that knockdown of Kank2, Dusp19 and PABPC1 impaired both OL process extension (cells accumulated in earlier morphological stages and did not progress to later stages, when compared to control) and myelin production (the percentage of MBP^+ cells was significantly reduced when compared to control).

Kank2 is an inhibitor of RhoA in podocytes, through interaction with RhoGDI (Gee et al., 2015). When Kank2 is knocked down, levels of active RhoA rise and when it is over-expressed in NIH3T3 cells they decrease, which is accompanied by a reduction in the formation of actin stress fibers (Zhu et al., 2008). In OL, RhoA is an inhibitor of process extension and branching: when RhoA (Liang et al., 2004) or ROCK (O'Meara et al., 2013) is inhibited, OL become more differentiated. In our experiments, knockdown of Kank2 led to a delayed morphological differentiation of OL and to lower levels of MBP production, consistent with the putative role of Kank2 as an inhibitor of RhoA.

Dusp19 is a serine/threonine and tyrosine phosphatase involved in the regulation of ASK1/MKK7/JNK signaling (Zama et al., 2002b). Knockdown of Dusp19 may impair JNK-MAP1B signaling, which could inhibit OL process extension (given its role in neurite elongation (Feltrin et al., 2012)), consistent with our observations. Given the role of c-Jun as an inhibitor of MBP transcription, Dusp19 knockdown could inactivate c-Jun and cause an increase in MBP mRNA levels, which we did not observe. On the other hand, the delay in process extension could compromise the reception of MBP production-inducing signals by the cell, without interfering with c-Jun. Therefore, other molecules must be at play, which requires further investigation.

PABPC1 is an RNA-binding protein necessary for the regulation of mRNA translation (Kahvejian et al., 2005) and degradation (Ford et al., 1997). Given its ubiquitous role in binding the polyA tails of mRNAs and its putative binding to the 3’UTR of OL markers of differentiation and myelin genes, its knockdown should impair many cellular functions. In fact, we observed a delay in OL process extension and MBP expression, which means PABPC1 may be an essential promoter of both processes.

On the other hand, knockdown of YBX1 delayed process extension but increased MBP levels, suggesting a decoupling of the two mechanisms. YBX1 is an RBP that can act as a packaging protein of RNPs (Minich and Ovchinnikov, 1992) regulating translation in a dose-dependent manner, either inhibiting or promoting it depending on the YBX1-mRNA ratio (Skabkin et al., 2004) In OL, it binds directly to MBP mRNA (RNA immunoprecipitation assay, Cruz, A., unpublished data, not shown) and may bind to other markers of OL differentiation (*in silico* analysis, Cruz, A., unpublished data, not shown). Regarding MBP production, there was a non-significant increase in the percentage of MBP^+ cells at OL5d and mRNA levels of MBP were higher than those of control cells. Despite being transcribed at early stages of OL development, MBP is not translated until a later stage is reached (Laursen et al., 2011). Binding of YBX1 to MBP mRNA could be a silencing mechanism to prevent MBP production until the cell receives an appropriate stimulus. By depleting OL of YBX1, we may have induced MBP translation at an earlier time point, which is why YBX1 knockdown cells have a slightly greater percentage of MBP positive staining compared to control at OL5d. This alteration in the rate of MBP translation may also be accompanied by changes in transcription and/or degradation, which may be responsible for the increase in mRNA levels observed.

5. Future perspectives

The next steps in this project are the dissection of signaling pathway mechanisms involving Kank2, Dusp19, PABPC1 and YBX1, and to continue the improvement of the automated high-throughput analysis protocol.

We are currently working with CG4 (a rat oligodendrocyte cell line) and NIH3T3 cells (a mouse fibroblast cell line) to perform biochemical analysis of RhoA activity by pulldown in control and Kank2 knockdown cells. This will allow us to see if there are any alterations in RhoA levels and activity. We are also going to look at the expression of other Kank family members (Kank1, 3 and 4) in control and Kank2 knockdown cells to see if there is any compensatory or synergistic effect with Kank2 in OL differentiation. We are also going to evaluate the effect of over-expressing the different Kank isoforms (plasmids were a courtesy of Dr. Ryoiti Kiyama, Japan).

Regarding Dusp19, we are focusing on the JNK pathway by looking at JNK protein levels and phosphorylation state in control and Dusp19 knockdown cells. We will also look at the levels other JNK pathway molecules like MKK7 and MAP1B, total and phosphorylated forms. In collaboration with Dr. Fatiha Nothias (France), we will analyze the role of Dusp19 in MAP1B phosphorylation through JNK (Barnat et al., 2010).

In what respects the RNA-binding proteins, PABPC1 and YBX1, we will look at their relationship after knockdown (collaboration with Dr. Andrea Cruz). We hypothesize they regulate each other during OL development. We are also investigating whether MBP production in YBX1 knockdown cells is increased at an earlier time point, OL3d. Our preliminary data suggest that there is, in fact, a higher percentage of MBP^+ cells at OL3d after YBX1 knockdown, relative to control (19% vs. 5%, data not shown), but we still need to confirm by increasing the number of experiments. Finally, we could do an *in silico* analysis to look for putative binding sites in the 3’UTR of cytoskeleton and myelin-related genes, such as molecules involved in RhoA, integrin and MAPK signaling pathways.

6. Challenges

The main challenge encountered in this project was the high variability among experiments. This is due to several factors: first, we were working with primary mixed glial cell cultures from wild-type Wistar rats. Each of these cultures were prepared from brain cortices of at least 10 individuals, a minimum of three independent OPC/OL cultures was done. Second, we used lentivirus as a vector for shRNA delivery, because OL are cells very difficult to transfect. Although viral preparations were titrated to estimate the number of transducing units per microliter and a multiplicity of infection of 1:1 was used, efficiency of infection was variable and relatively low – 50% or less in some cases. In addition, cells were classified as infected when exhibiting green fluorescence, due to the expression of GFP included in the plasmid. It should be noted that GFP and the shRNA were expressed under different promoters, so a higher intensity of fluorescence does not necessarily correlate with a higher knockdown effect, and vice-versa. We may have overlooked many cells that were effectively undergoing mRNA knockdown but did not reach the arbitrary fluorescence threshold applied. Thirdly, it is not possible to obtain pure differentiation stages in OL primary cultures, but only enriched populations. Though OPC were initially cultured in a proliferative medium and then switched to a differentiation medium, differentiation was not completely synchronous among all cells. This means that some cells would differentiate faster than others, despite being cultured in the same conditions. Another difficulty was related to cell confluency: OPC were plated on laminin-2-coated surfaces, which cannot dry otherwise it will become inactive, but it cannot be too wet because the cell suspension would spread too much and cells would be plated farther apart. It was challenging to achieve a consistent technique that would result in cultures with similar confluencies throughout experiments. OL differentiate better when they are in closer physical proximity thanks to chemotactic cues; however it is difficult to visualize cellular morphology in these conditions. High cell confluency is the main reason why it was so difficult to perform Sholl Analysis and to optimize the automated high-throughput analysis protocol for process extension. Finally, and as previously mentioned, OL have very thin processes which makes them difficult to visualize by wide-field fluorescence microscopy. Staining with anti-α-tubulin antibodies was irregular and faint at the tips of OL processes, even when the sample was overexposed. However, overexposure had as a consequence an increase in background noise, which made it difficult to identify processes using the automated protocol.

As a final commentary, I would like to say that I found the technical demands of this project to be good for my training as a scientist. I learned to solve problems and fine-tune procedures and techniques, which I think are essential skills for a good scientist.

7. References

Aggarwal, S., Snaidero, N., Pähler, G., Frey, S., Sánchez, P., Zweckstetter, M., Janshoff, A., Schneider, A., Weil, M.-T., Schaap, I. A. T., et al. (2013). Myelin membrane assembly is driven by a phase transition of myelin basic proteins into a cohesive protein meshwork. *PLoS Biology* **11**, 1-14.

Alberts, B., Johnson, A., Lewis, J., Raff, M., Roberts, K. and Walter, P. (2002a). Cell Junctions, Cell Adhesion, and the Extracellular Matrix. In *Molecular Biology of the Cell*. New York: Garland Science.

---- (2002b). Histology: The Lives and Deaths of Cells in Tissues. In *Molecular Biology of the Cell*. New York: Garland Science.

---- (2002c). How Cells Read the Genome: From DNA to Protein. In *Molecular Biology of the Cell*. New York: Garland Science.

---- (2002d). Proteins. In *Molecular Biology of the Cell*. New York: Garland Science.

Anderson, P. and Kedersha, N. (2009). RNA granules: post-transcriptional and epigenetic modulators of gene expression. *Nature Reviews Molecular Cell Biology* **10**, 430-436.

Arquint, M., Roder, J., Chia, L.-S., Down, J., Braun, P. and Dunn, R. (1987). Molecular cloning and primary structure of myelin-associated glycoprotein. *Proceedings of the National Academy of Sciences* **84**, 600-604.

Back, S. A., Luo, N. L., Borenstein, N. S., Levine, J. M., Volpe, J. J. and Kinney, H. C. (2001). Late oligodendrocyte progenitors coincide with the developmental window of vulnerability for human perinatal white matter injury. *The Journal of Neuroscience* **21**, 1302-1312.

Bakhti, M., Aggarwal, S. and Simons, M. (2014). Myelin architecture: zippering membranes tightly together. *Cellular and Molecular Life Sciences* **71**, 1265-1277.

Barnat, M., Enslen, H., Propst, F., Davis, R. J., Soares, S. and Nothias, F. (2010). Distinct roles of c-Jun N-terminal kinase isoforms in neurite initiation and elongation during axonal regeneration. *The Journal of Neuroscience* **30**, 7804-7816.

Barros, C. S., Nguyen, T., Spencer, K. S. R., Nishiyama, A., Colognato, H. and Müller, U. (2009). β1 integrins are required for normal CNS myelination and promote AKT-dependent myelin outgrowth. *Development* **136**, 2717-2724.

Bengtsson, S. L., Nagy, Z., Skare, S., Forsman, L., Forssberg, H. and Ullén, F. (2005). Extensive piano practicing has regionally specific effects on white matter development. *Nature Neuroscience* **8**, 1148-1150.

Benninger, Y., Colognato, H., Thurnherr, T., Franklin, R. J. M., Leone, D. P., Atanasoski, S., Nave, K.-A., ffrench-Constant, C., Suter, U. and Relvas, J. B. (2006). β1-Integrin Signaling Mediates Premyelinating Oligodendrocyte Survival But Is Not Required for CNS Myelination and Remyelination. *The Journal of Neuroscience* **26**, 7665-7673.

Besirli, C. G., Wagner, E. F. and Johnson, E. M. (2005). The limited role of NH2-terminal c-Jun phosphorylation in neuronal apoptosis Identification of the nuclear pore complex as a potential target of the JNK pathway. *The Journal of Cell Biology* **170**, 401–411.

Bhat, M. A., Rios, J. C., Lu, Y., Garcia-Fresco, G. P., Ching, W., St. Martin, M., Li, J., Einheber, S., Chesler, M., Rosenbluth, J., et al. (2001). Axon-glia interactions and the domain organization of myelinated axons requires neurexin IV/Caspr/Paranodin. *Neuron* **30**, 369-383.

Binley, K. E., Ng, W. S., Tribble, J. R., Song, B. and Morgan, J. E. (2014). Sholl analysis: a quantitative comparison of semi-automated methods. *Journal of Neuroscience Methods* **225**, 65-70.

Biogen anti-LINGO-1(BIIB033) Pipeline.

Bizzozero, O. A., McGarry, J. F. and Lees, M. B. (1986). Acylation of rat brain myelin proteolipid protein with different fatty acids. *Journal of Neurochemistry* **47**, 772-778.

Blaschuk, K. L., Frost, E. E. and ffrench-Constant, C. (2000). The regulation of proliferation and differentiation in oligodendrocyte progenitor cells by alphaV integrins. *Development* **127**, 1961-1969.

Brakebusch, C. and Fässler, R. R. (2003). The integrin–actin connection, an eternal love affair. *The EMBO Journal* **22**, 2324-2333.

Brent, R. (2000). Genomic Biology. *Cell* **100**, 169-183.

Brück, W. and Stadelmann, C. (2003). Inflammation and degeneration in multiple sclerosis. *Neurological Sciences* **24**, 265-267.

Buttermore, E. D., Thaxton, C. L. and Bhat, M. A. (2013). Organization and maintenance of molecular domains in myelinated axons. *Journal of Neuroscience Research* **91**, 603-622.

Buttery, P. C. and ffrench-Constant, C. (1999). Laminin-2/integrin interactions enhance myelin membrane formation by oligodendrocytes. *Molecular and Cellular Neurosciences* **14**, 199–212.

Cahoy, J. D., Emery, B., Kaushal, A., Foo, L. C., Zamanian, J. L., Christopherson, K. S., Xing, Y., Lubischer, J. L., Krieg, P. A., Krupenko, S. A., et al. (2008). A Transcriptome Database for Astrocytes, Neurons, and Oligodendrocytes: A New Resource for Understanding Brain Development and Function. *The Journal of Neuroscience* **28**, 264–278.

Câmara, J., Wang, Z., Nunes-Fonseca, C., Friedman, H. C., Grove, M., Sherman, D. L., Komiyama, N. H., Grant, S. G., Brophy, P. J., Peterson, A., et al. (2009). Integrin-mediated axoglial interactions initiate myelination in the central nervous system. *The Journal of Cell Biology* **185**, 699–712.

Camps, M., Nichols, A. and Arkinstall, S. (2000). Dual specificity phosphatases: a gene family for control of MAP kinase function. *The FASEB Journal* **14**, 6-16.

Chang, A., Tourtellotte, W. W., Rudick, R. and Trapp, B. D. (2002). Premyelinating oligodendrocytes in chronic lesions of multiple sclerosis. *The New England Journal of Medicine* **346**, 165-173.

Charles, P., Reynolds, R., Seilhean, D., Rougon, G., Aigrot, M. S., Niezgoda, A., Zalc, B. and Lubetzki, C. (2002). Re-expression of PSA-NCAM by demyelinated axons: an inhibitor of remyelination in multiple sclerosis? *Brain* **125**, 1972-1979.

Chen, Y., Balasubramaniyan, V., Peng, J., Hurlock, E. C., Tallquist, M., Li, J. and Lu, Q. R. (2007). Isolation and culture of rat and mouse oligodendrocyte precursor cells. *Nature Protocols* **2**, 1044-1051.

Cheng, H., Gao, Q., Jiang, M., Ma, Y., Ni, X., Guo, L., Jin, W., Cao, G., Ji, C., Ying, K., et al. (2003). Molecular cloning and characterization of a novel human protein phosphatase, LMW-DSP3. *The international Journal of Biochemistry & Cell Biology* **35**, 226–234.

Chew, L.-J., Coley, W., Cheng, Y. and Gallo, V. (2010). Mechanisms of regulation of oligodendrocyte development by p38 mitogen-activated protein kinase. *The Journal of Neuroscience* **30**, 11011–11027.

Chittajallu, R., Aguirre, A. and Gallo, V. (2004). NG2 positive cells in the mouse white and grey matter display distinct physiological properties. *The Journal of Physiology* **561**, 109-122.

Clarke, L. E., Young, K. M., Hamilton, N. B., Li, H., Richardson, W. D. and Attwell, D. (2012). Properties and fate of oligodendrocyte progenitor cells in the corpus callosum, motor cortex, and piriform cortex of the mouse. *The Journal of Neuroscience* **32**, 8173–8185.

Colello, R. J., Pott, U. and Schwab, M. E. (1994). The role of oligodendrocytes and myelin on axon maturation in the developing rat retinofugal pathway. *The Journal of Neuroscience* **14**, 2594-2605.

Colognato, H., Baron, W., Avellana-Adalid, V., Relvas, J. B., Baron-Van Evercooren, A., Georges-Labouesse, E. and ffrench-Constant, C. (2002). CNS integrins switch growth factor signalling to promote target-dependent survival. *Nature Cell Biology* **4**, 833-841.

Colognato, H., Ramachandrappa, S., Olsen, I. M. and ffrench-Constant, C. (2004). Integrins direct Src family kinases to regulate distinct phases of oligodendrocyte development. *The Journal of Cell Biology* **167**, 365–375.

Compston, A. and Coles, A. (2008). Multiple Sclerosis. *Lancet* **372**, 1502–1517.

Constantinescu, C. S., Farooqi, N., O'Brien, K. and Gran, B. (2011). Experimental autoimmune encephalomyelitis (EAE) as a model for multiple sclerosis (MS). *British Journal of Pharmacology* **164**, 1079–1106.

Craig, A., Luo, N. L., Beardsley, D. J., Wingate-Pearse, N., Walker, D. W., Hohimer, A. R. and Back, S. A. (2003). Quantitative analysis of perinatal rodent oligodendrocyte lineage progression and its correlation with human. *Experimental Neurology* **181**, 231-240.

Dai, L., Taylor, M. S., O'Donnell, K. A. and Boeke, J. D. (2012). Poly (A) binding protein C1 is essential for efficient L1 retrotransposition and affects L1 RNP formation. *Molecular and Cellular Biology* **32**, 4323-4336.

Dawson, M. R. L., Polito, A., Levine, J. M. and Reynolds, R. (2003). NG2-expressing glial progenitor cells: an abundant and widespread population of cycling cells in the adult rat CNS. *Molecular and Cellular Neuroscience* **24**, 476-488.

de Rosbo, N. K., Milo, R., Lees, M. B., Burger, D., Bernard, C. A. and Ben-Nun, A. (1993). Reactivity to myelin antigens in multiple sclerosis. Peripheral blood lymphocytes respond predominantly to myelin oligodendrocyte glycoprotein. *Journal of Clinical Investigation* **92**, 2602-2608.

Dugas, J. C., Tai, Y. C., Speed, T. P., Ngai, J. and Barres, B. A. (2006). Functional Genomic Analysis of Oligodendrocyte Differentiation. *The Journal of Neuroscience* **26**, 10967–10983.

Ebner, S. and Dunbar, M. (2000). Distinct roles for PI3K in proliferation and survival of oligodendrocyte progenitor cells. *Journal of Neuroscience Research* **62**, 336 – 345.

England, J. D., Levinson, S. and Shrager, P. (1996). Immunocytochemical investigations of sodium channels along nodal and internodal portions of demyelinated axons. *Microscopy Research and Technique* **34**, 445-451.

Feltrin, D., Fusco, L., Witte, H., Moretti, F., Martin, K., Letzelter, M., Fluri, E., Scheiffele, P. and Pertz, O. (2012). Growth Cone MKK7 mRNA Targeting Regulates MAP1b-Dependent Microtubule Bundling to Control Neurite Elongation. *PLoS Biology* **10**, 1-23.

Ferreira, T. A., Blackman, A. V., Oyrer, J., Jayabal, S., Chung, A. J., Watt, A. J., Sjöström, J. P. and Meyel, D. J. (2014). Neuronal morphometry directly from bitmap images. *Nature methods* **11**, 982-984.

Flores, A. I., Narayanan, S. P., Morse, E. N., Shick, H. E., Yin, X., Kidd, G., Avila, R. L., Kirschner, D. A. and Macklin, W. B. (2008). Constitutively active Akt induces enhanced myelination in the CNS. *The Journal of Neuroscience* **28**, 7174-7183.

Ford, L. P., Bagga, P. S. and Wilusz, J. (1997). The poly (A) tail inhibits the assembly of a 3'-to-5'exonuclease in an in vitro RNA stability system. *Molecular and Cellular Biology* **17**, 398–406.

Fukui, Y. (1993). Toward a new concept of cell motility: cytoskeletal dynamics in amoeboid movement and cell division. *International Review of Cytology* **144**, 85–127.

Gardinier, M. V., Amiguet, P. and Linington, C. (1992). Myelin/oligodendrocyte glycoprotein is a unique member of the immunoglobulin superfamily. *Journal of Neuroscience Research* **133**.

Gee, H. Y., Zhang, F., Ashraf, S., Kohl, S., Sadowski, C. E., Vega-Warner, V., Zhou, W., Lovric, S., Fang, H., Nettleton, M., et al. (2015). KANK deficiency leads to podocyte dysfunction and nephrotic syndrome. *The Journal of Clinical Investigation* **125**, 2375–2384.

Gittes, F., Mickey, B., Nettleton, J. and Howard, J. (1993). Flexural rigidity of microtubules and actin filaments measured from thermal fluctuations in shape. *The Journal of Cell Biology* **120**, 923-934.

Goodin, D. S., Frohman, E. M., Garmany, J. G. P., Halper, J., Likosky, W. H., Lublin, F. D., Silberberg, D. H., Stuart, W. H. and van den Noort, S. (2002). Disease modifying therapies in multiple sclerosis. *American Academy of Neurology* **58**, 169-178.

Goold, R. G., Owen, R. and Gordon-Weeks, P. R. (1999). Glycogen synthase kinase 3beta phosphorylation of microtubule-associated protein 1B regulates the stability of microtubules in growth cones. *Journal of Cell Science* **112**, 3373-3384.

Gupta, S., Barrett, T., Whitmarsh, A. J., Cavanagh, J., Sluss, H. K., Dérijard, B. and Davis, R. J. (1996). Selective interaction of JNK protein kinase isoforms with transcription factors. *The EMBO Journal* **15**, 2760-2770.

Gutowski, N. J., Newcombe, J. and Cuzner, M. L. (1999). Tenascin-R and C in multiple sclerosis lesions: relevance to extracellular matrix remodelling. *Neuropathology and Applied Neurobiology* **25**, 207–214.

Haak, L. L., Grimaldi, M. and Smaili, S. S. (2002). Mitochondria regulate Ca2+ wave initiation and inositol trisphosphate signal transduction in oligodendrocyte progenitors. *Journal of Neurochemistry* **80**, 405-415.

Han, S. P., Friend, L. R., Carson, J. H., Korza, G., Barbarese, E., Maggipinto, M., Hatfield, J. T., Rothnagel, J. A. and Smith, R. (2010). Differential subcellular distributions and trafficking functions of hnRNP A2/B1 spliceoforms. *Traffic* **11**, 886-898.

Hardy, R. J. and Friedrich, J., V. L. (1996). Progressive remodeling of the oligodendrocyte process arbor during myelinogenesis. *Dev Neurosci-Basel* **18**, 243-254.

Hartline, D. K. and Colman, D. R. (2007). Rapid conduction and the evolution of giant axons and myelinated fibers. *Current Biology* **17**, 29-35.

Healthcare, G. (2008a). *IN Cell Developer Toolbox v1.6 High-content image analysis software User's Reference Manual*.

---- (2008b). *INCell Analyzer 2000 Acquisition Software Manual*.

Hilpelä, P., Vartiainen, M. K. and Lappalainen, P. (2004). Regulation of the actin cytoskeleton by PI(4, 5)P2 and PI(3, 4, 5)P3. *Current Topics in Microbiology and Immunology* **282**, 117-163.

Hirokawa, N., Noda, Y. and Okada, Y. (1998). Kinesin and dynein superfamily proteins in organelle transport and cell division. *Current Opinion in Cell Biology* **10**, 60-73.

Hoek, K. S., Kidd, G. J., Carson, J. H. and Smith, R. (1998). hnRNP A2 selectively binds the cytoplasmic transport sequence of myelin basic protein mRNA. *Biochemistry* **37**, 7021-7029.

Holmgren, B., Urbá-Holmgren, R., Riboni, L. and Vega-SaenzdeMiera, E. C. (1989). Sprague Dawley rat mutant with tremor, ataxia, tonic immobility episodes, epilepsy and paralysis. *Laboratory Animal Science* **39**, 226-228.

Holt, C. E. and Schuman, E. M. (2013). The central dogma decentralized: new perspectives on RNA function and local translation in neurons. *Neuron* **80**, 648-657.

Hoshina, N., Tezuka, T., Yokoyama, K., Kozuka-Hata, H., Oyama, M. and Yamamoto, T. (2007). Focal adhesion kinase regulates laminin-induced oligodendroglial process outgrowth. *Genes to Cells* **12**, 1245–1254.

Intermountain Medical Imaging, B., Idaho MRI of Multiple Sclerosis. http://img.webmd.com/dtmcms/live/webmd/consumer_assets/site_images/media/medical/hw/h9991221.jpg.

Jackman, N., Ishii, A. and Bansal, R. (2009). Oligodendrocyte Development and Myelin Biogenesis: Parsing Out the Roles of Glycosphingolipids. *Physiology* **24**, 290-297.

John, G. R., Shankar, S. L., Shafit-Zagardo, B., Massimi, A., Lee, S. C., Raine, C. S. and Brosnan, C. F. (2002). Multiple sclerosis: re-expression of a developmental pathway that restricts oligodendrocyte maturation. *Nature medicine* **8**, 1115-1121.

Kahvejian, A., Svitkin, Y. V., Sukarieh, R., M'Boutchou, M.-N. and Sonenberg, N. (2005). Mammalian poly (A)-binding protein is a eukaryotic translation initiation factor, which acts via multiple mechanisms. *Genes & development* **19**.

Kakinuma, N., Roy, B., Zhu, Y., Wang, Y. and Kiyama, R. (2008). Kank regulates RhoA-dependent formation of actin stress fibers and cell migration via 14-3-3 in PI3K–Akt signaling. *The Journal of Cell Biology* **181**, 537-549.

Kaplan, M. R., Meyer-Franke, A., Lambert, S., Bennett, V., Duncan, I. D., Levinson, S. R. and Barres, B. A. (1997). Induction of sodium channel clustering by oligodendrocytes. *Nature* **386**, 724-728.

Kawauchi, T., Chihama, K., Nishimura, Y. V., Nabeshima, Y.-i. and Hoshino, M. (2005). MAP1B phosphorylation is differentially regulated by Cdk5/p35, Cdk5/p25, and JNK. *Biochemical and Biophysical Research Communications* **331**, 50–55.

Keene, J. D. and Tenenbaum, S. A. (2002). Eukaryotic mRNPs may represent posttranscriptional operons. *Molecular cell* **9**, 1161-1167.

Kelm, S., Pelz, A., Schauer, R., Filbin, M. T., Tang, S., de Bellard, M.-E., Schnaar, R. L., Mahoney, J. A., Hartnell, A., Bradfield, P., et al. (1994). Sialoadhesin, myelin-associated glycoprotein and CD22 define a new family of sialic acid-dependent adhesion molecules of the immunoglobulin superfamily. *Current Biology* **4**, 965–972.

Kessaris, N., Fogarty, M., Iannarelli, P. and Grist, M. (2006). Competing waves of oligodendrocytes in the forebrain and postnatal elimination of an embryonic lineage. *Nature Neuroscience* **9**, 173-179.

Kosturko, L. D., Maggipinto, M. J., Korza, G., Lee, J. W., Carson, J. H. and Barbarese, E. (2006). Heterogeneous nuclear ribonucleoprotein (hnRNP) E1 binds to hnRNP A2 and inhibits translation of A2 response element mRNAs. *Molecular Biology of the Cell* **17**, 3521-3533.

Kotter, M. R., Li, W. W. and Zhao, C. (2006). Myelin impairs CNS remyelination by inhibiting oligodendrocyte precursor cell differentiation. *The Journal of Neuroscience* **26**, 328-332.

Kreis, T. E. and Birchmeier, W. (1980). Stress fiber sarcomeres of fibroblasts are contractile. *Cell* **22**, 555-561.

Kuhlmann, T., Miron, V., Cuo, Q., Wegner, C., Antel, J. and Brück, W. (2008). Differentiation block of oligodendroglial progenitor cells as a cause for remyelination failure in chronic multiple sclerosis. *Brain* **131**, 1749-1758.

Laursen, L. S., Chan, C. W. and ffrench-Constant, C. (2011). Translation of myelin basic protein mRNA in oligodendrocytes is regulated by integrin activation and hnRNP-K. *The Journal of Cell Biology* **192**, 797-811.

Lawler, S., Fleming, Y., Goedert, M. and Cohen, P. (1998). Synergistic activation of SAPK1/JNK1 by two MAP kinase kinases in vitro. *Current Biology* **8**, 1387–1390.

Lee, K. K., de Repentigny, Y., Saulnier, R., Rippstein, P., Macklin, W. B. and Kothary, R. (2006). Dominant-negative beta1 integrin mice have region-specific myelin defects accompanied by alterations in MAPK activity. *Glia* **53**, 836-844.

Legate, K. R., Montañez, E., Kudlacek, O. and Füssler, R. (2006). ILK, PINCH and parvin: the tIPP of integrin signalling. *Nature Reviews Molecular Cell Biology* **7**, 20-31.

Levine, J. M., Stincone, F. and Lee, Y.-S. (1993). Development and differentiation of glial precursor cells in the rat cerebellum. *Glia* **7**, 307-321.

Liang, X., Draghi, N. A. and Resh, M. D. (2004). Signaling from integrins to Fyn to Rho family GTPases regulates morphologic differentiation of oligodendrocytes. *The Journal of Neuroscience* **24**, 7140-7149.

Ma, S., Musa, T. and Bag, J. (2006). Reduced Stability of Mitogen-activated Protein Kinase Kinase-2 mRNA and Phosphorylation of Poly(A)-binding Protein (PABP) in Cells Overexpressing PABP. *Journal of Biological Chemistry* **281**, 3145-3156.

Mangus, D. A., Evans, M. C. and Jacobson, A. (2003). Poly (A)-binding proteins: multifunctional scaffolds for the post-transcriptional control of gene expression. *Genome Biology* **4**, 1-14.

Mattila, P. K. and Lappalainen, P. (2008). Filopodia: molecular architecture and cellular functions. *Nature Reviews Molecular Cell Biology* **9**, 446-454.

McCarthy, K. D. and de Vellis, J. (1980). Preparation of separate astroglial and oligodendroglial cell cultures from rat cerebral tissue. *Journal of Cell Biology* **85**, 890-902.

McDonald, W. I. and Sears, T. A. (1969). Effect of demyelination on conduction in the central nervous system. *Nature* **221**, 182-183.

McKenzie, I. A., Ohayon, D., Li, H., Paes de Faria, J., Emery, B., Tohyama, K. and Richardson, W. D. (2014). Motor skill learning requires active central myelination. *Science* **346**, 318-322.

Mi, S., Miller, R. H., Lee, X., Scott, M. L., Shulag-Morskaya, S., Shao, Z., Chang, J., Thill, G., Levesque, M., Zhang, M., et al. (2005). LINGO-1 negatively regulates myelination by oligodendrocytes. *Nature Neuroscience* **8**, 745-751.

mikeclaffey.com Saltatory conduction.

Mili, S., Moissoglu, K. and Macara, I. G. (2008). Genome-wide screen reveals APC-associated RNAs enriched in cell protrusions. *Nature* **453**, 115-119.

Milner, R. and ffrench-Constant, C. (1994). A developmental analysis of oligodendroglial integrins in primary cells: changes in alpha v-associated beta subunits during differentiation. *Development* **120**, 3497-3506.

Minich, W. B. and Ovchinnikov, L. P. (1992). Role of cytoplasmic mRNP proteins in translation. *Biochimie* **74**, 477-483.

Moore, C. S., Abdullah, S. L., Brown, A., Arulpragasam, A. and Crocker, S. J. (2011). How factors secreted from astrocytes impact myelin repair. *Journal of Neuroscience Research* **89**, 13-21.

Müller, C., Bauer, N. M., Schäfer, I. and White, R. (2013). Making myelin basic protein-from mRNA transport to localized translation. *Frontiers in Cellular Neuroscience* **7**, 1-7.

Nave, K.-A. (2010). Myelination and support of axonal integrity by glia. *Nature* **468**, 244-252.

Nawaz, S., Kippert, A., Saab, A. S., Werner, H. B., Lang, T., Nave, K.-A. and Simons, M. (2009). Phosphatidylinositol 4,5-Bisphosphate-dependent interaction of myelin basic protein with the plasma membrane in oligodendroglial cells and its rapid perturbation by elevated calcium. *The Journal of Neuroscience* **29**, 4794-4807.

Nawaz, S., Sánchez, P., Schmitt, S., Snaidero, N., Mitkovski, M., Velte, C., Brückner, Bastian R., Alexopoulos, I., Czopka, T., Jung, S. Y., et al. (2015). Actin Filament Turnover Drives Leading Edge Growth during Myelin Sheath Formation in the Central Nervous System. *Developmental Cell* **34**.

Nicholson, P. and Mhlemann, O. (2010). Cutting the nonsense: the degradation of PTC-containing mRNAs. *Biochemical Society Transactions* **38**, 1615–1620.

Nishiyama, A., Lin, X. H., Giese, N., Heldin, C. H. and Stallcup, W. B. (1996). Interaction between NG2 proteoglycan and PDGF receptor on O2A progenitor cells is required for optimal response to PDGF. *Journal of Neuroscience Research* **43**, 315-330.

NMSS Medications.

Nobes, C. D. and Hall, A. (1995). Rho, rac, and cdc42 GTPases regulate the assembly of multimolecular focal complexes associated with actin stress fibers, lamellipodia, and filopodia. *Cell* **81**, 53-62.

Noll, E. and Miller, R. H. (1993). Oligodendrocyte precursors originate at the ventral ventricular zone dorsal to the ventral midline region in the embryonic rat spinal cord. *Development* **118**, 563-573.

O'Meara, R. W., Michalski, J.-P., Anderson, C., Bhanot, K., Rippstein, P. and Kothary, R. (2013). Integrin-linked kinase regulates process extension in oligodendrocytes via control of actin cytoskeletal dynamics. *The Journal of Neuroscience* **33**, 9781–9793.

Paluch, E. K. and Raz, E. (2013). The role and regulation of blebs in cell migration. *Current Opinion in Cell Biology* **25**, 582-590.

Parkinson, D. B., Bhaskaran, A., Arthur-Farraj, P., Noon, L. A., Woodhoo, A., Lloyd, A. C., Feltri, M., Wrabetz, L., Behrens, A., Mirsky, R., et al. (2008). c-Jun is a negative regulator of myelination. *The Journal of Cell Biology* **181**, 625–637.

Pfeiffer, S. E., Warrington, A. E. and Bansal, R. (1993). The oligodendrocyte and its many cellular processes. *Trends in Cell Biology* **3**, 191-197.

Poliak, S., Salomon, D., Elhanany, H., Sabanay, H., Kiernan, B., Pevny, L., Stewart, C. L., Xu, X., Chiu, S.-Y. Y., Shrager, P., et al. (2003). Juxtaparanodal clustering of Shaker-like K+ channels in myelinated axons depends on Caspr2 and TAG-1. *The Journal of Cell Biology* **162**, 1149-1160.

Prineas, J. W. and Connell, F. (1979). Remyelination in Multiple Sclerosis. *Annals of Neurology* **5**, 22-31.

Pringle, N. P., Mudhar, H. S., Collarini, E. J. and Richardson, W. D. (1992). PDGF receptors in the rat CNS: during late neurogenesis, PDGF alpha-receptor expression appears to be restricted to glial cells of the oligodendrocyte lineage. *Development* **115**, 535-551.

Quarles, R. H. (2002). Myelin sheaths: glycoproteins involved in their formation, maintenance and degeneration. *Cellular and Molecular Life Sciences* **59**, 1431-1448.

Quarles, R. H. and Morell, P. (1999). Characteristic Composition of Myelin. In *Basic Neurochemistry: Molecular, Cellular and Medical Aspects* (ed. A. B. Siegel GJ, Albers RW, et al.). Philadelphia: Lippincott-Raven.

Raff, M. C., Miller, R. H. and Noble, M. (1983). A glial progenitor cell that develops in vitro into an astrocyte or an oligodendrocyte depending on culture medium. *Nature* **303**, 390-396.

Ramot, Y., Molho-Pessach, V., Meir, T., Alper-Pinus, R., Siam, I., Tams, S., Babay, S. and Zlotogorski, A. (2014). Mutation in KANK2, encoding a sequestering protein for steroid receptor coactivators, causes keratoderma and woolly hair. *Journal of Medical Genetics* **51**, 388-394.

Readhead, C. and Hood, L. (1990). The dysmyelinating mouse mutations shiverer (shi) and myelin deficient (shi mld). *Behavior Genetics* **20**, 213-234.

Redford, E. J., Kapoor, R. and Smith, K. J. (1997). Nitric oxide donors reversibly block axonal conduction: demyelinated axons are especially susceptible. *Brain* **120**, 2149–2157.

Relucio, J., Tzvetanova, I. D., Ao, W., Lindquist, S. and Colognato, H. (2009). Laminin Alters Fyn Regulatory Mechanisms and Promotes Oligodendrocyte Development. *The Journal of Neuroscience* **29**, 11794-11806.

Relvas, J. B., Setzu, A., Baron, W., Buttery, P. C., LaFlamme, S. E., Franklin, R. J. and ffrench-Constant, C. (2001). Expression of dominant-negative and chimeric subunits reveals an essential role for beta1 integrin during myelination. *Current Biology* **11**, 1039-1043.

Reynolds, R. and Wilkin, G. P. (1988). Development of macroglial cells in rat cerebellum. II. An in situ immunohistochemical study of oligodendroglial lineage from precursor to mature myelinating cell. *Development* **102**, 409-425.

Ridley, A. J. and Hall, A. (1992). The small GTP-binding protein rho regulates the assembly of focal adhesions and actin stress fibers in response to growth factors. *Cell* **70**, 389-399.

Ridley, A. J., Paterson, H. F., Johnston, C. L., Diekmann, D. and Hall, A. (1992). The small GTP-binding protein rac regulates growth factor-induced membrane ruffling. *Cell* **70**, 401-410.

Roy, B., Kakinuma, N. and Kiyama, R. (2009). Kank attenuates actin remodeling by preventing interaction between IRSp53 and Rac1. *The Journal of Cell Biology* **184**, 253-267.

Sarkar, S., Roy, B., Hatano, N., Aoyagi, T., Gohji, K. and Kiyama, R. (2002). A Novel Ankyrin Repeat-containing Gene (Kank) Located at 9p24 Is a Growth Suppressor of Renal Cell Carcinoma. *Journal of Biological Chemistry* **277**, 36585-36591.

Schaeffer, H. J. and Weber, M. J. (1999). Mitogen-activated protein kinases: specific messages from ubiquitous messengers. *Molecular and Cellular Biology* **19**, 2435–2444.

Schindelin, J., Arganda-Carreras, I., Frise, E., Kaynig, V., Longair, M., Pietzsch, T., Preibisch, S., Rueden, C., Saalfeld, S., Schmid, B., et al. (2012). Fiji: an open-source platform for biological-image analysis. *Nature methods* **9**, 676–682.

Sedgwick, S. G. and Smerdon, S. J. (1999). The ankyrin repeat: a diversity of interactions on a common structural framework. *Trends in Biochemical Sciences* **24**, 311-316.

Shahbabian, K. and Chartrand, P. (2012). Control of cytoplasmic mRNA localization. *Cellular and Molecular Life Sciences* **69**, 535-552.

Shi, J., Marinovich, A. and Barres, B. A. (1998). Purification and characterization of adult oligodendrocyte precursor cells from the rat optic nerve. *The Journal of Neuroscience* **18**, 4627–4636.

Sholl, D. A. (1953). Dendritic organization in the neurons of the visual and motor cortices of the cat. *Journal of Anatomy* **87**, 387-407.

Skabkin, M. A., Kiselyova, O. I., Chernov, K. G., Sorokin, A. V., Dubrovin, E. V., Yaminsky, I. V., Vasiliev, V. D. and Ovchinnikov, L. P. (2004). Structural organization of mRNA complexes with major core mRNP protein YB-1. *Nucleic acids research* **32**, 5621-5635.

Skabkina, O. V., Skabkin, M. A., Popova, N. V., Lyabin, D. N., Penalva, L. O. and Ovchinnikov, L. P. (2003). Poly(A)-binding protein positively affects YB-1 mRNA translation through specific interaction with YB-1 mRNA. *The Journal of biological chemistry* **278**, 18191-18198.

Small, J. V., Stradal, T., Vignal, E. and Rottner, K. (2002). The lamellipodium: where motility begins. *Trends in Cell Biology* **12**, 112-120.

Snaidero, N., Möbius, W., Czopka, T., Hekking, L., Mathisen, C., Verkleij, D., Goebbels, S., Edgar, J., Merkler, D., Lyons, D., et al. (2014). Myelin Membrane Wrapping of CNS Axons by PI(3,4,5)P3-Dependent Polarized Growth at the Inner Tongue. *Cell* **156**, 277-290.

Sobel, R. A., Chen, M., Maeda, A. and Hinojoza, J. R. (1995). Vitronectin and integrin vitronectin receptor localization in multiple sclerosis lesions. *Journal of Neuropathology & Experimental Neurology* **54**, 202-213.

Sobottka, B., Ziegler, U., Kaech, A., Becher, B. and Goebels, N. (2011). CNS live imaging reveals a new mechanism of myelination: the liquid croissant model. *Glia* **59**, 1841-1849.

Sommer, I. and Schachner, M. (1981). Monoclonal antibodies (O1 to O4) to oligodendrocyte cell surfaces: an immunocytological study in the central nervous system. *Developmental Biology* **83**, 311-327.

Song, J., Carson, J. H., Barbarese, E., Li, F.-Y. Y. and Duncan, I. D. (2003). RNA transport in oligodendrocytes from the taiep mutant rat. *Molecular and Cellular Neurosciences* **24**, 926-938.

Song, J., Goetz, B. D., Baas, P. W. and Duncan, I. D. (2001). Cytoskeletal reorganization during the formation of oligodendrocyte processes and branches. *Molecular and Cellular Neuroscience* **17**, 624–636.

Sternberger, N. H., Quarles, R. H., Itoyama, Y. and Webster, H. d. (1979). Myelin-associated glycoprotein demonstrated immunocytochemically in myelin and myelin-forming cells of developing rat. *Proceedings of the National Academy of Sciences* **76**, 1510-1514.

Stewart, S. A., Dykxhoorn, D. M., Palliser, D., Mizuno, H., Yu, E. Y., An, D. S., Sabatini, D. M., Chen, I. S. Y., Hahn, W. C., Sharp, P. A., et al. (2003). Lentivirus-delivered stable gene silencing by RNAi in primary cells. *Rna* **9**, 493-501.

Thomsen, R. and Nielsen, A. (2011). A Boyden chamber-based method for characterization of astrocyte protrusion localized RNA and protein. *Glia* **59**, 1782-1792.

Thurnherr, T., Benninger, Y., Wu, X., Chrostek, A., Krause, S. M., Nave, K.-A., Franklin, R. J. M., Brakebusch, C., Suter, U. and Relvas, J. B. (2006). Cdc42 and Rac1 Signaling Are Both Required for and Act Synergistically in the Correct Formation of Myelin Sheaths in the CNS. *The Journal of Neuroscience* **26**, 10110-10119.

Tiscornia, G., Singer, O. and Verma, I. M. (2006). Production and purification of lentiviral vectors. *Nature Protocols* **1**, 241-245.

Ulloa, L., Diez-Guerra, F. J., Avila, J. and Diaz-Nido, J. (1994). Localization of differentially phosphorylated isoforms of microtubule-associated protein 1B in cultured rat hippocampal neurons. *Neuroscience* **61**, 211-223.

Ventura, A., Meissner, A., Dillon, C. P., McManus, M., Sharp, P. A., Parijs, L., Jaenisch, R. and Jacks, T. (2004). Cre-lox-regulated conditional RNA interference from transgenes. *Proceedings of the National Academy of Sciences of the United States of America* **101**, 10380-10385.

Vouyioukiis, D. A. and Brophy, P. J. (1993). Microtubule-associated protein MAP1B expression precedes the morphological differentiation of oligodendrocytes. *Journal of Neuroscience Research* **35**, 257-267.

Wang, Y., Kakinuma, N., Zhu, Y. and Kiyama, R. (2006). Nucleo-cytoplasmic shuttling of human Kank protein accompanies intracellular translocation of β-catenin. *Journal of Cell Science* **119**, 4002-4010.

White, R., Gonsior, C., Krämer-Albers, E.-M. M., Stöhr, N., Hüttelmaier, S. and Trotter, J. (2008). Activation of oligodendroglial Fyn kinase enhances translation of mRNAs transported in hnRNP A2-dependent RNA granules. *The Journal of Cell Biology* **181**, 579-586.

Wilkie, G. S., Dickson, K. S. and Gray, N. K. (2003). Regulation of mRNA translation by 5′-and 3′-UTR-binding factors. *Trends in Biochemical Sciences* **28**, 182-188.

Williams, A., Piaton, G., Aigrot, M.-S., Belhadi, A., Théaudin, M., Petermann, F., Thomas, J.-L., Zalc, B. and Lubetzki, C. (2007). Semaphorin 3A and 3F: key players in myelin repair in multiple sclerosis? *Brain* **130**, 2554-2565.

Willis, D. E., van Niekerk, E. A., Sasaki, Y., Mesngon, M., Meriand, T. T., Williams, G. G., Kendall, M., Smith, D. S., Bassell, G. J. and Twiss, J. L. (2007).

Extracellular stimuli specifically regulate localized levels of individual neuronal mRNAs. *The Journal of Cell Biology* **178**, 965-980.

Windebank, A. J., Wood, P., Bunge, R. P. and Dyck, P. J. (1985). Myelination determines the caliber of dorsal root ganglion neurons in culture. *The Journal of Neuroscience* **5**, 1563-1569.

Wolf, R. M., Wilkes, J. J., Chao, M. V. and Resh, M. D. (2001). Tyrosine phosphorylation of p190 RhoGAP by Fyn regulates oligodendrocyte differentiation. *Journal of neurobiology* **49**, 62-78.

Yamamoto, Y., Mizuno, R., Nishimura, T., Ogawa, Y., Yoshikawa, H., Fujimura, H., Adachi, E., Kishimoto, T., Yanagihara, T. and Sakoda, S. (1994). Cloning and expression of myelin-associated oligodendrocytic basic protein. A novel basic protein constituting the central nervous system myelin. *Journal of Biological Chemistry* **269**, 31725-31730.

Yeung, M. S. Y., Zdunek, S., Bergmann, O., Bernard, S., Salehpour, M., Alkass, K., Perl, S., Tisdale, J., Possnert, G., Brundin, L., et al. (2014). Dynamics of oligodendrocyte generation and myelination in the human brain. *Cell* **159**, 766–774.

Yool, D., Montague, P., McLaughlin, M., McCulloch, M. C., Edgar, J. M., Nave, K.-A., Davies, R. W., Griffiths, I. R. and McCallion, A. S. (2002). Phenotypic analysis of mice deficient in the major myelin protein MOBP, and evidence for a novel Mobp isoform. *Glia* **39**, 256 –267.

Yool, D. A., Edgar, J. M., Montague, P. and Malcolm, S. (2000). The proteolipid protein gene and myelin disorders in man and animal models. *Human Molecular Genetics* **9**, 987-992.

Zama, T., Aoki, R., Kamimoto, T., Inoue, K., Ikeda, Y. and Hagiwara, M. (2002a). A Novel Dual Specificity Phosphatase SKRP1 Interacts with the MAPK Kinase MKK7 and Inactivates the JNK MAPK Pathway. *Journal of Biological Chemistry* **277**, 23909-23918.

Zama, T., Aoki, R., Kamimoto, T., Inoue, K., Ikeda, Y. and Hagiwara, M. (2002b). Scaffold Role of a Mitogen-activated Protein Kinase Phosphatase, SKRP1, for the JNK Signaling Pathway. *Journal of Biological Chemistry* **277**, 23919-23926.

Zannat, M. T., Bhattacharjee, R. B. and Bag, J. (2011). Depletion of cellular poly (A) binding protein prevents protein synthesis and leads to apoptosis in HeLa cells. *Biochemical and Biophysical Research Communications* **408**, 375-381.

Zawadzka, M., Rivers, L. E., Fancy, S. P. J., Zhao, C., Tripathi, R., Jamen, F., Young, K., Goncharevich, A., Pohl, H., Rizzi, M., et al. (2010). CNS-resident glial progenitor/stem cells produce Schwann cells as well as oligodendrocytes during repair of CNS demyelination. *Cell Stem Cell* **6**, 578–590.

Zhai, J., Lin, H., Shamim, M., Schlaepfer, W. W. and Cañete-Soler, R. (2001). Identification of a novel interaction of 14-3-3 with p190RhoGEF. *Journal of Biological Chemistry* **276**, 41318-41324.

Zhang, J.-X., Feng, Y.-F., Qi, Q., Shen, L., Wang, R., Zhou, J.-S., Lü, H.-Z. and Hu, J.-G. (2014a). JNK Is Necessary for Oligodendrocyte Precursor Cell Proliferation Induced by the Conditioned Medium from B104 Neuroblastoma Cells. *Journal of Molecular Neuroscience* **52**, 269–276.

Zhang, Y., Chen, K., Sloan, S. A., Bennett, M. L., Scholze, A. R., O'Keeffe, S., Phatnani, H. P., Guarnieri, P., Caneda, C., Ruderisch, N., et al. (2014b). An RNA-sequencing transcriptome and splicing database of glia, neurons, and vascular cells of the cerebral cortex. *The Journal of Neuroscience* **34**, 11929-11947.

Zhang, Y. Y., Zhang, Y. P., Pepinsky, B., Huang, G., Shields, L. B. E., Shields, C. B. and Mi, S. (2015). Inhibition of LINGO-1 promotes functional recovery after experimental spinal cord demyelination. *Experimental Neurology* **266**, 68-73.

Zheng, Y., Wong, M. L., Alberts, B. and Mitchison, T. (1995). Nucleation of microtubule assembly by a gamma-tubulin-containing ring complex. *Nature* **378**, 578-583.

Zhu, Y., Kakinuma, N., Wang, Y. and Kiyama, R. (2008). Kank proteins: A new family of ankyrin-repeat domain-containing proteins. *Biochimica et Biophysica Acta* **1780**, 128-133.

Zuchero, J. B., Fu, M.-m., Sloan, S. A., Ibrahim, A., Olson, A., Zaremba, A., Dugas, J. C., Wienbar, S., Caprariello, A. V., Kantor, C., et al. (2015). CNS Myelin Wrapping Is Driven by Actin Disassembly. *Developmental Cell* **34**, 1-16.

Notes